The African Membrane Society

First International Congress:

SFAX 2016 – May 3rd – 5th 2016 - Tunisia

http://www.sam-ptf.com/sfax.html

IMPLEMENTATION OF MEMBRANE PROCESSES FOR WATER TREATMENT IN SMALL COMMUNITIES & CITIES

PARTNERS:

THE AFRICAN MEMBRANE SOCIETY &

THE *FACULTE DES SCIENCES DE SFAX*

Editorial par :

Pr. Raja Ben Amar

Dr. Abdoulaye Doucouré

L'African Membrane Society (AMS) est une société savante internationale qui regroupe les spécialistes de l'eau et des technologies membranaires.

L'AMS a vu officiellement le jour au mois d'Août 2014. Son siège est établi à l'École Nationale d'Ingénieurs Abderrahmane Baba Toure de Bamako au Mali. Elle compte plus de 70 membres originaires de toutes les grandes régions d'Afrique (Afrique du Nord, Afrique de l'Ouest, Afrique Centrale, Afrique Australe et Afrique de l'Est) et quelques acteurs installés en Amérique du Nord et en Europe :

La liste des membres du Conseil de l'AMS (composé de douze représentants) se trouve en page suivante.

Notre association milite pour l'**étude et l'exploitation des procédés de filtration et s'intéresse aux axes stratégiques suivants : Eau, Santé, Énergie et Environnement.** La priorité et les défis pour l'AMS consistent à stimuler l'appropriation technologique via la formation d'une masse critique d'experts et la dissémination du savoir scientifique sur le continent africain tout en favorisant le rapprochement avec les acteurs de l'industrie.

Nous organisons cette année notre premier congrès international, AMSIC-1, du 3 au 5 Mai 2016 à Sfax. Cette manifestation sera tenue chaque deux ans dans différents pays d'Afrique.

Cette rencontre internationale s'appuie sur la participation d'éminents experts scientifiques, des professionnels et décideurs institutionnels du domaine de l'eau et des technologies à membrane.

Le congrès AMSIC-1 inclut des conférences sessions plénières et key-notes, des communications orales, des posters et la visite d'une station de dessalement d'eau de mer dans la région de Sfax.

Nous remercions nos collaborateurs membres du bureau de l'AMS et les différents sponsors. Nos remerciements s'adressent également aux participants qui contribuent à la réussite de cette grande manifestation scientifique. Nous sommes heureux d'avoir pu mobiliser toutes les pôles géographiques de l'Afrique en invitant d'éminents chercheurs, des experts européens et plusieurs décideurs issus de structures gouvernementales et industrielles.

Editorial by:

Pr. Raja Ben Amar

Dr. Abdoulaye Doucouré

The African Membrane Society (AMS) is an international scientific society that brings together experts in membrane filtration and water treatment technologies.

The AMS was formally established in August 2014 and its headquarters are located at the National School of Engineers Abderrahmane Baba Toure in Bamako, Mali. It has over 70 members from all major regions of Africa (North Africa, West Africa, Central Africa, Southern Africa and East Africa) and some members are settled in North America and Europe:

AMS office is composed of twelve members (next page).

Our association is actively engaged in studying and implementing filtration processes and focuses its efforts on the following strategic areas: Water, Health, Energy and Environment. Our priorities and challenges are to promote technological ownership via the formation of a critical mass of experts, to disseminate scientific knowledge on the African continent and to foster academy-industry-government partnerships.

This year AMS first international congress (AMSIC-1) occurs between May 3rd and 5th in Sfax. Our goal is to organize AMSIC meetings every two years in different African countries.

This international meeting attracts world scientific experts, institutional professionals and decision makers from the membrane filtration and water treatment community.

The AMSIC-1 convention includes lectures plenary sessions and key-notes, oral presentations, posters and the visit of a seawater desalination plant in the Sfax region.

We would like to acknowledge the crucial support of all African Membrane Society members and our various sponsors. We are thankful to everyone that has been working closely with us to turn AMSIC-1 into a productive and memorable scientific gathering. This convention brings together many prominent researchers originating from all regions of Africa, several experts from western countries, and decision makers from the industrial and government sectors.

AMS BOARD / BUREAU DE L'AMS

President Président :	Abdoulaye Doucouré (France– Mali)
General Secretary Secrétaire Générale :	Raja Ben Amar (Tunisia)
Vice-President Vice Président :	Courfia Diawara (Senegal)
Treasurer Trésorier :	Arona Coulibaly (Mali)
Director of Science & Technology Directeur des Sciences &Technologies :	Mady Cissé (Senegal)
Director of Visual Content & Webmaster Directeur du Contenu Visuel & Administrateur du Réseau :	Jim Barry (USA)
Director of Communication Directeur de la Communication:	Nachida Kasbadji-Merzouk (Algeria)
Directors of External Relations Directeurs des Relations Extérieures:	G. Fred Molelekwa (South Africa) Tata Toure Diarra (Mali)
Director of Fundraising Directeur des Levées de Fonds :	Chimezie Anyakora (Nigeria)
Director of Publication & Editing Directeur de la Publication & de l'Edition:	Sidy Ba (Mali)
Director of Academy-Industry Partnership Directeur du Partenariat Académie-Industrie :	Alex Anim-Mensah (Ghana)

AMSIC-1 Program (Golden Tulip Hotel)

Time	Monday, May 2nd	
17:00-19:30	**Registration & "O. Expo" installation**	
Time	**Tuesday May 3rd - Clean Water/ Desalination**	
08:00-9:00	**Registration**	
08:30-9:00	**Opening Ceremony**	
09:00-09:45	**Plenary conference 1** Design of membrane systems for drinking water supply in small communities **Michel FARCY**, President - Aclaira S.A.S – France	
09:45-10:15	**Keynote 1** Energy supply in desalination processes? **Sadok BEN JABRALLAH** - Université de Carthage, Bizerte – Tunisia	
10:15-10:40	**Coffee Break**	
10:40-12:30	**Oral session A (I)** Carbon-based UF/NF Membranes for Water Treatment	**Oral session A (II)** Removal of Dissolved Minerals/Metals : Membranes Filtration for Water Consumption
	Oral presentation numbers: OC 1: OC 5	**Oral presentation numbers** OC6 : OC10
12:30-13:55	**Lunch & Learn** La stratégie de la SONEDE dans le domaine du dessalement **M. Abderaouf NOUICIR** - SONEDE - Tunisia Water treatment using membranes: desalination of brackish water and/or seawater resources? Treatment of surface water and/or non-conventional water resources? Which kind of membranes and at which scale**?** **Maxime PONTIE** - Université d'Angers - France	
14:00-14:45	**Keynote 2** Membrane materials for desalination **Andre DERATANI** - Institut Européen des Membranes, Université de Montpellier - France	
14:45-15:25	**Introduction to UNESCO-SIMEV** Une décennie d'Initiatives de SIMEV au Service des Nouvelles Formes de Collaboration Nord-Sud **Pierre MAGNES** (Firmus - France)	
15:30-17:10	**Oral session B(I)** Renewable Energy and Desalination Technologies	**Oral session B(II)** Surface Modified Membranes - Water Treatment Systems
	Oral presentation numbers OC11 : OC15	**Oral presentation numbers** OC6 - OC20

17:15-17:30	**Coffee Break**	
17:30-19:00	**Round table** Implementation of Water Treatment Technologies in Small Communities and Urban Centers Moderators : **Courfia DIAWARA, Senegal/ Roger BEN AIM, France**	
14:30-19:30	**O. Expo Exhibition (start)**	
19:15-20:30	**City Hall reception (Sfax Mayor)**	
22:00-23:00	**AMS members meet**	
Time	**Wednesday May 4th- Water reuse/ Industrial filtration**	
08:00-9:00	**Registration**	
09:00-09:45	**Plenary conference 2** Membrane bioreactor: recent evolution and present status. A key technology for a more sustainable management of wastewater. **Roger BEN AIM**, Institut de la Filtration & des Techniques Séparatives - Agen – France	
09:45-10:15	**Keynote 3** 2IE contribution in research and capacity building for water quality and water treatment in Africa. **Amadou HAMA MAIGA**, International Institute for Water & Environmental Engineering, Ouagadougou - Burkina Faso	
10:15-10:40	**Coffee Break**	
10:45-12:30	**Oral session C (I)** Facilitated Transport Membranes: Performance and Applications	**Oral session C (II)Wastewater** Treatment by Membranes and Alternative Technologies
	Oral presentation numbers: OC 21- OC 25	**Oral presentation numbers:** OC 25 - OC 30
12:30-13:55	**Lunch & Learn** Treatment of industrial wastewater by membrane bioreactor with consideration of microbial community dynamics **Sami SAYADI**, L.B.E. Centre de Biotechnologie de Sfax – Tunisia L'assainissement en Tunisie : l'expérience de l'ONAS **Mohamed Ben MAKHLOUF** (ONAS -Tunisia)	
14:00-14:45	**Keynote 4** Membrane science and technology research at the Nanotechnology and Water Sustainability Research Unit, of the University of South Africa. **Mhlanga SABELO** - UNISA, Johannesburg - South Africa	
14:45-15:25	**IFTS presentation** Testing protocols & standards in filtration and transport studies: **Vincent EDERY** & **Hafedh SAIDANI**	

15:30-17:10	**Oral session D(I) :** Novel Membranes/Characterization Methods and Experimental Designs	**Oral session D(II) :** Membranes for Industrial Effluent Removal
	Oral presentation numbers OC31- OC35	**Oral presentation numbers** OC36 - OC40
17:15-17:30	**Coffee Break**	
17:30-19:00	**Poster session**	
08:30-17:00	**O. Expo Exhibition (ongoing)**	
19:00-19:45	**Poster review (AMSIC-1 JURY only)**	
Special time	**Dinner Gala - Poster awards**	
Time	**Thursday, May 5th - RO desalination (tour)**	
9:00-2:45	**Site tour of desalination station organized by Le Groupe Chimique Tunisien (GCT)**	
13:00-14:30	**Lunch (hosted by GCT)**	
14:45-15:45	**Downtown tour in Sfax**	
14:30-16:00	**O. Expo Exhibition (End)**	
16:00-17:30	**Closing ceremony & awards**	
18:00-19:30	**Reception:** Sponsored by the Institut des Hautes Etudes de Tunis	

List of oral contribution (OC)

DAY 1 - Tuesday May 3rd, 2016 - *Clean Water Access & Desalination*

Morning: Session A - Afternoon: Session B

OC	AUTHORS	TITLE	SESSION
1	A. Lhassani	Potabilisation des eaux saumâtres par les procédés membranaires	Removal of Dissolved Minerals/Metals Membranes for Water Consumption 10:45 – 12:30 (Session A)
2	R. Fakhfekh C. Charcosset R. Ben Amar	Removal of iron from Tunisian drinking water by an hybrid membrane process using oxidation/microfiltration	
3	S. N. Diop M. C. Faye M. M. Diém Diémé	Elimination du fluor et de la salinité par système membranaire en milieu rural au Sénégal : bilan de 02 ans de fonctionnement dans le village de Keur Mariama	
4	M. Cisse	Application de la nanofiltration pour la production d'eau potable au Sénégal	
5	D. Berdous D. E. Akretche	Ion Exchange Membrane textile bioreactor : A novel alternative approach for drinking water denitrification	
6	A. Oun R. Ben Amar S. Maouch-Chergui B Charbonnier G. Sahoo	Membrane d'ultrafiltration à base de dioxyde de titane déposé sur un support d'argile-alumine et destinée au traitement d'une eau de lac	Carbon-based Materials and UF/NF Membranes for Water Treatment 15:30 – 17:10 (Session B1)
7	E. N. Nxumalo S.D. Mhlanga B. B Mamba	Diverse Physicochemical and Performance Properties for CNT-based Membranes	
8	N. Tahri R. Ben Amar	Formation of an asymmetric carbon nanofiltration membrane for the treatment of industrial effluent	
9	K. Yokwana	Performance evaluation of nitrogen-doped carbon nanotubes/polysulfone mixed matrix membranes	
10	A. Karim M. Ouammou B. Achiou K. Khiat M. Bouhria A. Abdellah	Elaboration of flat ultrafiltration membrane fabricated from nano-pozzolan and obtained by a sono-chemical method	

DAY 1 - Tuesday May 3rd, 2016 - *Clean Water Access & Desalination*

Afternoon: Sessions B (II, III)

OC	AUTHORS	TITLE	SESSION
11	N. Kasbadji Merzouk Z. Tigrine D. Tassalit	L'apport des énergies renouvelables au dessalement: Relevance of renewable energy technologies in desalination	Renewable Energy and Desalination Technologies 15:30 – 17:10 (Session BII)
12	N. Frikha	Performance evaluation of an autonomous vacuum membrane distillation unit coupled with solar energy	
13	Z. Tigrine N. Kasbadji Merzouk H. Aburideh M. Abbas D. Belhout D. Zioui S. Hout M. Khateb	Characterization of pilot-scale desalination reverse osmosis membranes coupled with a sustainable energy source	
14	M. Haudebourg M. Vergnet	OMOSUN: an autonomous photovoltaic-solar desalination unit operating without electric storage battery	
15	P. Magnes	Water treatment derived from the coupling of membrane and renewable energy technologies	
16	P. Margnes	Introduction to a grey water recycling System	Surface Modified Membranes - Water Treatment Systems 15:30 – 17:10 (Session BIII)
17	K. Fethi	Performance de la station de dessalement de Gabes (30000 m3/j) après 20 ans de fonctionnement	
18	M. Khemakhem M. Lejeune S. Khemakhem R. Ben Amar	Study of ceramic membrane surface modification by thin-film deposition using PECVD technique	
19	A. Chaabouni F. Guesmi B. Hamrouni	Modification of CMX ion-exchange membrane: effect of temperature on ion-exchange equilibrium	
20	S. Gassara E. Dufour W. Chinpa Y. Shih D. Quemener R. Ben Amar Y. Chang O. Lorain A. Deratani	Improvement of membrane filtration performance by use of hydrophilic polymers	

DAY 2 - Wednesday May 4th - *Water reuse & Industrial filtration*

Morning: Session C - Afternoon: Session D

OC	AUTHORS	TITLE	SESSION
21	I. Khouni S. Abdelkader L. Bousselmi A.hmed Ghrabi	Investigation of cheese whey wastewater treatment using coagulation/flocculation and membrane filtration: New hybrid process	Facilitated Transport Membranes FTM: Performance & Applications 10:45 – 12:30 (Session C)
22	T. Eljaddi M. Riri, M. Hor Y. Chaouqi L. Lebrun M. Hlaibi	Preparation of new polymeric membranes used for studying the facilitated transport of cadmium ions in aqueous solutions	
23	T. Eljaddi A. Benjjar M. Riri, H.E. Atmani I. Mourtah L. Lebrun M. Hlaibi	New supported liquid membranes containing TBP and MC as carriers for the facilitated transport of cadmium ions from acidic mediums: Parameters and mechanism	
24	E.A. El Houssaine M. Habib Y. Chaouqi I. Touarsi L. Laurent M. Hlaibi	Influence des facteurs acidité et température sur l'évolution des paramètres relatifs au processus de l'extraction facilitée des cations Co2+ et Ni2+ à travers une membrane polymère type SLM contenant des agents extractifs phosphatés	
25	M. Habib S. Majid E.A. El Houssaine S. Tarhouchi M. Hlaibi L. Laurent	Determination of specific parameters related to the directed process of facilitated extraction of Oleic acid through polymer inclusion membranes.	
26	K. Touaj S. Majid N. Sefiani L. Lebrun M. Hlaibi	L'Association substrat-agent extractif: principe de base pour l'extraction et la séparation facilitée par procédés membranaires	Wastewater Treatment by Membranes & Alternative Technologies: 15:30 – 17:10 (Session D I)
27	B. Moslah A. Jrad	Decontamination of residual antibiotics-loaded wastewater by combining solar TiO2 photocatalysis and biological treatment	
28	H. I. Abdel-Shafy	Treatment enhancement of blackwater Using ZnO-nanoparticles coupled with an efficient mixed micro-organism and membrane bioreactor	
29	A. Tolofoudye	Challenges of residential, domestic and industrial wastewater management in Mali: case study in Bamako city	
30	C. Fersi	Wastewater treatment of tannery effluents via an hybrid process of coagulation-flocculation / NF	

DAY 2 - Wednesday May 4th - *Water reuse & Industrial filtration*

Afternoon: Sessions D (II, III)

OC	AUTHORS	TITLE	SESSION
31	H. Aloulou A. Ghorbel R. Ben Amar Raja S. Khemakhem	Elaboration et caractérisation d'un nouveau support membranaire à base de zéolite : Elaboration and characterization of a new membrane support derived from a zeolite	Novel Membranes/Characterization Methods and Experimental Designsn **15:30 – 17:10 (Session DII)**
32	I. Louati F. Guesmi C. Hannachi B. Hamrouni	Optimization of nitrate removal from water by electrodialysis	
33	A. Doucoure	Advanced nonwoven filtration materials for enhanced water pretreatment	
34	So. Rekik A. Deratani	Study of ceramic membranes from naturally-occuring Kaolin clays for microfitration applications	
35	D. Tassalit N. Kasbadji Merzouk O. Mouzaoui W. Naceur Wahib N. Chekir O. Benhabiles	Use of an experimental design for the heterogeneous photocatalysis of organic pollutants in aqueous TiO2 suspension	
36	A. Hammami C. Charcosset R. Ben Amar	Removing of AO7 dye by an hybrid process based on adsorption/membrane separation	Membranes for Industrial Effluent Removal (MIER): **15:30 – 17:10 (Session DIII)**
37	D. Dadi B. Van der Bruggen	Bioethanol production from coffee waste fractions and quality upgrading using an alcohol selective pervaporation membrane	
38	B. Dembele A. Tolofoudye A. Doucoure	Traitement des eaux de drainage minier du Mali par nanofiltration / Treatment of Mali drainage mining water by nanofiltration	
39	S. Louhichi A. Ghorbel S. Khemakhem	Elaboration of a new ceramic membrane from Turkish zeolite for hydrogen sulfide removal by ultrafiltration.	
40	R. Haouche H. Mabrouki D. E. Akretche	Membrane treatment of an effluent derived from the pharmaceutical industry	

Poster session (Golden Tulip Hotel)

Wednesday, May 4th: 17:30 – 19:00		
N°	**AUTHORS**	**TITLE**
1	Catherine Charcosset Assma Alharati Koffi Fiaty	Elimination du bore contenu dans l'eau par un procédé membranaire hybride associant résine échangeuse d'ions et microfiltration
2	Imen Derbel Mouna Khemakhem Raja Ben Aamar	Elaboration and characterization of a carbon-based ultrafiltration Membrane: Application to membrane distillation
3	Diaf Amine Seddini Abdelali Debbal Zakaria	Traitement des eaux sur des filtres gravitaire à composition variée/Water treatment based on trickling filters of various compositions
4	Kholiswa Yokwana Sabelo.D Mhlanga Bhekie.B Mamba Edward.N Nxumalo	Performance evaluation of nitrogen-doped carbon nanotubes/polysulfone mixed matrix membranes
5	Jamel Kheriji Béchir Hamrouni	Le bore comme élément problématique dans le domaine de dessalement
6	Ghazza Masmoudi Raja Ben Amar	Comparison between coagulation/ultrafiltration hybrid treatment and combination of membrane processes for the treatment and reuse of deying effuents
7	Aloulou Wala Hamza Wiem Khemakhem Sabeur Ben Zina Mourad Ben Amar Raja	Développement de membranes poreuses de filtration à base de nano-composites argileux.
8	Imen Ben Belgacem, Hazem Bouhamed and Sabeur Khemakhem	Elaboration and characterization of ZnO-SiO2 nano-composite made of a nanofiltration layer
9	Sofian Louhichi Ghorbel Ali Sabeur Khemakhem	Elaboration and characterization of a novel ceramic microfiltration membrane From Tunisian natural kaolinite
10	Mahzoura Missaoui Fakhfekh Rahma Ben Amar Raja Charcosset Catherine	Defluorination of Tunisian drinking water (region of Gafsa, South)
11	Mohamad M. Dieme	Sustainable conversion of agricultural wastes into activated carbons devoted to arsenic (V) and fluoride removal from natural water
12	Nabil Jallouli Mohamed Ksibi	UV and solar photo-degradation of Naproxen: Reaction kinetics, product identification and assessment of toxicity
13	Ahmed Hammami Ghazza Masmoudi Catherine Charcosset Raja Ben Amar	Application of microfiltration and ultrafiltration in hybrid processes for dyeing wastewater treatment

14	Mohamed Aiman Kammoun Sana Gassara André Deratani Raja Ben Amar	Adoucissement des eaux saumâtres par membrane de nanofiltration NF270
15	Radek Oborný	Sustainable and robust DEWATS- sidestream AnMBR with the Helix Technology
16	Hassen Khazri Ibtissem Ghorbel-Abid Rafik Kalfat	Removal of drugs in aqueous solution onto natural clay
17	Tassalit Djilali Kasbadji M. Nachida Mouzaoui Oussama Naceur Wahib Chekir Nadia Benhabiles Ouassila	Use of an experimental design for the heterogeneous photocatalysis of organic pollutants in aqueous TiO2 suspension
18	Ilhem Ben Salah Sayadi	Study of CaCO3 scaling of ion-exchange membranes
19	Hafedh Saidani Vincent Edery Roger Ben-Aim	New testing method: Effectiveness of submicron cartridges and membranes

Chers collègues,

Les organisateurs du congrès de Sfax ont le plaisir de vous informer que les quatre candidats ci-dessous (étudiants ou professionnels en début de carrière) ont été choisis pour représenter les premiers lauréats de l'AMSIC. L'association European Membrane Society ayant sponsorisé cette compétition chaque lauréat recevra un diplôme cosigné par les responsables de l'EMS et de l'AMS et une récompense de 150 euros.

Dear colleagues,

The Sfax congress organizers are delighted to inform you that the four candidates whose names are listed below (students and early career professionals) were selected as first laureates of AMSIC. Since this activity is sponsored by the European Membrane Society the award recipients will receive a certificate signed by EMS and AMS leadership as well 150 euros.

Best Oral Presentation by Students & Young Professionals		
1	**Kholiswa YOKWANA (South Africa)**	
	Performance evaluation of nitrogen-doped carbon nanotube/polysufone mixed matrix membranes	
Best 3 Posters by Students & Young Professionals		
1	**Ghazza MASMOUDI Tunisia**	Comparison between coagulation /ultrafiltration and combination of membrane processes for the treatment of dyeing effluent
2	**Jamel KHERIJI Tunisia**	Le bore comme élément problématique dans le domaine du dessalement
3	**Zahia TIGRINE Algeria**	Characterization of a pilot-scale reverse osmosis membrane coupled with a self-sustained energy source

Nous remercions l'EMS pour ce geste généreux et félicitons Kholiswa, Ghazza, Jamel, et Zahia pour leur excellent travail. L'AMS et ses partenaires sont extrêmement reconnaissants envers tous les sponsors et les participants qui ont contribué au succès de cette rencontre et vous donnent rendez-vous en Afrique du Sud pour l'AMSIC-2 prévu en 2018.

We would like thank EMS for its generous support and congratulate Kholiswa, Ghazza, Jamel, et Zahia for their outstanding work. AMS and its partners are deeply grateful to their sponsors and participants who have made this meeting successful. We would like to invite you to join us again during AMSIC-2 in South Africa in 2018.

Salutations Cordiales / Kindest regards.

Participant à la rencontre / 04 mai 2016, Hotel Golden Tulip

Visite de la station d'Osmose Inverse (Groupe Chimique Tunisien) de dessalement de mer de Skhira, e, banlieue de Sfax, Tunisia

Cérémonie d'inauguration du congrès à l'intérieur de la Mairie de Sfax

Mairie de Sfax by night

Objectifs de la Conférence

Une gestion rigoureuse des ressources en eau s'impose dans toutes les régions du globe à cause principalement de l'assèchement des sols ou des contraintes d'ordre économique et géopolitique.

La croissance de la demande en eau, associée à la situation de stress hydrique, et aux contraintes d'ordre économique et géopolitique, nécessite la mobilisation de nouvelles richesses et une gestion rigoureuse des ressources avérées. En Afrique, les menaces climatiques ont causé une baisse sensible en approvisionnement en eau de surface, ce qui entrave le développement économique de la région. Ainsi, il devient urgent d'exploiter les technologies filtrantes, certaines ressources non conventionnelles et les énergies renouvelables pour favoriser l'accès à l'eau potable, l'irrigation des sols, et l'épuration des eaux usées à des fins de réutilisation ou de recyclage.

La rencontre internationale de Sfax (Tunisie), mettra l'accent sur les principales avancées de la recherche académique et industrielle dans le domaine des technologies membranaires et de filtration pour le traitement de l'eau.

Les experts se réuniront pour échanger les données et résultats des projets de recherche engagés en Afrique, et formuler les recommandations et orientations futures en matière de gestion efficace de l'eau. Les objectifs à long terme visent à renforcer les capacités scientifiques et technologiques, stimuler la croissance économique à travers la valorisation des ressources en eau et énergie afin de freiner la progression de la pauvreté en Afrique et ses conséquences dévastatrices.

Objective of the conference

The prevalence of physical water scarcity, economic limits, and complex geopolitical development around the globe call for pressing action and better management of water resources. In Africa, environmental and climate challenges have resulted in diminishing surface water supply that has hindered economic development.

In this context, it is worth assessing the relevance of filtration processes vis-a-vis potable water resource management, land irrigation, renewable energy production, and wastewater treatment for reuse or recycling.

The international meeting in Sfax (Tunisia) will focus on key advances in academic and industrial research targeting membrane technologies for water treatment. Experts will gather to share research data, discuss water projects initiated in Africa, and make recommendations for future directions. The underlying goals for Africa are to build scientific and technological capacity, stimulate economic growth, and play an active role in the fight against poverty.

AMS will organize two days of research sessions and training to discuss membrane filtration in developing countries (May 3rd and 4th). The third and final day will be devoted to visiting a water desalination plant followed by the closing ceremony.

Comité d'Edition et de Publication

Edition & Publishing team:

Nachida Kasbadji Merzouk, (Leader)
Sidy Ba
Raja Benamar
Mady Cisse
Abdoulaye Doucoure
Soraya Malinga

Comité Scientifique International

International scientific committee

Raja Benamar, Chairwomen, Tunisia
Abdoulaye Doucoure, Chairman, USA

Andre Ayral, France
Jas Pal S. Badyal, United Kingdom
Amina Bakhrouf, Tunisia
Merlin L. Bruening, USA
Bart Van der Bruggen, Belgium
Catherine Charcosset, France
Mady Cisse, Senegal
André Deratani, France
Ludovic Dumee, South Africa
Tarik Eljaddi, Morocco
Sana Gassara, Tunisia
Amel Jrad, Tunisia
Nachida Kasbadji Merzouk, Algeria
Sabeur Khemakhem, Tunisia
Mohamed Ksibi, Tunisia
Abdelhadi Lhassani, Morocco
Soraya Malinga, South Africa
Wahib Naceur, Algeria
Abdallah Ouagued, Algeria
Gilbert Rios, France
Ganesh Sahoo, India
Sami Sayadi, Tunisia
Anthony Szymczyk, France
Saad Alami Younssi, Marrocco

Sponsors Acknowledgement/Remerciements

Institut de la Filtration et des Techniques Séparatives(Fra)

Institut Européen des Membranes de Montpellier(Fra)

Chaire UNESCO SIMEV European Membrane Society Hollingsworth & Vose (USA)

Caltech

Faculté des Sciences de Sfax (Tun)Université de Sfax (Tun)

Groupe Chimique Tunisien(Tun)Instituts des Hautes Etudes de Tunis (Tun)

Instituts des Hautes Etudes de Paris(Fra)Confection idéale du sud (Tun)

Plastic Sfax (Tun) Masmoudi Patisserie (Tun)

Al Koutaf (Tun) Groupe Triki(Tun)

Chahia (Tun) BIAT (Tun)

CHO Group(Tun)Sopal (Tun)

SIVO (Tun)Sonede (Tun)

Sommaire /Table of Contents

Preparation a New Polymeric Membranes for Studying the Facilitated Transport of Cadmium Ions from Aqueous Solutions

Tarik Eljaddi, Mohamed Riri, Mustapha Hor, Youssef Chaouqi, Laurent Lebrun, Miloud Hlaibi..... 1

Osmosun, Un Système de Dessalement Solaire Photovoltaïque Autonome, au Fil Du Soleil Sans Batterie de Stockage Electrique

Pierre Hamon, Maxime Haudebourg Et Marc Vergnet 6

Preparation of Asymmetric Carbon Nanofiltration Membrane for the Treatment of Indusrial Textile Effluent

Nouha Tahri And Raja Benamar 9

Le Bore comme Elément Problématique dans le Domaine du Dessalement

Jamel Kheriji, Bachir Hamrouni..... 14

Comparison Between Coagulation/ Ultrafiltration Hybrid Treatment and Combination of Membrane Processes for Treatment and Reuse of Dyeing Effluents

Ghazza Masmoudi And Raja Ben Amar..... 19

Investigation Of Cheese Whey Wastewater Treatment Using Coagulation/Flocculation And Membrane Filtration: New Hybrid Process

Imen Khouni, Sana Abdelkader, Latifa Bousselmi, Ahmed Ghrabi 24

Study Of Ceramic Membrane From Naturally Occurring-Kaolin Clays For Microfiltration Applications

Sonia Rekik, Semia Baklouti, Jamel Bouaziz, André Deratani..... 27

Adoucissement des Eaux Saumâtres par Membrane de Nanofiltration Nf270. Etude de la Rétention et des Mécanismes de Transport

Mohamed Aiman Kammoun, Sana Gassara, André Deratani, Et Raja Ben Amar..... 33

L'appoint des Energies Renouvelables au Dessalement

Nachida Kasbadji Merzouk, Zahia Tigrine et Djillali Tassalit..... 38

Tannery waste water treatment using hybrid process: Coagulation-Flocculation/Nanofiltration

Cheima Fersi, Chiraz Gorgi, A. Irmani..... 43

Performance Evaluation of an Autonomous Vacuum Membrane Distillation Unit Coupled with Solar Energy

Slimane Gabsi, Nader Frikha, Béchir Chaouachi..... 46

Improvement Of Membrane Filtration Performances By Using Hydrophilic Polymers

Sanna Gassara, Elsa Dufour, Watchanida Chinpa, Y.-J. Shih, Damien Quémener, Raja Ben Amar,Yung Chang, Olivier Lorain And Alain Deratani..... 52

Contribution To Understand Caco3 Scaling Of Ion Exchange Membranes During Conventional Electrodialysis

Ilhem Ben Salah Sayadi, T. Mansour, H. Boughanmi, M. Ben Amor..... 57

African Membrane Society
Water & Environment, Process, Energy
Sfax, Tunisia, May 3-5, 2016 - Membrane Water Treatment in Small Urban and Village Centers

Preparation a New Polymeric Membranes for Studying the Facilitated Transport of Cadmium Ions from Aqueous Solutions

Tarik ELJADDI[1], Mohamed RIRI[1], Mustapha HOR[1], Youssef CHAOUQI[1], Laurent LEBRUN[2], Miloud HLAIBI[1]

[1]*Laboratoire Génie des Matériaux Pour l'Environnement et la Valorisation, University of HASSAN II Casablanca, Morocco*
[2]*Laboratoire des Polymères, Biopolymères, Membranes, UMR 6522 du CNRS, University of Rouen, France*
eljaddi@gmail.com

Abstract: In this work, we have developed asymmetric membranes using PSU as a support, PVP as a co-polymer and Cholic acid (CA) as a carrier by the phase inversion method, we have characterized prepared membranes by various techniques like SEM, IR, angle contact. Then, we have realized the facilitated transport of some ions like cadmium ions in acidic solutions (pH=1). A kinetic model is used to determine the Macroscopic parameters (permeability P and initial flux J_0), for understanding this phenomenon of facilitated transport and therefore extraction of these ions by this type of membranes, we have developed a mechanism based on the association between substrate (ion) and carrier (CA), flowed by diffusion of the formed complex through membrane phase. The experimental results verify this mechanism and, allow finding the microscopic parameters: (association constant Kass and apparent diffusion coefficient D*) related to the migration of the complex (Substrate-Carrier) formed through the membrane. Finally, we have developed a stable membrane at different conditions like pH or Temperature.

Keywords: facilitated extraction; PSU/PVP; ions; initial flux; permeability.

I. INTRODUCTION

Actually, we need to develop some techniques for treating or produce the fresh water because the population in our planet grows rapidly and, we don't have enough resources for water or it is polluted by solid, liquid or gas waste like toxic metals (cadmium, chromium,...). Many researches are conducted to extract cadmium ions by several types of polymeric membranes: supported liquid membrane (SLM) [1], polymer inclusion membrane (PIM) [2], Bulk liquid membrane (BLM) [3], in addition, Membranes formed by polysulfone PSU and polyvinyl pyrrolidone (PVP), have better physicochemical properties [4].

In this work, we will introduce the Cholic acid (CA) as a carrier in the matrix of PSU / PVP for studying the facilitated transport of cadmium ions through the functionalized polymer membrane (FPM) that are characterized by several techniques. Also, we have used kinetics and theoretical models for determining the macroscopic (P, J0) and microscopic (Kass, D*) parameters for facilitated extraction of cadmium ions.

II. MATERIALS AND METHODS

2.1 Chemical products

All reagents, solvents and chemicals used in this study are pure commercial products (Aldrich, Fluka and Alpha Aesar). Cadmium and copper ions acids are prepared from solutions of cadmium nitrate hydratedand copper sulfates and the pH was adjusted with HCl and NaOH.

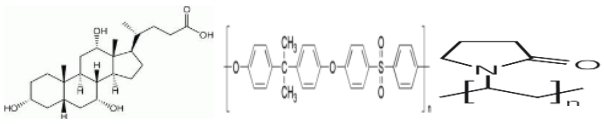

A: CA B: PSU C: PVP

Figure 1: Structures of components.

2.2 Membrane preparation

The membrane was prepared by phase inversion method the mixture of polysulfone and polyvinylpyrrolidone (PVP) in NMP as solvent followed by addition of Cholic acid (CA) as an extractant, we have used a pure water bath of phase inversion at room temperature [5].

2.3 SEM observation

The samples were fractured in liquid nitrogen and coated with gold–palladium and then observed by a scanning electron microscope (ZEISS EVO40EP).

2.4 FTIR spectroscopy

The equipment used is an infrared Fourier transform spectrometer AVATAR 360 ESP FTIR Nicolet piloted by OMNIC as computer program, measurements are

performed in the laboratory of PBS Rouen in France, analysis of the membranes is made at normal pressure and room temperature [6].

2.5 Transport experiments

Transport experiments were performed in a cell (Fig.2), that contains two compartments, the source phase (F) and the receiving phase (R) the system is immersed in a thermostatic bath (TB) and agitation provided by a multi-station magnetic stirring (MS), to follow the evolution of the facilitated extraction of cadmium or copper ions, we took samples from the receiving phase as a function of time, and we used atomic absorption spectroscopy (Shimadzu) to analyze the samples.

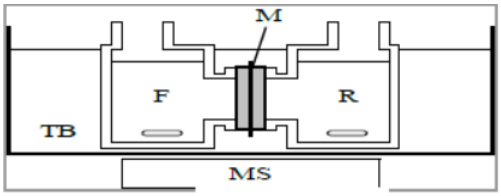

Figure 2: Transport cell.

III RESULTS AND DISCUSSION

3.1 Characterization of the membrane

3.1.1 Contact Angle

In the present study, all prepared membrane are relatively hydrophilic (ɵ<90°) table 1.

The hydrophilicity character increases with addition of PVP and it increases more after addition of Cholic acid, this evolution can be attributed to functional groups in PVP and CA added. We can be explained this by the mechanism of action involved during the phase inversion process. During membrane formation, the hydrophyilic functions migrate towards the top of the membrane as the top layer is more exposed to water[7].The thickness of the membrane was measured using the Palmer; it is in the order of 106µm.

Table 1 : Contact angle

membrane	Contact angle (°)
PSU alone	68.60
PSU/PVP	65.9
PSU/PVP/AC	58.6

3.1.2 FTIR

Figure 3 shows the spectra relating to prepared membranes: (PSU / PVP)-AC ,PSU alone, PSU/PVP, Cholic acid alone ,PVP alone, the group are identified in the spectrum, we find that the membrane contains the matrix the base polymer PSU and PVP polymer, essentially, the first characterized by the group “S” is present the spectrum.

For the PSU / PVP-AC membrane, we note that there has apparition a band about 1700cm-1 characteristic of “C=O” group which confirms that the extractive agent is grafted in the membrane matrix, other evidence that confirms this results , the apparition of a wide band about 3400cm-1, which also exists in the spectrum of the extractive agent only and does not exist in the spectrum of PSU alone, so the source of this group is probably the “CA”, more than that, there is the disappearance of a band characteristic of group “C-OH” carboxylic about 1395-1440 cm-1 thus confirming that the grafting of the function of “CA” is in matrix PSU / PVP. Similar results were found by addition the citric acid in the PSU in the work of Xinyu et al [8].

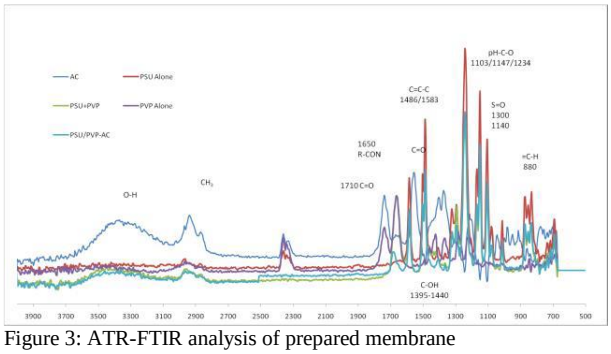

Figure 3: ATR-FTIR analysis of prepared membrane

3.1.3 Membrane morphology:

The SEM images of prepared membranes were recorded and shown in Figure 4, membrane exhibited characteristic asymmetric structure of dense top layer followed by macro-voids. Membranes with PVP and CA demonstrated noticeable changes in top layer. The macro-void structure was altered by the addition of PVP and CA to PSU polymer matrix. this change can be explain by the relative hydrophilic character of PVP and CA which is responsible for the fast exchange of solvent (NMP) and non-solvent (water) during the phase inversion process which leads to extended porosity as well as changes in the macro-voids structure. Membranes are homogeneous and contain cavities of different sizes, communicative through pores. Despite the existence of pores in PSU/PVP membranes, we have not observed any transport of cadmium or copper ions through these membranes, this result can confirm the existence the interaction between ions and cholic acid (CA).

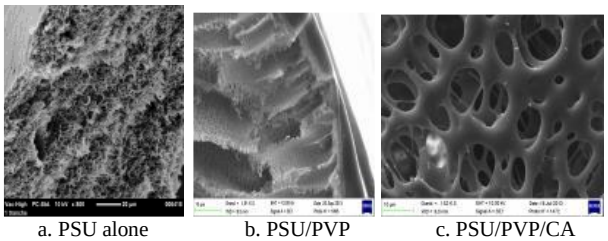

a. PSU alone b. PSU/PVP c. PSU/PVP/CA

Figure 4: Micrographs of the cross-sections of membranes

3.2 Facilitated transport of Cadmium ions

3.2.1 Quantity of extractiveagent (CA)

We have transported the cadmium ions using the membrane PSU/PVP/CA at T = 25 °C and pH = 1 for initial concentrations of 0.0125 M to 0.1 M, we used the calculation model [9]–[11]. The figure 4 represents the linear evolution of -Ln (C0-2CR) = f (time, and shows that kinetic model is verified and the mechanism for this process is the same for ions extracted through both

membranes prepared. The slopes of these line segments allow to determine the macroscopic parameters P and J0 relating to performance of each of the membrane-type PSU / PVP-AC adopted for facilitated extraction of Cd (II) ions), and the different values obtained are listed in Table 2.

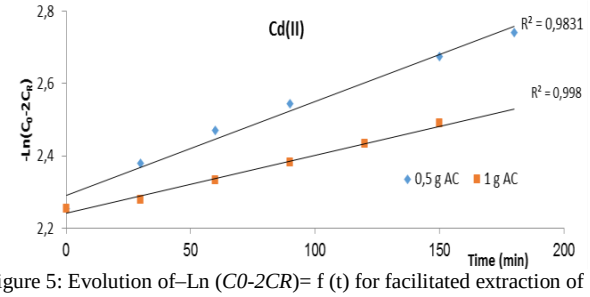

Figure 5: Evolution of–Ln (*C0-2CR*)= f (t) for facilitated extraction of Cd(II) ions throught membranePSU /PVP-AC. pHF=pHR= 1,C0=0.1 Mand K= 298K.

Table2: Kinetic parameters

Masse of CA	***C0*M**	***P*x 10^7 cm^2 s^{-1}**	***J0*x10^5 mmole s^{-1} cm^{-2}**
0.5g	0.1	20.10	1.90
	0.05	20.87	0.98
	0.025	21.64	0.51
	0.0125	22.41	0.26
1 g	0.1	17.50	1.17
	0.05	18.59	0.62
	0.025	19.69	0.33
	0.0125	20.78	0.17

$l_{0,5gAC}$=106µm, l_{1gAC}=150µm, $pH_R = pH_F$=1 et T=298 K.

Analysis of the results summarized in the table 2, indicates that the membrane PSU / PVP-AC 0.5 g of CA agent is performing better than membrane of 1g of CA. Certainly is an optimum concentration of the extractive agent for this type of functionalized membranes, and optimum mass is less than 1g in CA agent. Moreover, these parameters P and J0have a reverse variation with initial substrate concentration C0, a low of C0 in the feed phase results in decreased flux J0and an increased permeability P, for this reason, the search for an adequate concentration C0is necessary for a better compromise for the parameter values P and J0 for getting a better performance of membrane.. therefore, the introduction of PVP polymer only improve the performance of this new type of membranes (PSU / PVP-AC) by increasing their porosity and certainly giving of freedom of movement to the CA agent molecules present in the membrane.

To explain and better understand this phenomenon, we have adopted a thermodynamic model (Ref), based on the interactions between the substrate (ion) and the extractive agent, and which are necessary for diffusion of these ions through membrane phase.

Figure 6 relative to the Line weaver-Burk representation of curves 1 / J0 = f (1 / C0) provided by this model show linear evolution with positive slopes of straight segments. These results confirm the proposed mechanism in the model. The slopes and intercepts of these lines allow to determine the values of the microscopic parameters, Kass association constant of the substrate (ion) with the extractive agent(CA), and the apparent diffusion coefficient D* of migration step which is the rate-determining step of the mechanism. All values obtained for these two parameters Kass and D * relating to the studied process are summarized in Table **3,**the analysis shows a clear inverse evolution of microscopic parameters Kass and D *, in other words, a low value of Kass corresponds to a high value of coefficient D * and therefore a better performance of the membrane adopted, and vice versa. These results confirm the low performance of membrane (1 g CA) with a high value of the constant Kass and low value of the coefficient D *. So the addition of a small amount of PVP polymer for the preparation of this new type of membranes, provides more porous membranes (SEM images) and more efficient for the studied process. . Finally, the variation of specific parameters Kass and D * indicates that certainly the diffusion of a substrate (ion) from feed phase to receiving phase through the membrane, is made according to a result of reversible reactions (Association / Dissociation) with formation and decomposition of a pseudo entity (ion-CA) required for this migration.

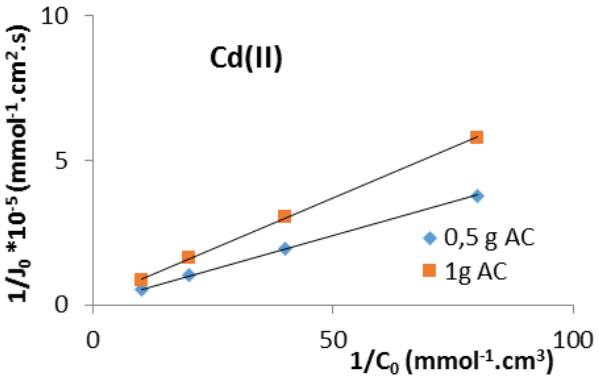

Figure 6: Lineweaver-Burkrepresentation of (1/*J0*= f(1/*C0*))

Table 3: microscopic parameters

Cholic Acid (CA)	*D**x 106cm2s-1	*Kass*
0.5 g	9.3	1.75
1g	2.6	2.83

$l_{0,5gAC}$=106µm et l_{1gAC}=150µm

3.2.2Influence of pH

In the aqueous solutions, acidity factor is very important and can influence the soluble forms of the metal captions, for example, depending on the pH of the environments studied some forms become unstable and with very small concentrations [12], [7].To check the influence of this factor on the evolution of the performance of membranes PSUPVP-AE. We performed kinetic experiments for facilitated extraction of Cd (II) ions through a membrane-type PSU / PVP-CA with best performing containing 10% of in PSU, PVP and [AC] = 0.10 M. at T = 298 K, of initial concentrations of substrate (ion) C0ranging from 0.10 to 0,0125 M and the three respective acidities pH = 1, 2

and 3 of the two compartments (feed and receiver).We used the same model by following the evolution of Ln (C_0-2C_R) = f (time) (figure 7). The slopes of various lines quantify the parameters P and J_0 according to the terms established by the kinetic model, and all the values for these parameters are listed in Table4. The P and J_0 parameters changes lightly with the acidity of feed and receiving phases, the table show the performance of membranes is best for environments with high acidity (low pH).

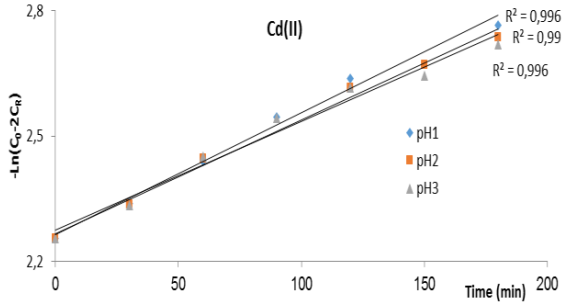

Figure 7: Evolution of–Ln (C_0-2C_R) = f (t) for facilitated extraction of Cd (II) ions through the membrane PSU /PVP-AC. pH_F=pH_R= 1,2 and 3,C0=0.1 M and K= 298K.

Table4: Kinetic parameters

pH	*C0*M	***P***x 10^7 cm^2s^{-1}	***J0***x 10^5 mmole s^{-1} cm^{-2}
1	0.1	31.93	2.11
	0.05	33.03	1.09
	0.025	34.13	0.57
	0.0125	35.23	0.29
2	0.1	29.95	1.98
	0.05	31.05	1.03
	0.025	32.04	0.53
	0.0125	33.47	0.28
3	0.1	28.63	1.90
	0.05	29.73	0.98
	0.025	30.83	0.51
	0.0125	32.26	0.27

l = 151µm et [AC] = 0,10 M

The study of the evolution of the function $1/J_0=f(1/C_0)$ according to Line weaver-Burk method (figure 8) shows linear evolution for the three acidities. Which confirms the proposed mechanistic model. The slopes and intercepts of the straight lines were used to calculate the values of Kass and D* parameters according to equations prescribed by the thermodynamic model, and all results obtained for these parameters are summarized in Table 5.

After analyze of the results, the interactions between ions and CA are low in acidic medium which allows the formation of (ion-CA) unstable, and therefore a high diffusion of the substrate through the membrane and better performance of PSU / PVP-AC membrane, for facilitated extraction of Cd (II) ions.

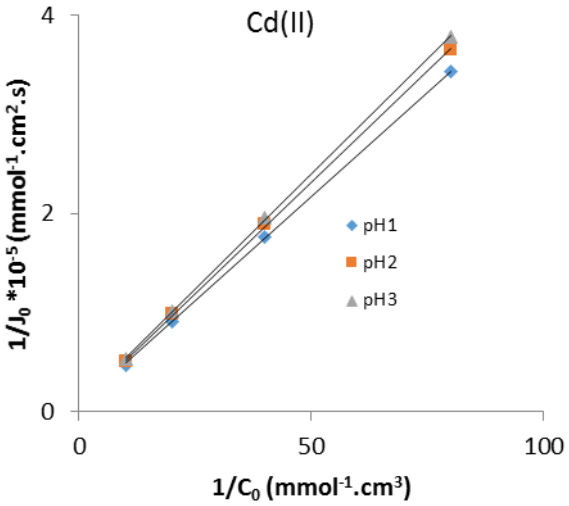

Figure 8: Line weaver-Burk representation of (1/*J0*= f(1/*C0*))

Table 5: microscopic parameters

pH	D* 10^6 cm2 s2	K_{ass}
1	22.8	1.57
2	18.2	1.89
3	16.2	2.07

l=151µm et [AC]=0,1M

These results show the free forms of ions are unstable in the membrane phase. Indeed, these free forms favored by high acidity are loaded and establish very weak interactions with CA molecules, with greater diffusion through the membrane phase. The overall results show that the influence of the acidity factor on the performance of such membranes for the studied process remains weak in the field of studied acidity (pH = 1, 2 and 3) as the free forms of Cd(II) are little affected. In contrast to low acidity (pH greater), this influence is more important because the forms-related will be favored.

Finally, studies by Gulsin A. et al. indicated similar trends as a function of acidity factor for the extraction of Cr (VI) ions [13].

IV. CONCLUSION

In this work, we have prepared by phase inversion method a new membrane at the base PSU / PVP and Cholic acid as an extractive agent, which was characterized by SEM, IR and contact angle,.

Also, we have verified our model calculation and calculated parameters related to facilitated extraction of cadmium ions through the membrane prepared and we have studied the effect of CA quantity and acidity of feed and receiving phase,

This study is a first step to develop a membrane for protect our environment by recovering a Cadmium ions for recycling and treating a wastewater.

REFERENCES

[1] T. Eljaddi, O. Kamal, E. H. El Atmani, I. Touarssi, L. Lebrun, and M. Hlaïbi, "Effective supported liquid membranes for facilitated extraction phenomenon of cadmium (II) ions from acidic environments: parameters and mechanism," *Can. J. Chem. Eng.*, vol. 9999, pp. 1–9, Dec. 2014.

[2] C. Fontàs, R. Tayeb, M. Dhahbi, E. Gaudichet, F. Thominette, P. Roy, K. Steenkeste, M.-P. Fontaine-Aupart, S. Tingry, and E. Tronel-Peyroz, "Polymer inclusion membranes: The concept of fixed sites membrane revised," *J. Memb. Sci.*, vol. 290, no. 1–2, pp. 62–72, Mar. 2007.

[3] S. Koter, P. Szczepański, M. Mateescu, G. Nechifor, L. Badalau, and I. Koter, "Modeling of the cadmium transport through a bulk liquid membrane," *Sep. Purif. Technol.*, vol. 107, pp. 135–143, 2013.

[4] N. Ghaemi, S. S. Madaeni, A. Alizadeh, P. Daraei, M. M. S. Badieh, M. Falsafi, and V. Vatanpour, "Fabrication and modification of polysulfone nanofiltration membrane using organic acids: Morphology, characterization and performance in removal of xenobiotics," *Sep. Purif. Technol.*, vol. 96, pp. 214–228, Aug. 2012.

[5] T. Eljaddi, A. Benjjar, O. Kamal, M. Riri, L. Lebrun, and M. Hlaibi, "Preparation and characterization of new membranes PSU / PVP for the extraction of cadmium ions from acidic solutions," *Moroccan J. Chem.*, vol. 5, pp. 470–474, 2014.

[6] E. Goormaghtigh, V. Cabiaux, and J.-M. Ruysschaert, "Physicochemical Methods in the Study of Biomembranes," 1994. [Online]. Available: http://www.springerlink.com/index /10.1007/978-1-4615-1863-1. [Accessed: 07-Mar-2014].

[7] B. M. Ganesh, A. M. Isloor, and a. F. Ismail, "Enhanced hydrophilicity and salt rejection study of graphene oxide-polysulfone mixed matrix membrane," *Desalination*, vol. 313, pp. 199–207, Mar. 2013.

[8] X. Wei, Z. Wang, J. Wang, and S. Wang, "A novel method of surface modification to polysulfone ultrafiltration membrane by preadsorption of citric acid or sodium bisulfite," *Membr. water Treat.*, vol. 3, no. 1, pp. 35–49, 2012.

[9] A. Benjjar, T. Eljaddi, O. Kamal, K. Touaj, L. Lebrun, and M. Hlaibi, "The development of new supported liquid membranes (SLMs) with agents: Methyl cholate and resorcinarene as carriers for the removal of dichromate ions (Cr2O7 2-)," *J. Environ. Chem. Eng.*, vol. 2, no. 1, pp. 503–509, Mar. 2014.

[10] T. Eljaddi, O. Kamal, A. Benjjar, M. Riri, M. E. Elatmani, L. Lebrun, and M. Hlaibi, "New supported liquid membranes containing TBP and MC as carriers for the facilitated transport of cadmium ions from acidic mediums : Parameters and mechanism," *J. Mater. Environ. Sci.*, vol. 5, no. 6, pp. 1994–1999, 2014.

[11] T. Eljaddi, A. Benjjar, O. Kamal, M. Riri, L. Lebrun, and M. Hlaibi, "Recovering copper ions from industrial environments by supported liquid membranes : parameters and mechanism," *Moroccan J. Chem.*, vol. 1, pp. 1–7, 2015.

[12] S. Rouaix, C. Causserand, and P. Aimar, "Experimental study of the effects of hypochlorite on polysulfone membrane properties," *J. Memb. Sci.*, vol. 277, no. 1–2, pp. 137–147, Jun. 2006.

[13] G. Arslan, A. Tor, H. Muslu, M. Ozmen, I. Akin, Y. Cengeloglu, and M. Ersoz, "Facilitated transport of Cr(VI) through a novel activated composite membrane containing Cyanex 923 as a carrier," *J. Memb. Sci.*, vol. 337, no. 1–2, pp. 224–231, Jul. 2009.

African Membrane Society
Water & Environment, Process, Energy
Sfax, Tunisia, May 3-5, 2016 - Membrane Water Treatment in Small Urban and Village Centers

Osmosun, un Système de Dessalement Solaire Photovoltaïque Autonome, au Fil du Soleil Sans Batterie de Stockage Electrique

Pierre HAMON, Maxime HAUDEBOURG et Marc VERGNET

MASCARA NT, Espace Atlantic LOT 21, 20 rue Gustave Eiffel, 28630 Gellainville, France.
m.vergnet@mascara-nt.fr

Résumé : Le dessalement par osmose inverse apparait comme une solution pour satisfaire les besoins croissants en eau d'une population mondiale qui sera sous stress hydrique pour 3,9 milliards de personnes en 2030 (source : OCDE). Les technologies actuelles sont fortement consommatrices de combustibles fossiles et ne sont pas adaptées aux besoins inférieurs à 1000m3/jour ni aux réalités économiques, techniques et organisationnelles des petites collectivités. La Société MASCARA NT a développé une technologie nouvelle, OSMOSUN, de dessalement solaire autonome, sans stockage électrique avec de très faibles consommations énergétiques (2,5 KWh/m3 d'eau dessalée), des couts de production de l'ordre de 1€ /m3. Robustes, automatiques et en télé-suivi/télémaintenance, ces équipements ont été conçus pour une gestion à la portée des petites collectivités. Un démonstrateur a été installé sur la plateforme d'expérimentation des technologies avancées de dessalement de Ghantoot en partenariat avec MASDAR à Abu Dhabi.

Mots Clés énergie renouvelables, Energie solaire, dessalement, osmose inverse, système autonome.

I. INTRODUCTION

Le dessalement par osmose inverse apparait comme une solution pour la satisfaction des besoins croissants en eau d'une population mondiale qui sera sous stress hydrique pour 3,9 milliards de personnes en 2030, [1]. Le dessalement annuel de 21 milliards de m^3 d'eau génère aujourd'hui un rejet de 80 millions de tonnes de CO_2 et 240 millions de tonnes en 2040 si rien n'est fait d'ici là. Un tel risque a conduit à la signature, pendant la COP 21, le 5 décembre 2015, de l'Initiative Climat Dessalement « **Global Clean Water Desalination Alliance H_2O minus CO_2** » qui fixe des objectifs ambitieux d'utilisation des Energies Renouvelables pour les nouvelles installations de dessalement réalisées dans le monde (20% en 2020 croissants jusqu'à 80% à partir de 2035) et engage de nombreux programmes d'amélioration des process de dessalement et de réduction des consommations énergétiques [2].

Par ailleurs, il n'existait pas d'équipements de dessalement de faibles capacités (inférieures à 1000 m^3/jour) adaptés aux contextes économiques, techniques, logistiques des petites collectivités. Dans les équipements conventionnels diesels, les coûts élevés de production de l'eau potable avec des approvisionnements récurrents en combustible et la difficulté à assurer l'exploitation et surtout la maintenance des équipements conduisaient souvent à l'abandon des unités de dessalement.

L'usage de l'énergie solaire photovoltaïque dont les coûts ont été réduits d'un facteur 3 en 6 ans pour atteindre aujourd'hui 8 à 10 cents d'€/KWh avec des garanties de production de plus de 20 ans permet une réduction importante des coûts de production d'eau dessalée.

Pour la première fois au monde, la Société MASCARA NT a développé des équipements industriels de dessalement d'eau de mer, OSMOSUN, fonctionnant de façon autonome, à l'énergie solaire, sans stockage électrique et avec zéro émission de CO_2.

Les très faibles consommations spécifiques (2,5 KWh/m^3) et l'usage de l'énergie solaire conduisent à des coûts de production de l'ordre de 1 € /m^3. La conception robuste, le fonctionnement automatique directement piloté par l'énergie solaire, l'absence de coûts récurrents élevés et la facilité d'exploitation maintenance sont parfaitement adaptés à une gestion par de petites collectivités. La société MASCARA NT est une entreprise nouvellement créée par Marc VERGNET, fondateur du groupe VERGNET (hydraulique villageoise : 55 millions de personnes alimentées par l'hydropompe VERGNET en Afrique, ENR : 700 éoliennes anticycloniques installées dans le monde et plusieurs centaines d'équipements solaires photovoltaïques)

II. ETAT DE L'ART DU DESSALEMENT SOLAIRE

L'utilisation de batteries a toujours été mise en œuvre pour permettre un fonctionnement continu des installations 24/24. A notre connaissance, pour des systèmes produisant plusieurs dizaines de m^3 par jour, un osmoseur alimenté par des panneaux solaires photovoltaïques associés à des batteries de stockage de l'énergie semble être la seule technologie ayant dépassé le stade de R&D (Tableau 1).

Beaucoup de petits systèmes de dessalement photovoltaïque ont été implantés dans le monde spécialement dans les zones isolées et les iles. Il ressort

que :

- Les projets de dessalement au fil du soleil n'ont concerné que de faibles capacités de production et sont souvent limités au dessalement d'eaux saumâtres.
- Les projets plus significatifs en termes de capacité incluent un stockage de l'énergie sur batteries et présentent des coûts de production de l'ordre de 6 à 8 US$/m^3 d'eau produite (voire 40 US$/m^3 d'eau produite (voir Vanuatu) compte tenu d'un surcoût de 1,1€ du kWh stocké [4].

Table 1. Comparative costs for common renewable desalination, [3]

	Technical Capacity	Energy Demand (kWh/m³)	Water Cost (USD/m³)	Development Stage
Solar stills	< 0.1 m³/d	Solar passive	1.3–6.5	Application
Solar-Multiple Effect Humidification	1–100 m³/d	thermal: 100 electrical: 1.5	2.6–6.5	R&D Application
Solar- Membrane Distillation	0.15–10 m³/d	thermal: 150–200	10.4–19.5	R&D
Solar/CSP-Multiple Effect Distillation	> 5,000 m³/d	thermal: 60–70 electrical: 1.5–2	2.3–2.9 (possible cost)	R&D
Photovoltaic-Reverse Osmosis	< 100 m³/d	electrical: BW: 0.5–1.5 SW: 4-5	BW: 6.5–9.1 SW: 11.7–15.6	R&D Application
Photovoltaic-Electrodialysis Reversed	< 100 m³/d	electrical: only BW:3–4	BW:10.4–11.7	R&D
Wind- Reverse Osmosis	50–2,000 m³/d	electrical: BW: 0.5–1.5 SW: 4–5	Units under 100 m³/d, BW:3.9–6.5 SW:6.5–9.1 About 1,000 m³/d, 2–5.2	R&D Application
Wind- Mechanical Vapor Compression	< 100 m³/d	electrical: only SW:11–14	5.2–7.8	Basic Research
Wind-Electrodialysis	–	–	BW: 2.0–3.5	–
Geothermal-Multi Effect Distillation	–	–	SW: 3.8–5.7	–

De nombreux travaux de R&D ont été menés sur le développement d'unités flexibles compatibles avec un fonctionnement au fil du soleil, sans batterie (en vert sur la Figure 1), cependant « aucun projet ayant dépassé le stade de la R&D n'a mis en œuvre de systèmes au fil du soleil, c'est-à-dire sans batterie de stockage » [5]. Ainsi, il n'existe pas aujourd'hui sur le marché d'équipements industriels de dessalement fonctionnant au fil du soleil, c'est-à-dire sans batterie.

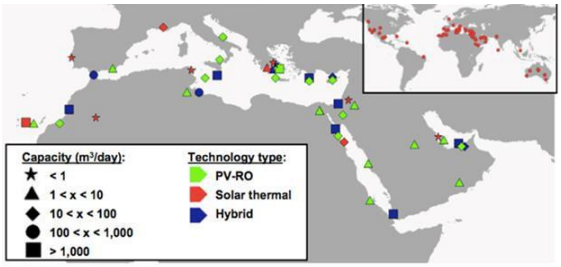

Figure 1. Solar-driven RO desalination systems: geographical distribution and type in Mediterranean and MENA countries, and worldwide.

III PRESENTATION DE LA TECHNO- LOGIE OSMOSUN ET COLLABORATION AVEC MASDAR

Pour la première fois au monde, MASCARA NT a développé et breveté **une unité d'osmose inverse totalement flexible et adaptée aux variations de la puissance solaire d'un générateur photovoltaïque (Figure 2)**. Cet équipement permet la production automatique d'eau en fonction de l'énergie solaire disponible, tout en optimisant et contrôlant les paramètres de longévité des membranes (variation de pression et de débit) avec le soutien de l'IEM, les consommations énergétiques les plus basses au monde : 2.5 kWh/m^3 d'eau potable à partir d'eau de mer à 35 g et la salinité des perméats.

Figure 2. Autonomous PV solar desalination unit developed by MASCARA NT

Dans le cadre d'un **Programme de Collaboration Avec Masdar** (Abu Dhabi), un démonstrateur OSMOSUN est en cours d'installation sur la plateforme des technologies avancées de dessalement de Ghantoot aux côtés des quatre pilotes des plus grands industriels du dessalement (SUEZ, VEOLIA, ABENGOA et TREVI System) (Figure 3). **OSMOSUN** devient ainsi la première technologie entièrement solaire mise en œuvre industriellement.

Figure 3. MASCARA NT demonstrator set-up on the experimentation platform of advanced technologies in Ghantoot in partnership with MASDAR in Abu Dhabi.

IV. LES AVANTAGES DECISIFS DE LA TECHNOLOGIE OSMOSUN

4.1 Un système respectueux de l'environnement

Ce système évite toute émission de CO2 grâce à l'alimentation solaire ou énergie renouvelable. Les taux de salinité des concentras rejetés en mer sont faibles (40 à 45 g/l contre 80 à 90 g/l dans les unités conventionnelles.

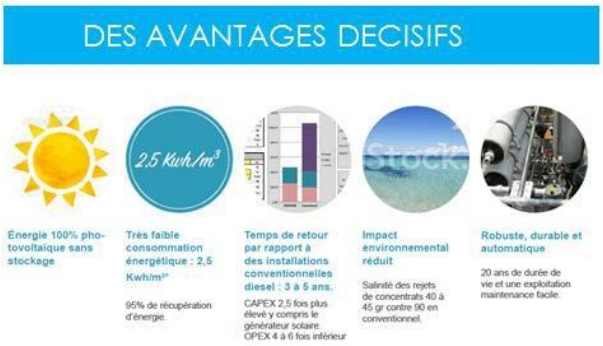

Figure 4. Advantages of the OSMOSUN technology.

4.2 Un système compétitif

Malgré un coût d'investissement deux fois supérieur (y compris le générateur solaire photovoltaïque) pour OSMOSUN par rapport à des unités conventionnelles consommatrices de pétrole, les coûts de production d'eau potable sont deux fois moins élevés (1,2 à 1,5 €/m^3) avec des temps de retour sur investissement de l'ordre de 3 à 5 ans (Figure 5).

Cette très forte compétitivité est liée aux faibles consommations spécifiques d'OSMOSUN et aux très bas coûts actuels du solaire photovoltaïque (8 à 12 cents d'€/kWh).

V. OSMOSUN, UN SYSTEME ADAPTE A L'ALIMENTATION DES COLLECTIVITES ISOLEES

Les équipements OSMOSUN ont été conçus pour être :
- Robustes
-Automatiques
- Faciles d'exploitation et maintenance
-Télésuivis et télémaintenus

à l'image des 110 000 équipements de pompage installés par Marc VERGNET en Afrique. Avec une gamme de 40 m^3 à 300 m^3/jour en 2016 et 1 000 m^3/jour en 2017, MASCARA pourra alimenter des collectivités de plusieurs milliers de personnes en eau potable et permettre des irrigations maraichères ou ferreuses.

VI. CONCLUSION

MASCARA s'est spécialisé dans les traitements membranaires solaires de l'eau pour des petites communautés ou des sites isolés. La réussite du programme OSMOSUN permet d'envisager le développement de nouveaux produits tels que :

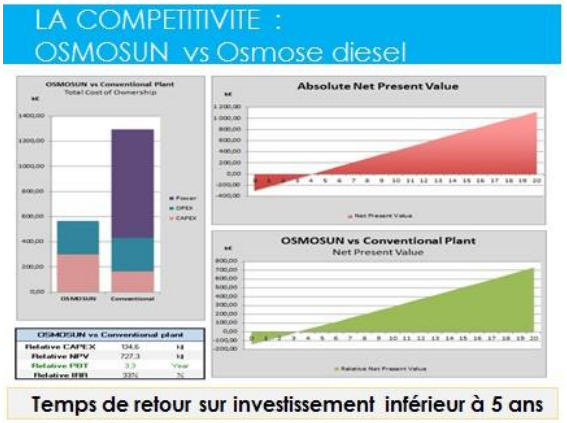

Figure 5. Comparison of return on investment between the OSMOSUN technology vs conventional RO plant.

- le dessalement solaire d'eaux saumâtres (nanofiltration ou osmose inverse) en relation avec l'Institut Européen des Membranes (IEM)les traitements solaires des eaux fluorées, arsenicales

Par ailleurs, en relation avec POLYMEM, un système d'ultrafiltration solaire fait également l'objet d'un programme de recherche développement.

REMERCIEMENTS

Les auteurs remercient la région Centre-Val de Loire pour son support financier (Projet CAP CREATION N ° 00096998 – 2014).

REFERENCES

[1] «Managing water for all» OCDE 2009.
[2] «Global Clean Water Alliance – H2O minus CO2» launches in Paris during COP21 www.wam.ae/en/news/economics/ 1395288855730.html
[3] «Water desalination using renewable energy», Technology Brief IEA-ETSAP and IRENA , Brief 112, March 2012
[4] V. Jülch, N. S. Hussein, J. Koschikowski, J. Skeer, « Technology options for renewable desalination on Islands» http://irena.org/martinique/sessionT3.aspx
[5] «Water desalination using renewable energy», Technology Brief IEA-ETSAP and IRENA, Brief 112, March 2012)

African Membrane Society
Water & Environment, Process, Energy
Sfax, Tunisia, May 3-5, 2016 - Membrane Water Treatment in Small Urban and Village Centers

Preparation of Asymmetric Carbon Nanofiltration Membrane for the Treatment of Indusrial Textile Effluent

Nouha TAHRI and Raja BENAMAR

Laboratoire Sciences des Matériaux et Environnement, Faculté des Sciences de Sfax, Route de Soukra Km 4,3000 Sfax, Tunisie.
tahri.nouha@yahoo.fr

Abstract : An asymmetric nanofiltration carbon membrane has been prepared by carbonizing a phenolic resin using as polymer precursor and source of carbon. The membrane was composed of a mesoporous interlayer with an average pore size of 0.6µm deposited by slip casting process on the inner face of a macroporous support. The nanofiltration top layer was deposited by vacuum slip casting process using an alcoholic solution of phenolic resin during 60 s. A crack-free membrane with a thickness layer of 1.36 µm, an average pore size of 1.1 nm and a molecular cut-off of 400Da was obtained in one step. The application of the carbon NF membrane to the treatment of industrial textile wastewater shows good performances in term of permeate flux and removal of pollutants efficiency. It was found that the treated wastewater could be recycled into the textile industry processes or can be discharged into the municipal sewerage in compliance with Tunisian legislations.

Keywords: Carbon membrane, Nanofiltration, Phenolic resin, Treatment, Textile wastewater.

I. INTRODUCTION

Nanofiltration (NF) is a pressure driven separation process intermediate between reverse osmosis (RO) and ultrafiltration (UF), which rejects molecules having the size in the order of one nanometer [1–3]. NF membranes are potent in the separation of inorganic salts and small organic molecules with lower osmotic pressure difference, higher permeate flux compared to RO, relatively low investment and low operation and maintenance costs. These properties have allowed NF to be used in various applications in many areas especially for water and wastewater treatment, pharmaceutical, biotechnology, and food engineering [4-7].

Pure inorganic NF membranes have the advantages of polymeric membranes in addition to a high chemical, thermal and mechanical resistances, easy regeneration and long service life [8]. However, ceramic membranes are difficult to fabricate and may have many defects in the microstructure which require several additional steps to correct or compensate these defects. To overcame these problems and improve the performances of NF membranes, numerous studies have been focused on the production of organic-inorganic composite membranes that combine characteristics of polymers and ceramics [9-11]. The polymer/ceramic composite membranes are potentially the most suitable for nanofiltration, gas separation and membrane distillation. The preparation of the NF composite membrane consists of carbonizing a polymeric precursor deposited on a porous supported membrane. In this regard, considerable efforts have been made in terms of developing precursors with low cost and high carbon yield, a good choice of the supported membrane and the preparation process, in order to reduce the cost of production and obtain final material having a good structure [12]. Several parameters can affect the microstructure of the active layer, but the nature of the polymer precursor remains the crucial parameter that affects the final structure of carbon NF membranes [12, 13]. It was found by many researchers that the phenolic resin was the excellent carbonaceous material using for the preparation of microporous and nanoporous carbon layers due to its considerable fixed-carbon yield, high inherent purity and low cost.

Carbon membranes have been mainly used for gas separation but there lies a large potential for these membranes to be used for aqueous applications due to their high temperature and chemical resistance but only a few works have been interested in this application [13–14].The purpose of this paper is to demonstrate the effectiveness of the composite carbon NF membranes for the treatment and recycling of industrial textile effluent.

II. EXPERIMENTAL

2.1 Material

Mineral coal was used as the main carbon material source for preparing carbon membrane. This powder presents high carbon content, low ash content and moderated volatile components. According to previous

studies [15-16], it was found that the average pore size of carbon membrane decreases with decreasing coal particles size and then average particle sizes of 100µm and 1.8µm were selected for the preparation of the support and the microfiltration (MF) layer respectively. The second source of carbon was Novolac® phenolic resin (NPR) marketed by the company Irons Resins S.A, Spain (Sumitomo Bakelite co). High carbon yield and low price are the most important benefits of NPR precursors. The NPR was used for the preparation of NF top layer.

2.2 Membrane preparation

The membrane preparation involved two main steps: the production of high-quality macroporous support on which active layer was deposited. To achieve this, firstly, a macroporous carbon tube (OD/ID = 10mm/8mm) having a pore volume of 38% and a mean pore diameter of 9µm was prepared by extrusion-carbonization process. For this, an extruded paste was prepared from a mixture of mineral coal powder, organic additives and an alcoholic solution of NPR. The different percentages were determined in a previous work [16]. Secondly, an intermediate MF layer was then deposited by slip casting process to sustain the final layer and to avoid the infiltration of NF suspension inside the large pores of the tube. For this, a suspension made from carbon powder (1.8µm average particles size) and an alcoholic solution of NPR (Resin/Ethanol = 515/85° wt percentage) was slip-casted on the inner face of the support for 6 min at room temperature. MF layer with an average pore diameter of 0.6µm and a thickness of 22µm were obtained a curing-carbonization cycle at 700°C under a nitrogen stream of 1mL/min (Figure 1).

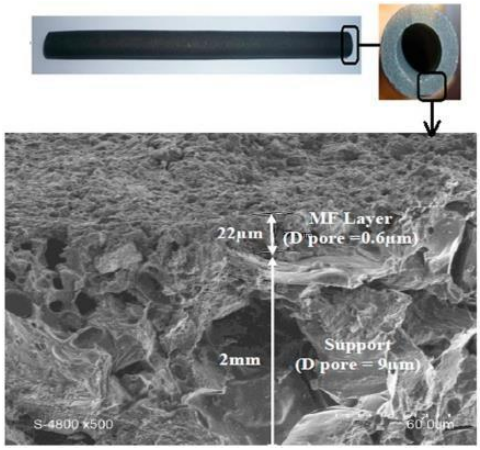

Figure 1. Picture and SEM micrograph of the tubular carbon microfiltration membrane

The carbon Nano filtration top layer was prepared using an alcoholic solution of NPR. The viscosity of the solution was adjusted to around 39 cp. The resin suspension was deposited in the inner face of the supported membrane by means of the vacuum slip casting (VSC) technique under the pressure difference of 0.05-0.07 MPa for 60 s. The prepared NF layer was carbonized at 650 °C for 2 hours under nitrogen atmosphere.

2.3. Permeation properties and pores size determination

Cross-flow filtration experiments were carried out with single channel tubular NF membrane having an active surface area of 13.6 cm. Before each run, the membrane was conditioned in ultrapure water (resistivity 18 M Ω cm) for 24 h to stabilize the permeate flux. Permeability was then obtained according to the Darcy's law:

$$J_w = TMP / \mu R_m \qquad (1)$$

Where R_m is membrane resistance, µ is water viscosity and TMP is operating transmembrane pressure.

The molecular weight cut-off (MWCO) was determined using 1 g/L aqueous solution of various polyethylene glycol (PEG) molecules with molecular weight ranging from 2 to 300 kDa. The system was thoroughly rinsed with pure water between runs to check that membranes were not fouled during the cut-off determination. The retention rate (R) was determined using the following classical relation:

$$R(\%) = 100\left[1-\left(C_p - C_f\right)\right] \qquad (2)$$

where C_p and C_f are the permeate and the feed concentration solution, respectively.

Pore size distribution of the top layer was obtained from nitrogen adsorption/desorption isotherm using a Micrometrics Asap 2010. Pore diameter was estimated by BJH (Barret–Joyner–Halenda) method.

III. RESULTS AND DISCUSSIONS

3.1 Characterization of the carbon NF membrane

Surface and cross-section morphologies of the obtained NF membrane were characterized by SEM. Results show a typical asymmetric structure composed of a macroporous support, an intermediate layer and a thin top layer almost dense (Figure 2). The used casting suspension with low viscosity flow easily into the pores of the intermediate layer and during a casting time of 1 min a good adhesion between NF layer and the supported membrane can be well observed.

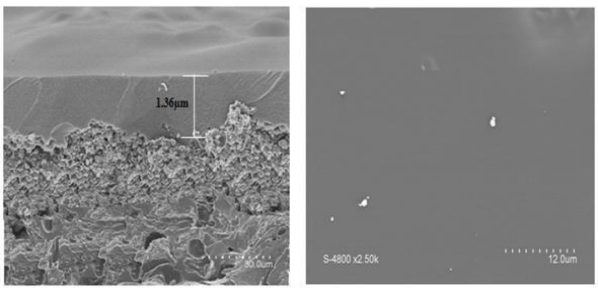

Figure 2. Micrographs of the section and the surface of the carbon NF membrane

The determination of UF pores size was done using adsorption/desorption isotherm of N_2 at 77 K.

Results show that the composite NF membranes exhibit a type I adsorption isotherm according to IUPAC, which is associated with microporous structure. The adsorption equilibrium was established at a very low relative pressure. The slight gain in uptake at the end (p/p0 ~ 1) can be attributed to the presence of mesopores or macropores (Figure 3).

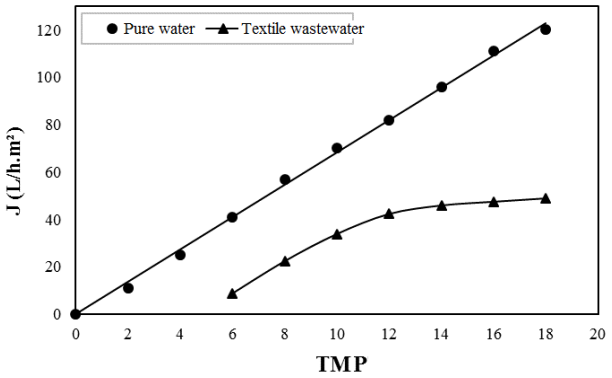

Figure 3. Nitrogen adsorption/desorption isotherm of the carbon NF membrane

Table 1 illustrates the main characteristic of the obtained composite NF membrane.

Table 1. Characteristics of the elaborated NF membrane

	NF membrane
Thickness (µm)	1.36
MWCO (Da)	400
Average pores size (nm)	1.1
Permeability (L/h.m².bar)	7.6

3.2 Application of the NF membrane to the treatment of real textile effluent

3.2.1 Wastewater characterization

The study was conducted with a real textile wastewater effluent supplied from a Tunisian textile factory that utilizes different dyes (reactive and direct) and chemical substances such as detergents, salts, auxiliaries (e.g. surfactants, emulsifiers) and caustic soda. Their amounts depend on the kind of process that generates different effluents (Table 2).

Table 2. Main characteristics of real textile effluent

Parameters	NF membrane
Turbidity (NTU)	1300
Salinity (g/L)	14.7
DCO (mg/L)	2100
Cl^- (mg/L)	1580
Color	47

3.2.2 Effect of temperature

The temperature used in this study was based on other works [17-18]. It was found that the effluent's quality and viscosity did not change with the temperature range of 25-50°C. Generally, the permeate flux increases slightly with temperature in the case of textile wastewater [17]. Such behavior is usually explained by the variation in the viscosity of the effluent. In the temperature range of 24-50°C, the viscosity of the treated effluent varied in the range 0.98-0.62 mPa s. These values are approximately the same as the one for pure water (0.91-0.55 mPa s) [17,19]. For these reasons, all the experiments were performed at ~~roo~~m around 30°C to minimize the energetic costs.

3.2.2 Effect of pressure

The evolution of the permeate flux with time at TMP varying from 6 to 18 bar and a temperature of 30 °C was illustrated in Figure 4. As can be seen there is a linear relationship between flux and TMP in the pressure range of 6-10 bar. Up to 10 bar, a deviation from the straight line was observed and then at high pressure values, the permeate flux becomes constant. This behavior was attributed to the establishment of polarization concentration phenomena due to the accumulation of the retained substances on the membrane surface resulting in an increase in the resistance to mass transport.

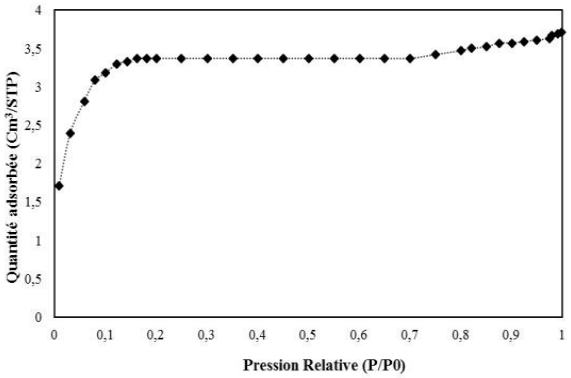

Figure 4. Evolution of filtration flux of pure water and textile wastewater with TMP.

The characterization of the NF permeates shows a total retention of turbidity and color over different TMP ~~v~~alues, while the dissolved organic and inorganic substances' retention increase until 12 bars. Beyond 12 bars, the retention of different parameters varies very little. Retention rates in terms of COD, salinity and chloride are then approximately 82%, 57% and 33% respectively (Figure 5). So, 12 bar can be considered as the optimal TMP value.

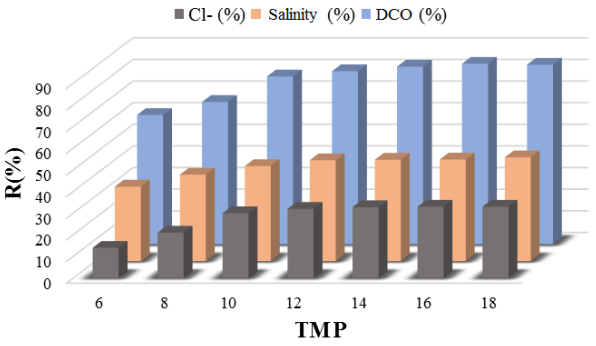

Figure 5. Evolution of the retention of different parameters with TMP

3.2.3 Effect of salinity: Critical flux concept

The composition of textile effluents, especially dye baths generally varies from one cycle to the next depending on the amount of articles to be treated and also to the used dye and additives. The application of the dyes depends on the grade and quality of fabric and requires varying amounts of fixing agents in terms of NaCl. To study the effect of salt on the performance of the carbon NF membrane, was modified the salinity of the treated effluent from the 7 g/L to 24 g/L. The concept of critical flux was adopted in this case to explain the fouling phenomena. It consists of varying the pressure of an ascending then descending, steady flux to be achieved before proceeding to the next pressure (Figure 6). The evolution of the critical flux as well as the retention of different parameters, depending on the NaCl content, is represented by the figure 7. The increase of salinity in the feed concentration of textile wastewater up to 13 g/L may cause a decrease of critical flux from 45 L/h m² at 7 g/L to 33 L/h m² at 13 g/L. Beyond this value the flux increases again and stabilizes at 41 L/h.m² for a salinity of 16 g/L. Moreover, the fouling seems to become irreversible between 8-10 bars for all concentrations of NaCl.

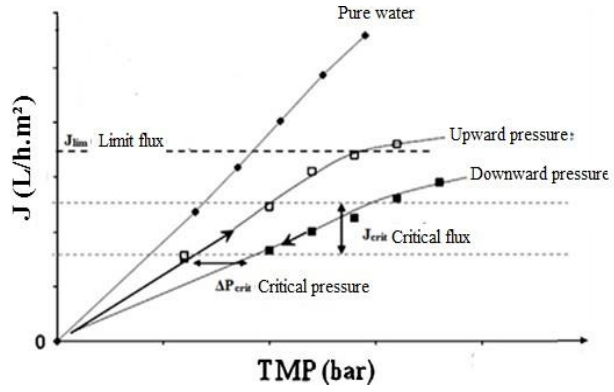

Figure 6. Permeate flux as a function of TMP in a filtration where pressure was alternately increased and decreased.

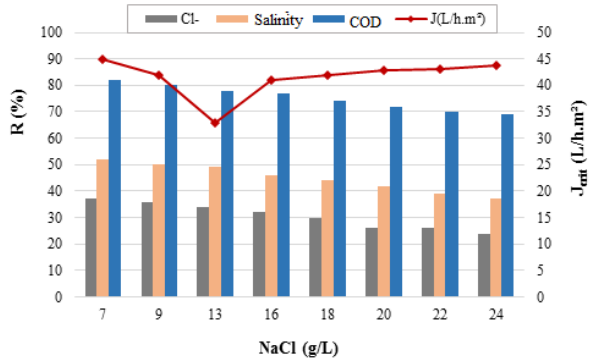

Figure 7: Evolution of critical flux and permeate performance with the salt content.

The evolution of the permeate characteristics with effluent salinity is illustrated. The retention of COD, salinity and Cl increases when the concentration of NaCl decreases. Similar results were obtained by Allègre et al. [17], who explain this behavior by the electrostatic interactions between effluent and membrane. As the NaCl is increases, electrostatic repulsions at the membrane wall are weak and the salts easily pass through the membrane. In contrast, a decrease in salt concentration induces an increase in the retention. When the concentration of NaCl is low, strong electrostatic repulsions occur near the membrane and hence salts are retained. It can therefore be seen that it is easy to eliminate the salts when their concentration in the solution is high, but this is appreciably more difficult when the concentration is higher than 13 g/L.

3.2.4 Characterization of treated wastewater

The treatment of textile wastewater using the elaborated carbon NF membrane under optimal conditions lead to a permeate with better quality than that of drilling water used in washing processes particularly in terms of chloride content. A total retention of color and turbidity were obtained. Table 3 shows the characteristics of the NF treated textile effluent after treatment at a temperature of 30°C and a pressure of 12bars. The treated wastewater can be reused as a refrigerating water, washing water and can be discharged into the municipal sewerage in compliance Tunisian legislations.

Table 3. Main characteristics of NF treated wastewater

Parameters	R (%)
Turbidity (NTU)	99
Salinity (g/L)	47
DCO (mg/L)	80
Cl^- (mg/L)	32
Color	98

IV. CONCLUSION

In the present study, microporous membranes for nanofiltration have been successfully prepared using the phenolic resin as precursor and source of carbon. The NF top layer has been deposited on the inner face of carbon MF membrane used as a supported membrane. Nanofiltration process was proposed for the treatment of industrial textile effluent coming from a Tunisian factory. Based on permeate flux performances and pollutant retention, the best operating conditions of NF were: 12 bar for TMP and 30 °C for operating temperature. Hence, considering these results, Nanofiltration could be used to preserve the environment since the treated water could be recycled into the textile industry processes as a refrigerating water, for washing water and can be discharged into the municipal sewerage in compliance with Tunisian legislations.

REFERENCES

[1] B.V. Der Bruggen, M. Mänttäri, M. Nyström, "Drawbacks of applying nanofiltration and how to avoid them: a review", *Sep. Purif. Technol.* Vol. 63, pp.251–263, 2008.

[2] T.V. Gestel, C. Vandecasteelea, A. Buekenhoudt, C. Dotremont, J. Luyten, R. Leysen, B.V. Der Bruggen, G. Maes, "Salt retention in nanofiltration with multilayer ceramic TiO2 membranes", *J. Membr. Sci.* vol. 209, pp. 379–389.

[3] S. Alami-Younssi, A. Larbot, M. Persin, J. Sarrazin, L. Cot, "Rejection of mineral salts on a gamma alumina nanofiltration membrane: application to environmental process", *J. Membr. Sci.* vol. 102, pp.123–129,1995.

[4] A. Bes-Pia, M.I. Iborra-Clar, A. Iborra-Clar, J.A. Mendoza-Roca, B. Cuartas-Uribe, M.I. Alcaina-Miranda, "Nanofiltration of textile industry wasterwater using physicochemical process as pre-treatment", *Desalination.* Vol. 178, pp.343-349, 2005.

[5] A. H. Hassani, R. Mirzayee, S. Nasseri, M. Borghei, M. Gholami, B. Torabifar, "Nanofiltration process on dye removal from simulated textile wastewater", *Int. J. Environ. Sci. Technl*. Vol. 5, pp. 401-408, 2008.

[6] L. Shao, X.Q. Cheng, Y. Liu, S. Quan, J. Ma, S.Z. Zhao, K.Y. Wang, "Newly developed nanofiltration (NF) composite membranes by interfacial polymerization for safranin O and aniline blue removal", *J. Membr. Sci*. vol. 430, 2013, pp.96–105.

[7] G. Baumgarten, D. Jakobs, H. Muller, "Treatment of AOX-containing waste- water partial flows from pharmaceutical production processes with nanofiltration and reverse osmosis", *Chem. Ing. Tech*. vol. 6, pp.321–325, 2004.

[8] Z. Chen, F. Chen, F. Zeng, J. Li, "Preparation and characterization of the charged PDMC/Al2O3 composite nanofiltration membrane", *Desalination*, Vol. 349, pp.106–114, 2014.

[9] C.M. Wu, T.W. Xu, W.H. Yang, Fundamental studies of a new hybrid (inorganic– organic) positively charged membrane: membrane preparation and characterizations, *J. Membr. Sci*. vol.216, pp.269–278, 2003.

[10] C.M. Wu, T.W. Xu, M. Gong, W.H. Yang, "Synthesis and characterizations of new negatively charged organic–inorganic hybrid materials. Part II.Membrane preparation and characterizations", *J. Membr. Sci*. vol. 247, pp.111–118, 2005.

[11] S.K. Nataraj, S. Roy, M.B. Patil, M.N. Nadagouda, W.E. Rudzinski, T.M. Aminabhavi, "Cellulose acetate-coated α-alumina ceramic composite tubular membranes for wastewater treatment", *Desalination.* Vol. 281, pp.348–353, 2011.

[12] B. Zhang, Y. Wu, Y. Lu, T. Wang, X. Jian, J. Qiu, "Preparation and characterization of carbon and carbon/zeolite membranes from ODPA–ODA type polyetherimide", *J. Membr. Sci*. vol. 474, pp.114–121, 2015.

[13] H.B. Park,Y.K. Kim, J.M. Lee, S.Y. Lee, Y.M. Lee, "Relationship between chemical structure of aromatic polyimides and gas permeation properties of their carbon molecular sieve membranes", *J. Membr. Sci.* vol. 229, pp.117–127, 2004.

[14] A.F. Ismail, "Basic aspects of polymeric and inorganic membrane preparation, in: E Drioli, L, Giorno (Eds.), Comprehensive *Membr. Sci. Eng*, *Elsevier, Japan*, pp.275–290, 2010.

[15] C. Song, T. Wang, Y. Pan, J. Qiu, "Preparation of coal based microfiltration carbon membrane and application in oily wastewater treatment", Sep. Purif. Technol. Vol. 51, pp.80–84, 2006.

[16] N. Tahri, I. Jedidi, S. Cerneaux, M. Cretin, R. Ben Amar, "Development of an asymmetric carbon microfiltration membrane: Application to the treatment of industrial textile wastewater", Sep. Purif. Technol. Vol. 118, pp.179–187, 2013.

[17] C. Allégre, P. Moulin, M. Maisseu, F. Charbit, Treatment and reuse of reactive dyeing effluents. J.Membr. Sci. vol. 269, pp.15-34, 2006.

[18] B. Van der Bruggen, B. Daems, D. Wilms, C. Vandecasteele, "Mechanisms of retention and flux decline for the nanofiltration of dye baths from the textile industry", Sep. Purif. Technol. Vol. 22, pp.519-528, 2001.

[19] E. Ellouze, S. Souissi, A. Jrad, R. Ben Amar, A. Ben Salah, "Performances of nanofiltration and reverse osmosis in textile industry wastewater treatment", Desalination. Vol. 22, pp.1-5, 2001.

African Membrane Society
Water * Environment, Process, Energy
Sfax, Tunisia, May 3-5, 2016 - Membrane Water Treatment in Small Urban and Village Centers

Le Bore comme Elément Problématique dans le Domaine du Dessalement

Jamel KHERIJI, Bachir HAMROUNI

Unité de recherche: Dessalement et traitement des eaux, Faculté des Sciences de Tunis, 2092 Université El Manar II, Tunisie
jamel.khriji@gmail.com

Résumé: Un apport d'eau de bonne qualité et en quantité suffisante est essentiel pour la santé. Un grand nombre des maladies liées à l'eau sont à mettre sur le compte de sa qualité, caractérisée par la présence de certaines substances chimiques comme le bore qui a été classé par l'Union Européenne et l'Organisation Mondiale de la Santé comme un polluant de l'eau potable. L'osmose inverse (OI) et la nanofiltration (NF) sont largement utilisés pour le dessalement des eaux. Le développement rapide dans ce domaine au cours des dernières décennies impose l'importance de l'élimination du bore. Bien que ces membranes d'OI et de NF offrent une efficacité exceptionnelle pour réduire la quantité des sels dans l'eau, l'efficacité à l'élimination du bore par les membranes commerciales disponibles reste relativement faible. Pour résoudre ce problème, on a proposé dans le cadre de ce travail d'optimiser l'élimination du bore par ces deux procédés.

Mots clés: Dessalement des eaux, Osmose inverse et Nanofiltration, Bore.

I. INTRODUCTION

L'eau est l'origine de la vie et de la civilisation. C'est une ressource indispensable non seulement pour le maintien de la vie et de la santé humaine mais aussi pour la préservation de l'écosystème et de toutes les activités économiques. Depuis quelques années, on entend de plus en plus parler de l'eau comme étant le grand enjeu du siècle, en raison de la croissance démographique, le changement de mode de vie, la pollution, l'utilisation inefficace de l'eau et les changements climatiques. Aujourd'hui, l'eau est devenue encore plus importante qu'elle ne l'était dans le passé en raison de l'urbanisation et de la croissance démographique rapide. Plus de 1.1 milliard de personnes, soit 18% de la population mondiale, n'ont pas accès à l'eau potable [1]. Environ 2.5 milliards de personnes, soit 42% de la population totale, n'ont pas des services d'assainissement de base [1]. Chaque semaine, on estime qu'environ 42000 personnes décèdent de maladies liées à la mauvaise qualité de l'eau potable et aux manques de services d'assainissement [2]. Plus de 90% de ces décès touchent des enfants de moins de 5 ans [2]. Pour être consommée sans danger, l'eau doit être traitée. La pollution croissante des réserves en eau rend cette opération plus délicate. A cet égard, la protection de l'environnement est très importante vu la présence de divers polluants dans l'eau comme le bore. Ce dernier présente des effets néfastes pour l'être humain et l'écosystème. Il a été classé par l'Union Européenne UE comme un polluant.

Sa concentration limite Recommandée par cette organisation est de 1 mg/L, [3]. De plus, l'organisation mondiale de la santé (OMS) a fixé une concentration maximale acceptable de 2.4 mg/L, [4]. Plusieurs techniques ont été employées pour l'élimination du bore. Parmi ces techniques, on peut citer les procédés membranaires particulièrement l'osmose inverse (OI) et nanofiltration (NF). Ces procédés ont pris leur essor dans les années 70 en particulier, grâce au développement des matériaux et des techniques de fabrication des membranes [5]. Plusieurs caractéristiques rendent ces techniques plus efficaces et plus économiques en termes de consommation d'énergie.

Les procédés de filtration par OI et NF semblent à être les procédés les plus efficaces en ce qui concerne le domaine de dessalement des eaux. Cette efficacité parait limitée dans l'élimination du bore. De ce fait, le but de cette étude est d'optimiser l'élimination du bore par ces deux techniques.

II. MATERIELS ET TECHNIQUES ANALYTIQUES

2.1 Dispositif expérimental utilisé

Le dispositif expérimental utilisé dans ce travail est un pilote conçu et réalisé au sein de notre laboratoire pour le traitement des eaux saumâtres. Ce pilote est désigné de telles façons qu'on peut modifier les paramètres opératoires tels que la température, le taux de conversion et la pression.Il comporte deux modules de filtration, un module d'OI (BW-30) et l'autre du NF (NF-90). Le reste d'équipement comprend un bac d'alimentation, une pompe à haute pression, un filtre à cartouche, des vannes, deux débitmètres et des capteurs de pression. Les différents éléments de l'installation sont montés sur un châssis mobile, permettant une certaine flexibilité d'exploitation du pilote.

2.2 Dosage du bore

La méthode de spectrophotométrie moléculaire à l'azométhine-H a été proposée pour le dosage du bore.

Elle est considérée comme une méthode précise, sensible et sélective par rapport aux autres méthodes d'analyse du bore. Le spectrophotomètre utilisé est de type 'TOMOS V-1100'.

III. RESULTATS ET DISCUSSION

3.1 Caractérisation des membranes

Cette étude fondamentale présente une caractérisation de deux membranes BW-30 et NF-90 par détermination de la perméabilité hydraulique et de la charge de la surface. La perméabilité à l'eau pure, notée Lp, est déterminée par la mesure du flux du perméat en fonction du temps et de la pression transmembranaire appliquée.

Les valeurs de flux de perméat pour les deux membranes BW-30 et NF-90 étudiées et leurs variations en fonction de la pression transmembranaire sont représentées sur la figure 1.

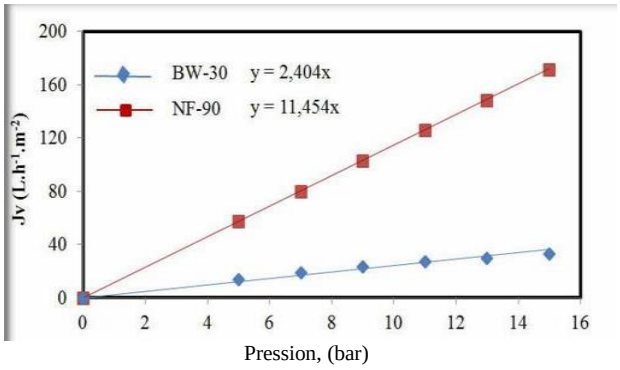

Figure 1. Mesure de la perméabilité à l'eau pure des membranes BW-30 et NF-90 à 27°C.

La perméabilité hydraulique à l'eau pure, Lp, est égale 11.45 pour la membrane NF-90 et 2.40 pour la membrane BW-30. La caractérisation des propriétés électriques de la surface membranaire représente une étape essentielle pour décrire les mécanismes de transfert des solutés. Dans cette étude, nous nous sommes intéressés à la détermination de la charge des membranes BW-30 et NF-90 par la méthode de rétention des sels. Cette méthode consiste à comparer la rétention ions monovalents et bivalents. En suivant l'ordre de rétention de ces ions, on peut déduire la charge de la membrane. Afin de savoir dans quelle catégorie se placent les deux membranes testées, trois solutions de sels : Na2SO4, CaCl2 et NaCl à la même concentration ont été préparées. Ensuite nous avons suivi la rétention de ces trois sels en fonction de la pression transmembranaire. Les résultats de cette étude sont présentés sur la figure 2.

D'après cette figure, la séquence de rétention des sels pour les membranes BW-30 et NF-90 est la suivante: $TR_{Na_2SO_4} > TR_{NaCl} > TR_{CaCl_2}$, cette séquence de rétention montre que ces deux membranes appartiennent à la catégorie où l'exclusion de Donnan joue un rôle important dans le mécanisme de rétention de sels. En outre, la rétention des anions bivalents est supérieure à celle des anions monovalents et la rétention des cations monovalents est supérieure à celle des cations bivalents. Ceci est un comportement typique d'une membrane chargée négativement. Ce comportement s'explique par la création d'une force de répulsion exercée sur les anions et d'une force d'attraction exercée sur les cations.

3.2 Influence des paramètres opératoires sur l'élimination du bore

De nombreux paramètres peuvent influencer l'élimination du bore par OI et NF. Nous nous attacherons dans cette partie à comprendre l'influence de la pression, le taux de conversion, le pH et la salinité sur la rétention.

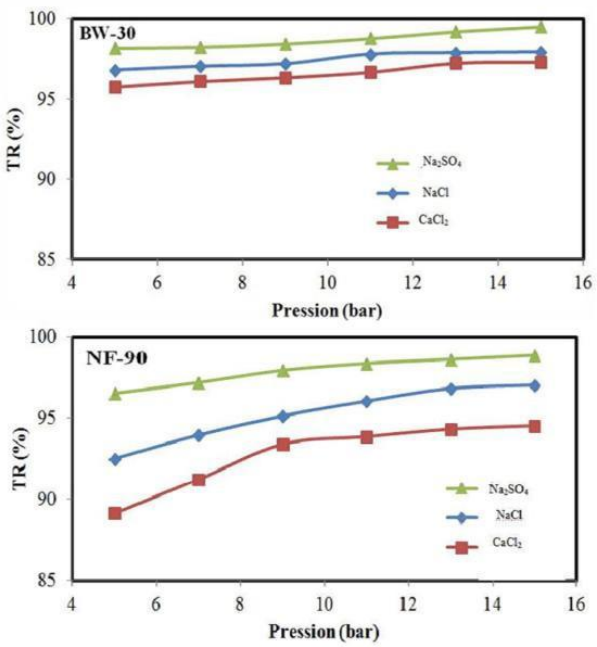

Figure 2. Variation des taux de rétention des sels en fonction de la pression transmembranaire (C0 = 10^{-3} mol.L-1, Y = 25 % et θ=27 °C).

L'influence de la pression d'alimentation sur les taux de rétention du bore par les deux membranes est représentée sur la figure 3. Ces résultats sont ajustés par le modèle de transfert Spiegler-Kedem.

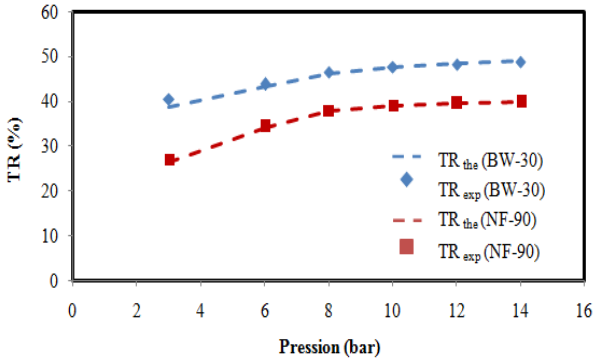

Figure 3. Influence de la pression sur l'élimination du bore (C0 =5 mg/L, Y = 25 % et θ=27 °C).

Les résultats obtenus montrent que la rétention du bore augmente avec la pression. De même, Wolska et al [6], Koseoglu et al. [7] et Parts et al. [8] ont mentionné qu'une élévation de rejet de bore a été observée lorsqu'on augmente la pression. Ce phénomène pourrait être attribué à l'augmentation du flux de solvant à une pression élevée. En fait, le flux de l'eau augmente proportionnellement avec la pression de fonctionnement

alors que le flux de soluté reste constant. La concentration en bore dans le perméat s'en trouve diminuée et par conséquent le taux de rétention augmente. Le pH est un facteur déterminant qui affecte à la fois la surface de la membrane et la répartition des espèces en solution. Afin d'évaluer l'influence de ce paramètre sur l'élimination du bore, une série d'expériences a été effectuée pour des pH variant de 7 à 11. La figure 4 illustre l'évolution du pourcentage du bore éliminé en fonction de la pression transmembranaire à différente valeur du pH.

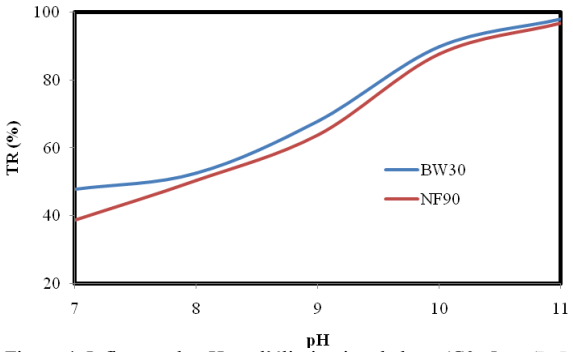

Figure 4. Influence du pH sur l'élimination du bore (C0=5 mg/L, P =10 bar, Y = 25 % et θ=27 °C).

Les résultats illustrés dans cette figure montrent que l'élimination du bore dépend fortement du pH. L'effet du pH peut être illustré par l'équilibre de dissociation de l'acide borique dans l'eau donnée par l'équation suivante :

$$H_3BO_3 + H_2O \leftrightarrow H_3O^+ + H_2BO_3^- \quad pKa_1 = 9{,}14$$

Une augmentation du pH entraine la dissociation de l'acide borique et la formation de l'ion borate (H_2BO_3). Pour des pH compris entre 9 et 10, la forme ionique prédomine, par contre pour un pH=11, la totalité de l'acide borique se transforme en ions borate. A des valeurs de pH neutre, l'acide borique sous sa forme moléculaire peut former un pont à hydrogène avec les groupes actifs de la membrane et diffuse d'une manière semblable à celle de l'acide carboxylique et de l'eau [9]. Par contre, à des valeurs de pH élevées (pH=11), l'élimination du bore atteint son maximum. En effet, des forces de répulsion seront formées entre les ions borates (H_2BO_3) et la surface membranaire chargé négativement. Ces interactions augmentent les taux de rétention du bore. Ce résultat est semblable à ceux trouvés par plusieurs auteurs [9,10]. La présence des sels peut provoquer un impact sur la rétention du bore par OI et NF. La variation des pourcentages d'élimination du bore pour différentes forces ioniques à pH = 11 est donnée dans la figure 5.

Les résultats illustrés dans la Figure 5 montrent que les pourcentages d'élimination du bore diminuent lorsque la force ionique augmente. Cette diminution peut être attribuée à la formation d'une couche des ions Na+ à la surface de la membrane. Cette couche permet de réduire la densité de charge de la membrane et par conséquence atténue les répulsions électrostatiques entre les charges négatives de la membrane et les ions borates et facilite leur migration à travers la membrane.

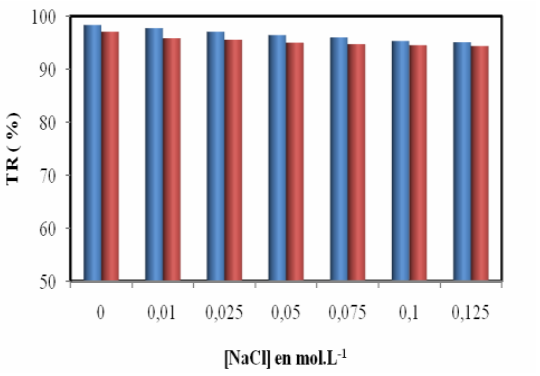

Figure 5. Influence de la force ionique sur l'élimination du bore (C0 =5 mg/L, P =10 bar, Y = 25 % et θ=27 °C).

3.4 Application à l'élimination du bore d'une eau naturelle

3.4.1 Essais d'élimination du bore

Les principales caractéristiques physicochimiques de cette eau sont résumées dans le tableau 1.

Table 1. Caractéristiques physicochimiques de l'eau naturelle à traiter.

Salinité (mg.L^{-1})	6883
pH	7,6
Bore (mg.L^{-1})	5,02
$[SO_4^{2-}]$ (mg.L^{-1})	728
$[HCO_3^-]$ (mg.L^{-1})	585
$[Cl^-]$ (mg.L^{-1})	3100
$[Na^+]$ (mg.L^{-1})	1022
$[K^+]$ (mg.L^{-1})	50
$[Mg^{2+}]$ (mg.L^{-1})	216
$[Ca^{2+}]$ (mg.L^{-1})	980

Le bore se trouve dans les eaux naturelles sous forme d'acide borique, un acide faiblement dissocié et sa rétention dépend fortement du pH. L'échantillon à analyser contient 5.02 mg/L du bore, une concentration qui dépasse les limites fixées par l'organisation mondiale de la santé (OMS) et la directive européenne (UE). La figure 6 donne la variation de concentration du bore dans le perméat ; les normes du bore dans l'eau potable fixées par l'OMS et l'UE sont représentées sur la même figure.

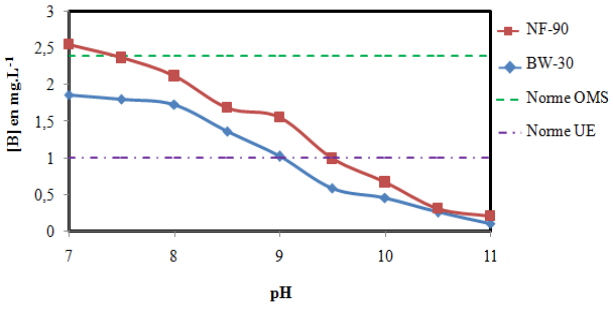

Figure 6 Variation de la concentration du bore dans le perméat en fonction de la pression et les normes fixées par l'OMS et l'UE.

L'eau produite par les deux membranes contient plus de 3 mg/L du bore. Ainsi avec ces conditions opératoires, on ne peut pas atteindre les normes fixées par l'OMS et l'UE. Dans la suite de ce travail, nous allons chercher des moyens pour améliorer la qualité d'eau produite par ces deux membranes et atteindre ces normes.

3.4.2 Ajustement du pH

On a montré, dans la partie 3.2, que l'élimination du bore dépend fortement du pH et que le maximum d'élimination est obtenu pour un pH au voisinage de 11. Or pour une eau chargée en sels, une augmentation du pH à des valeurs élevées peut provoquer la précipitation de certains sels et par conséquent, la formation des dépôts d'hydroxydes alcalins et des carbonates résultant ainsi le problème de colmatage. Afin de remédier à cette limitation, un système intégré de deux modules d'osmose inverse ou de nanofiltration, a été proposé. L'ajustement de pH est effectué à la fin de la première étape. La figure 7 représente le dispositif expérimental utilisé lors de cette application.

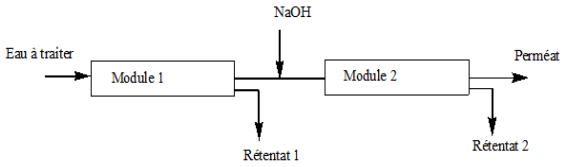

Figure 7. Dispositif expérimental utilisé pour l'élimination du bore après ajustement du pH.

Ce dispositif expérimental comprend deux modules de même référence. Le premier permet de réduire la quantité des sels présents dans l'eau (98.18% pour la membrane BW-30 et 96.29 % pour NF-90). A la sortie du premier module, on ajoute une quantité suffisante de NaOH pour atteindre le pH optimal pour l'élimination du bore. Cette eau est envoyée dans un deuxième module afin d'éliminer la quantité du bore restante. L'eau produite par le premier module contient 3.5 mg/L du bore pour la membrane BW-30 et 4.09 mg/L pour la membrane NF-90 avec des pourcentages d'éliminations respectives de 30,27 % et 18,52 %. La figure 8 donne la variation, en fonction du pH, de la concentration du bore dans l'eau produite après ajout de la soude.

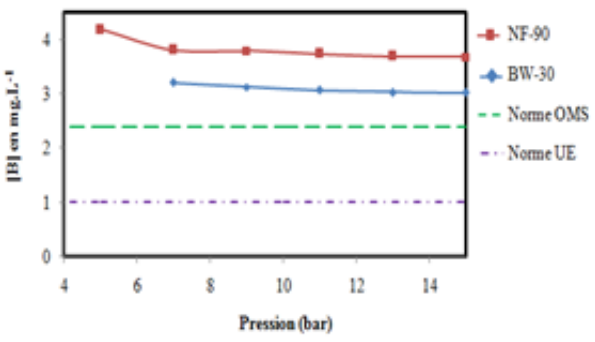

Figure 8. Variation de la concentration du bore dans l'eau produite après ajout de la soude en fonction du pH et les normes fixées par l'OMS et l'UE.

Comme montré dans la figure 8, en augmentant le pH, nous pouvons atteindre pour un pH =11 une concentration du bore de 0.2 mg/L pour la membrane NF-90 et 0.1 mg/L pour BW-30 avec deux taux d'élimination total de 96,015 % pour la première membrane et 98 % pour la deuxième. Pour la membrane BW-30, un deuxième traitement sans changement de pH permet d'atteindre la valeur limite fixée par l'OMS. Par contre, pour NF-90 une légère augmentation du pH (pH = 7.5) est suffisante pour atteindre cette norme. La qualité de l'eau produite devient conforme à la norme fixée par l'Union Européenne à un pH égal à 9 pour la membrane BW-30 et 9,5 pour la membrane NF-90.

L'inconvénient de cette application est lié à l'énergie consommée par le deuxième module et au produit d'ajustement du pH utilisé.

3.4.3 Complexation du bore

Une autre solution liée à la complexation de l'acide borique avec les composés polyhydroxylés, est proposé pour améliorer les pourcentages d'éliminations du bore. Les composés polyhydroxylés sont des composés organiques caractérisés par un certain nombre de groupements -OH. A pH des eaux naturelles, l'acide borique réagit avec ces composés, générant ainsi, des complexes stables qui peuvent être éliminés par OI et NF [53]. Trois complexants ont été testés : le mannitol, le sorbitol et l'acide gluconique. L'étude de détermination de l'effet de ces trois complexants est effectuée sur des échantillons d'eau réels. Différentes doses des complexants ont été ajoutées afin de déterminer l'effet des rapports molaires (n_C/n_B) sur les pourcentages d'élimination du bore par les deux membranes BW-30 et NF-90. Le rapport, a été varié de 0 à 4.

La figure 9, donnant ces résultats, montre qu'a partir du rapport n_C/n_B = 1, l'élimination du bore par les deux membranes reste constante. Ainsi, l'ajout de 85 mg de sorbitol, 85 mg de mannitol et 90 mg d'acide gluconique pour un litre d'eau à traiter (n_C/n_B= 1) améliore les pourcentages d'éliminations du bore par la membrane BW-30 de 38,11 % aux 53,73 % dans le cas de sorbitol, 50.43 % dans le cas de mannitol et 45.17 % dans le cas de l'acide gluconique. Les taux d'élimination du bore par la membrane NF-90 ont été améliorés de 24.72 % à 29.24, 32.64 % et 35.14 % lors de l'ajout respectif d'acide gluconique, de mannitol et de sorbitol.

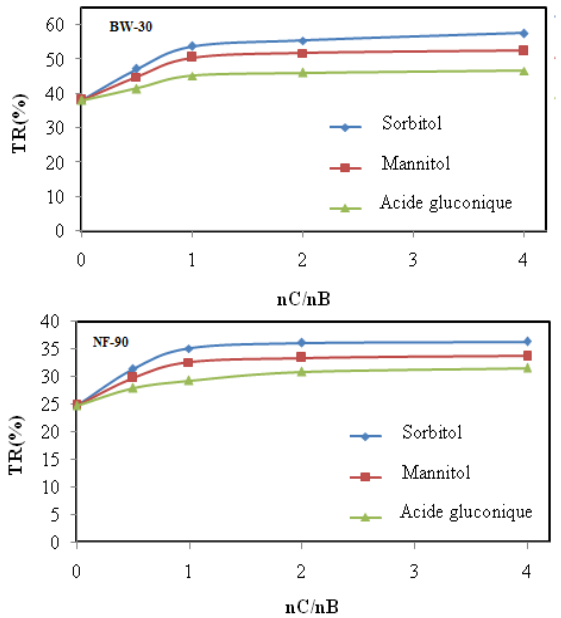

Figure 9. Variation des taux d'élimination du bore en fonction du rapport molaire nC/nB.

L'utilisation du sorbitol comme complexant est la meilleure solution pour améliorer l'élimination du bore

par les deux membranes utilisées. Ceci peut être expliqué par la configuration de la molécule de sorbitol (Figure 10). En effet, les groupements –OH, adjacents en position cis, sont les plus faciles pour former des complexes plus stables.

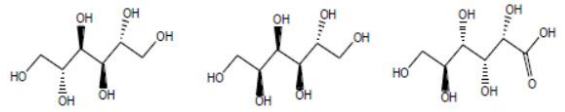

Mannitol Sorbitol Acide gluconique

Figure 10. Formule semi-développée des complexant.

Les composés polyhydroxylés augmentent l'acidité de l'acide borique. En effet lors d'une légère augmentation du pH, on peut augmenter les taux d'élimination du bore. La figure 11 donne la variation de taux de rétention du bore en fonction du rapport molaire n(Sorbitol)/n(Bore) à pH = 8,5. Cette figure 11, montre qu'à pH = 8.5, les taux de rétention du bore par les membranes BW-30 et NF-90 atteignent respectivement 65% et 46% en présence du sorbitol. Les eaux produites par les deux membranes sont caractérisées par des concentrations en bore de 1.7 mg/L pour BW-30 et 2.7 mg/L pour NF-90.

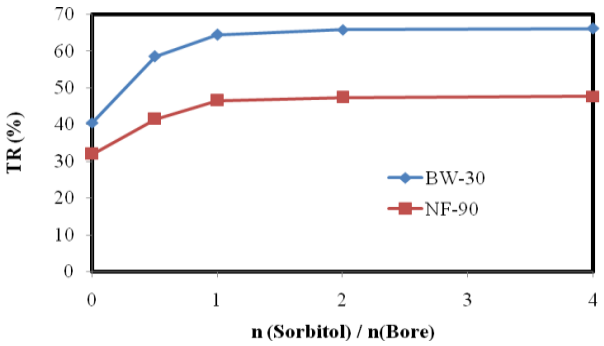

Figure 11. Variation des taux d'élimination du bore en fonction du rapport molaire n(sorbitol)/n(Bore) à pH = 8,5.

IV. CONCLUSION

Les performances des membranes en termes d'élimination du bore des solutions synthétiques et d'une eau saumâtre ont été déterminées. . Pour des solutions synthétiques, l'étude de l'effet des paramètres opératoires montre que le pH est le paramètre le plus influencé sur l'élimination du bore. Une meilleure élimination a été observée pour un pH égal à 11. Cette valeur du pH pose un problème au cours de l'application sur une eau naturelle. Deux solutions ont été proposées. La première consiste à ajuster le pH après la réduction de la salinité alors que la complexation de l'acide borique se présente comme une autre solution. Après ajustement du pH, des concentrations du bore de 0.2 mg/L pour la membrane NF-90 et 0.1 mg/L pour BW-30 avec deux taux d'élimination total de 96 ;015 % pour la première membrane et 98 % pour la deuxième ont été obtenus. D'une autre part, l'ajout de 58 mg/L du sorbitol, à pH = 8.5, améliore clairement les pourcentages d'élimination du bore (une augmentation de 27% pour la membrane BW-30 et 22% pour la membrane NF-90) pour produire des eaux caractérisées par des concentrations en bore de 1.7 mg/L pour BW-30 et 2.7 mg/L pour NF-90.

REFERENCES

[1] Nations unies, Rapport: objectifs du millénaire pour le développement, New York, 2009.
[2] P.J. Hotez, D.H. Molyneux, A. Fenwick, E. Ottesen, S.S. Ehrlich and J.D. Sachs, Incorporating a rapid-impact package for neglected tropical diseases with programs for HIV/AIDS, tuberculosis, malaria, PLoS Med, 2006, 3 (5), e-102.
[3] E.Weinthal, Y. Parag, A. Vengosh, A. Muti and W. Kloppmann, The EU drinking water directive: the boron standard and scientific uncertainty, European Environment, 2005, 15 (1), pp.1–12.
[4] OMS, Guidelines for Drinking-water Quality, 42éme Edition, 2011, Genève.
[5] A.K. Pabby, S.S.H. Rizvi and A.M. Saster, Handbook of membrane separation-Chemical, pharmaceutical, food and biotechnological application, Taylor and Francis group, 2009, New-York.
[6] J. Wolska and Bryjak M., Methods for boron removal from aqueous solutions- a review, Desalination, 2013, 310, pp.18-24.
[7] H. Koseoglu, N. Kabay, M. Yuksel, S. Sarp, O. Arar and M. Kitis, boron removal from seawater using high rejection SWRO membranes-impact of pH, feed concentration, pressure, and cross-flow velocity, Desalination, 2008, 227, pp. 253-263.
[8] D. Parts, M.F. Chillon-Arias and Pastor R.M. , Analysis of the influence of pH and pressure on the elimination of boron in reverse osmosis, Desalination, 2000,128 (3), pp.269-273.
[9] P.M. Rodriguez, R.M. Ferrandiz, T. Chillon and Prats R.D., Influence of pH in the elimination of boron by means of reverse osmosis, Desalination, 2001, 140 (2), pp.145-152.
[10] B. Tomaszewska and Bodzek M., Desalination of geothermal water using a hybrid UF-RO process, Part I: Boron removal in pilot-scale tests, Desalination, 2013, 319, pp. 99-106.

African Membrane Society
Water & Environment, Process, Energy
Sfax, Tunisia, May 3-5, 2016 - Membrane Water Treatment in Small Urban and Village Centers

Comparison between Coagulation/ Ultrafiltration Hybrid Treatment and Combination of Membrane Processes for Treatment and Reuse of Dyeing Effluents

Ghazza MASMOUDI and Raja BEN AMAR

Unit Laboratory of materials science and environment, Faculty of sciences of Sfax, Soukra road 4 th Km, 3028 Sfax, Tunisia
ghazza.masmoudi@gmail.com

Abstract- The objective of this work is to estimate quantitatively the potential of membrane distillation of seawater technology coupled with solar energy. The unit presented in this paper is designed to provide high quality drinking water in remote coastal areas with low infrastructure and without connection to an electrical network. The designed installation is completely autonomous, indeed the only energy source is the sun. The electrical energy required to operate the plant is produced by a photovoltaic cells field, and the sea water heating is provided by a thermic solar collectors field. A model describing the operation of a desalination membrane powered by solar energy is developed. This model determines the performance of the unit over time and for any day of the year.
This model is established from the balance equations of mass and heat on the different units (membrane, exchanger, condenser, field of solar collectors). The model is used to evaluate the evolution of the distillate flow and temperature changes for different flows. The model also allows to estimate the productivity of the unit during the year. The simulation of the operation of the unit shows that the daily production of distilled water is between 63 kg/m^2 and 188 kg/m^2 for the days of December 21 and June 21.

Keywords: membrane distillation, solar collectors, photovoltaic cells.

I. INTRODUCTION

In order to achieve a finished textile product many operations have to be done but the dyeing stills the operation releasing the most polluted effluent especially regarding to the high concentration of dyes and salts. To ovoid the contamination of the overall wastewater, treatment at source is proposed. In this approach, the dyeing effluent is recovered and treated separately. The treatment of concentrated dyeing wastewaters was the object of many studies since these effluents are extremely harmful for the environment and can cause irreversible damages touching different components of the ecosystem. Among the competitive treatment processes proposed for this approach, membrane processes showed to be promising technologies which respond to economical and space requirements of the modern industries. The choice of the membrane type depends on the nature of the compound to be removed. Microfiltration (MF) and ultrafiltration (UF) processes are generally used for the elimination of organic pollution such as suspended solids and colloids and can be applied as pretreatment [15] or main treatment [7,]. Nanofiltration (NF) and reverse osmosis (RO) can remove dissolved compounds, ions and dyes [13]. However, the main restriction of membranes use is fouling which can lead to permeate flux decrease with time and pollutants accumulation on the membrane surface.
To minimize membrane fouling and enhance membrane performances, pretreatment seems to be a good alternative. On one hand, possible combinations between membrane processes can be involved; MF and UF can be used as pretreatment for NF and RO [14, 10]. On the other hand, hybrid treatment represents another alternative, coagulation and/or flocculation [11, 4] and biological treatment [5, 16] can be used as pretreatment for membrane processes. Zahrim et al. , [17] stated that about 20% of NF flux improvement was achieved when a CF pretreatment was introduced. Rozzi et al. [12] tested the hybrid system C/MF for textile wastewater treatment and claimed that the coagulant use was necessary to obtain a satisfactory performance; otherwise, rapid fouling of the membrane occurred.
When coagulation and membrane processes are coupled, the coagulation conditions like the coagulant dose and nature as well as the shear applied, seems to affect the filtration performancesIn this work, a comparison between hybrid C/UF system and a combination of MF and NF membranes was investigated for the treatment of real dyeing effluent in pilot scale. Two different coagulants were tested in the C/UF experiments. The comparison was carried regarding the filtration performances and the quality of the treated effluent following the COD and color removals.

II. MATERIAL AND METHODS

2.1. Dyeing effluent

The studied effluent was collected from a dyeing machine in a textile company in Kasr Helal, Tunisia.

The effluent was released from a reactive dyeing operation and it represents a mixture of different baths used in the dyeing cycle; preparation, dyeing, neutralizing, washing and softening (Table1). As seen, different steps have to be done in order to accomplish the dyeing process, the wastewater object of this studied is a mixture of all these baths in the same proportions. The characteristics of the mixture to be treated are represented in table 2.

Table 1 : Operating conditions of the dyeing process steps

Operation	pH	T(°C)	t(min)	additives	Role
Preparation (P)	6-7	30	5	sequestering agent (anionic surfactant) Corrosion	attach hardening substances Prevent corrosion of
Dyeing (D)	9-11	60	110	Reactive dyes (anionic) Salt (sodium chloride) Sodium carbonate	Operation of attaching the dye molecule to the textile
Neutralizing (N)	6-7	50	5	Acetic acid	Add of acid to adjust the basic pH of
Washing (W)	6-7	80	5	Dispersing and degreasing detergent	Eliminate the excess of dyes
Softening (S)	5-6	40	20	Acetic acid Softening agent (cationic	Enhance the feel of textile

Table 2. The dyeing effluent characterization

pH	S (g/l)	TH (°F)	Cl^- (g/l)	COD (g/l)	Color[a]	Turb (NTU)
9.72	21.6	120	17.8	1.9	4.6	7.9

a: Integral of the absorbance curve in the whole visible range (400-800 nm)

2.2. Experimental set-up

The figure1 represents the experimental set-up of MF/NF combination. MEMBRALOX module (1P19-40/1R19-40) of 1020 mm length was used in the MF experiments. The membrane is multi-channel (19 channels) of 0.2 µm pore size made of ceramic based on Al_2O_3 with a surface exchange of 0.24 m^2. For NF experiments, a spiral DESAL membrane product (DK2540F1073) having a MWCO of 200 Da, a length of 1016 mm and an area of 2.5 m^2 was used. The operating temperature was the room temperature (20 °C) and the pressure was fixed at 2 bar and 12 bar for the MF and NF units, respectively.

2.3. Membrane performances evaluation

The filtration performances of the MF, UF and NF membranes were followed with the volume reduction factor (VRF) calculated as follows:

$$VRF = \frac{V_f}{V_c} \quad (1)$$

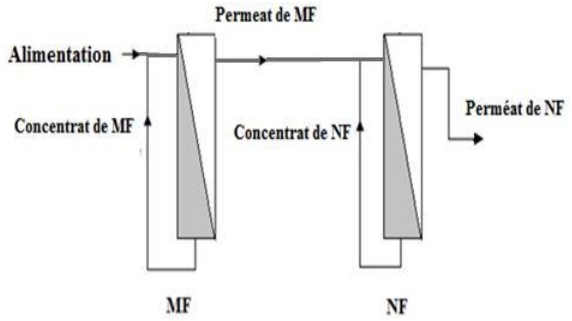

Figure 1: Schematic presentation of the experimental set-up of MF/NF combination

Figure 2 represents the hybrid treatment set-up. In the coagulation step, two different coagulants were used, inorganic (Aluminum sulfate (Alum)) and organic polymer with a cationic character (Amerfloc445). Optimal doses of coagulants were determined using jar test method and added in the feed tank of the UF unit before the beginning of the runs. The UF experiments were performed using KLEANSEP multichannel membrane (7 channels) of 1178 mm length. The membrane was made of ceramic based on TiO_2-Al_2O_3 with an area of 0.15
M^2 and a molecular cut-off of 15 kDa. The operating temperature was room temperature (20°C) and the pressure was fixed at 3 bar for the UF runs.

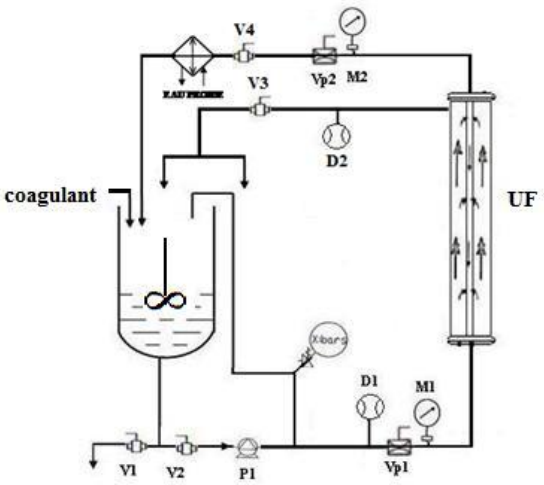

Figure 2. Schematic presentation of the hybrid treatment set-up of coagulation/UF

Where V_f and V_c are the volumes of the feed and the concentrate, respectively. The membranes performances were evaluated by the rejection rate of color and COD determined as follows:

$$R(\%) = \left(1 - \frac{C_p}{C_f}\right) * 100 \quad (2)$$

Where C_p and Cf are the concentrations in the permeate and in the feed respectively.

2.4. Analytical measurements

The dye amounts were followed by absorbance measurements at the visible maximum dye absorption wavelength using a UV-visible spectrophotometer (Perkin Elmer Lambda 20 UV/VIS).

COD was estimated by open reflux method. The protocol present a method derived from the standard AFNOR T90-101. The COD values were obtained using a Fisher Bioblock Scientific reactor COD 10119 type COD-meter.

Turbidity was measured using a turbidity-meter Hach RATIO 2100N. Chlorides amounts were calculated after a simple dosage by AgNO3, salinity was measured with a conductimeter Tascussel model 123 and total hardness was calculated following the complexometric titration method with EDTA.

The flocs size after the coagulation was determined using dynamic light scattering device Zetasizer Nano ZSP.

2.5. Textile color measurement

A point in a space formed by three orthogonal axes can represent color: the first describes color evolution from green (-a*) to red (+a*), the second identify color evolution from blue (-b*) to yellow (+b*) and the third one represents lightness L* ranging from 0 for black to 100 for perfect white. In this measurement method, a comparison against a color standard is required. So, total color differences ΔE can be calculated from analysis of samples and standard, following equation 3.

$$\Delta E = \sqrt{(\Delta a^*)^2 + (\Delta b^*)^2 + (\Delta L^*)^2} \quad (3)$$

Where $\Delta a^* = a^*_{sample} - a^*_{standard}$

$\Delta b^* = b^*_{sample} - b^*_{standard}$; $\Delta L^* = L^*_{sample} - L^*_{standard}$

The spectrocolorimeter used is Datacolor Spectrum 2520. Samples are textile items dyed with treated water. Standard reference is a textile dyed with fresh water using the same dyeing protocol. The samples giving the best results should have a total color difference ΔE close to zero.

III. RESULTS AND DISCUSSION

3.1. Coagulation step

For Alum, the dose of 0.9 g/l contributed to better COD and color eliminations, by 63% and 44% respectively. While for Amerfloc445, the optimum dosage was 0.5 g/l and achieved 69% and 67% of COD and color removals, respectively, (Figure 3).

The flocs size corresponding to the optimal dose of each coagulant was measured, for Alum flocs it was 488 µm while it was 845 µm for Amerfolc445 particles. It was obvious that smaller dose of Amerfloc445 contributed to better pollution removal efficiency as well as more aggregates that are voluminous, this could be attributed to better charge neutralization ability of the Amerfloc445 coagulant.

3.2. The filtration behavior

Figure 4 shows the variation of the MF and NF permeate fluxes with the VRF. The maximum VRF was only 2.5 for the NF, however it reached 4.3 in the MF runs.

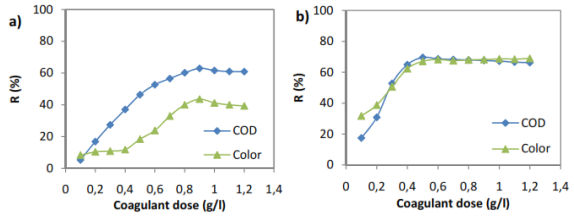

Figure 3. Variation of color and COD removals with coagulant dose for a) Alum and b) Amerfloc445

This indicate that the volume of produced permeate was noticeably higher for the MF membrane when compared to NF. This is principally due to the difference in the pore size between the MF and NF membranes. The obtained curves showed also that the MF behavior was severely influenced by fouling as the filtration flux dropped by more than 70% since the beginning of the filtration. However, fouling had not a significant effect on the NF behavior. This is due principally to the membranes characteristics since the main fouling mechanism of MF membrane is the cake layer formation, [1] while it is concentration polarization for the NF, [8].

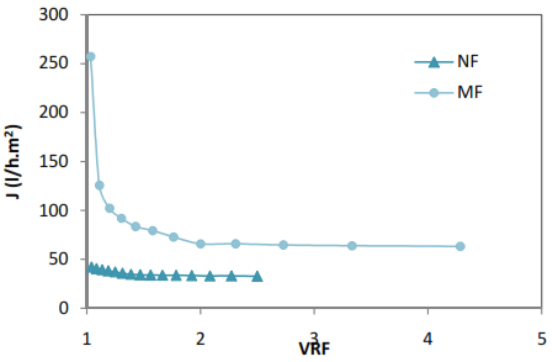

Figure 4. Variation of the MF and NF filtration flux with VRF

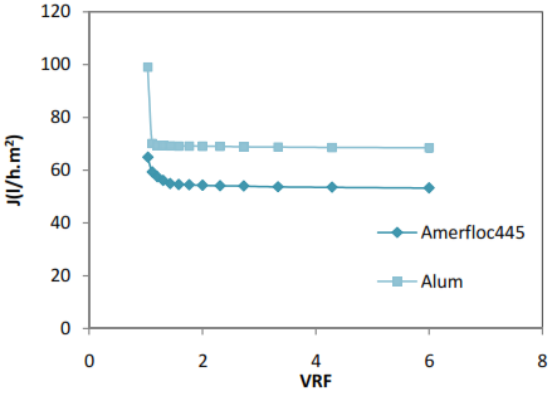

Figure 5. Variation of the UF normalized filtration flux with VRF for Alum and Amerfloc445 coagulants

Figure 5 represents the variation of the permeate flux during the UF filtration tests using Alum and Amerfloc445 coagulants. The results showed a typical behavior of UF membrane in which the permeate flux decreased until reaching a stabilized value. This is due to the matter accumulation close to the membrane surface, which caused membrane fouling. It was obvious that the stabilized filtration flux was higher with Alum coagulation; 68 l/h.m2against 52 l/h.m2 for Amerfloc 445 coagulation.

However, membrane fouling seems to be severer with Alum coagulant, indeed; the flux decline was about 30% for Alum coagulation while it did not exceed 10% with Amerfloc445. This behavior is attributed to the flocs size since the amerfloc445 flocs are bigger which make the formed cake layer thicker than that formed with smaller Alum flocs, which can reduce the filtration flux. On the other hand, more voluminous flocs can develop slowly a more porous cake layer contrarily to small flocs able to form rapidly a compact cake layer, [3] which increased the resistance to mass transfer. This can justify the high flux decline for Alum coagulation.

3.3. The treated effluents quality

In figure 6, the retentions of COD and color were represented for the followed treatment methods; C/UF (Alum), C/UF (Amerfloc445) and MF/ NF. The Alum coagulation coupled with UF showed the lowest retention values in term of COD (56%) as well as color (64%). C/UF (Amerfloc445) and MF/NF showed a comparable retention behavior; 92% and 89% of COD removal and 98.54 % and 99.58% of color retention, respectively. The high retentions given by the C/UF (Amerfloc445) system could be attributed to the bigger size of the flocs formed with the organic coagulant (845 µm) which make it easily retained by the membrane. The high COD and color retentions by MF/NF system was a predicted behavior of the NF membrane in agreement with results from He et al. (2009)

Regarding the permeate quality (Table 3), both approaches C/UF (Amerfloc445) and MF/NF showed similar retentions. The concentrations also were 0.17 mg/l and 0.2 g/l of COD and 0.07 and 0.03 in term of absorbance, respectively for C/UF (Amerfloc445) and MF/NF. Regarding the volume of the treated water produced, C/UF (Amerfloc445) treatment was able to produce higher volume of permeate since the filtration can reach a VRF of 6.

energy consumption as well as the required cleaning chemicals of the UF unit would certainly be smaller than those of both MF and NF units even if the coagulant cost was added.

3.4. Reuse of the treated water

Dyeing tests were done with the treated water obtained with different treatment approaches. In addition, a reference dyeing test was done with fresh water.

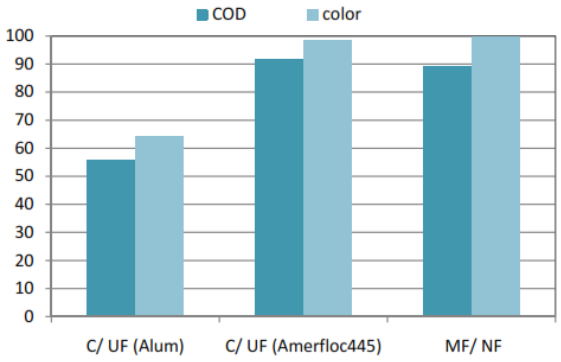

Figure 6. Retentions of COD and color for hybrid C/ UF treatment using Alum and Amerfloc445 coagulants and the combined membrane treatment MF/ NF

In addition, from the economical point of view, the

Table 3. Characterization of the treated effluents using different systems

	pH	S (g/l)	TH (°F)	Cl (g/l)	COD (g/l)	Color[a]
MF/NF	8.41	11.19	21	9.06	0.2	0.03
C/UF (Alum)	7.95	16.27	67	12.3	0.83	1.65
C/UF (Amerfloc445)	8.29	12.6	19	8.79	0.17	0.07

a: Integral of the absorbance curve in the whole visible range (400-800 nm).

Tests were performed in laboratory dyeing machine using a support of cotton material. As the treated effluents contain yet salt, in order to obtain the needed salt concentration in the dyeing bath, the quantity of NaCl added in the reuse tests corresponds just to the difference between the quantity of NaCl in the dyeing test with fresh water and in treated water.

Figure 6 shows the applied reactive dyeing protocol. It should be noticed that after dyeing no difference was perceptible between the different samples. Spectrocolorimetric measurements were represented in Table 4. The obtained results show that C/UF (Alum) system led to the highest ΔE value, which indicate that it represents the lowest similarity with the reference sample. This result is principally due to the important hardness of the effluent treated by C/UF (Alum) as well as its relatively high coloration (Table3). Generally, hard water has an unfavorable effect on dyeing results. Indeed, $Mg^{2+}$and Ca^{2+} ions which makes the color lighter as well as that discolored patches may also occur. This was confirmed by the positive ΔL^* value which indicate that L^*_{sample} was higher than $L^*_{standard}$, so L^*_{sample} tends to white.

Regarding the results obtained with MF/NF and C/UF (Amerfloc445) systems, the total color difference value ΔE was 0.2 and 0.17, respectively. This result confirmed the capacity of the C/UF (Amerfloc445) system to achieve comparable performances to that of the MF/NF system.

IV. CONCLUSION

A comparison between C/UF and MF/NF systems was carried in a paper the results indicated that the C/UF process can lead to similar results to those given by MF/NF treatment in term of COD and color removals if the adequate coagulant was used.

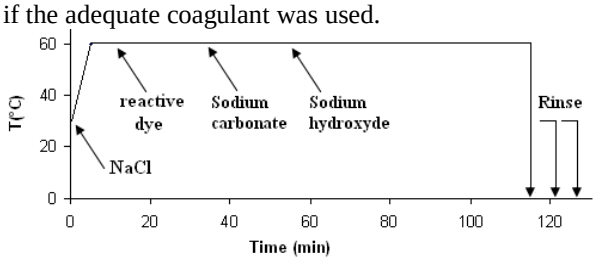

Figure7. Dyeing protocol with reactive dye.

Table 4. Color coordinates obtained after dyeing with treated water for each system

Configuration	Δa*	Δb*	ΔL*	ΔE
MF/NF	-0.05	0.12	0.15	0.2
C/UF (Alum)	-0.46	0.34	1.71	1.8
C/UF (Amerfloc445)	0.08	0.14	0.05	0.17

The combination of Amerfloc445 coagulation and UF led to 89% and 98.54% of COD and color retention, respectively. On the other hand, MF/NF system showed 92% and 99.58% of COD and color removals, respectively. Regarding the volume of the treated effluent, the C/UF system showed higher performances than MF/NF system since the UF runs can reach a VRF of 6 against only 2.5 for the NF.

Reuse tests confirmed that MF/NF and C/UF (Amerfloc445) can produce reusable water in the dyeing process, and that the hybrid system can lead to comparable performances to that of the MF/NF system.

REFERENCES

[1] P. Bacchin, D. Si-Hassen, V. Starov, M.J. Clifton, P. Aimar, A unifying model for concentration polarization, gel-layer formation and particle deposition in cross-'ow membrane filtration of colloidal suspensions. Chemical Engineering Science 57, pp. 77-91, 2002.

[2] L. Bae-Bok, C. Kwang-Ho, C. Daeic, C. Sang-June Choi, Optimizing the coagulant dose to control membrane fouling in combined coagulation/ultrafiltration systems for textile wastewater reclamation. Chemical egeneering journal 155, pp. 101-107, 2009.

[3] E. Barbot, S. Moustier, J. Bottero,P. Moulin. Coagulation and ultrafiltration: Understanding of the key parameters of the hybrid process. Journal of membrane science, 325, 520-527, 2008.

[4] F. Harrelkas, A. Azizi, A. A. Yaacoubi, Benhammou A., M.N. Pons. Treatment of textile dye effluents using coagulation–flocculation coupled with membrane processes or adsorption on powdered activated carbon. Desalination 235, pp.330-339, 2009.

[5] C. Fersi, L. Gzara, M. Dhahbi, Treatment of textile effluents by membrane technologies. Desalination 185, pp. 399-409, 2005.

[6] Y. He, G.M. Li, H. Wang, Z.W. Jiang, J.F. Zhao , H. X. Su, Q.Y. Huang, Experimental study on the rejection of salt and dye with cellulose acetate nanofiltration membrane. J. the Taiwan Institute of Chemical Engineers 40, pp. 289-295, 2009.

[7] M. Katarzyna M. Majewska-Nowak, Application of ceramic membranes for the separation of dye particles. Desalination, 254, pp. 185-191, 2010.

[8] I. Koyuncu, D. Topacik, Effects of operating conditions on the salt rejection of nanofiltration membranes in reactive dye/salt mixtures. Separation and purification technology 33, pp. 283-294, 2003.

[9] K.H. Choo, S.J. Choi, E.D. Hwang. Effect of coagulant types on textile wastewater reclamation in a combined Coagulation/ ultrafiltration system. Desalination 202, pp. 262-270, 2007.

[10] M. Marcucci, G. Nosenzo, G. Capannelli, L. Ciabatti, D. Corrieri, G. Ciardelli, Treatment and reuse of textile effluents based on new ultrafiltration and other membrane technologies. Desalination138, pp. 75-82, (2001).

[11] M. Rierra-Torres, C.G. Bouzan, M. Crespi, Combination of Coagulation- flocculation and nanofiltration techniques for dye removal and water reuse in textile effluents. Desalination 252, pp. 53-5, 2010.

[12] A. Rozzi, M. Antonelli, M. Arcarri, Membrane treatment of secondary textile effluents for direct reuse. Wat. Sci. Tech. 40(4-5), pp. 409-416, 1999.

[13] C. Suksaroj, M. Héran, C. Allègre, F. Persin, Treatment of textile plant effluent by nanofiltration and/or reverse osmosis for water reuse. Desalination 178, pp. 333-341, 2005.

[14] N. Tahri, G. Masmoudi, E. Ellouze, A. Jrad, P. Drogui, R. Ben Amar, Coupling of microfiltration and nanofiltration processes for the treatment at source of dyeing containing effluents. J. Clean. Prod. 33, pp. 226-235, 2012.

[15] N. Uzal, L. Yelmaz, U. Yetis, Microfiltration/ ultrafiltration as pretreatment for reclamation of rinsing water of indigo dyeing . Desalination 240, pp. 198-208, 2009.

[16] L. Xujie, L. Lin, L. Rongrong, J. Chen, Textile wastewater reuse as an alternative water source for dyeing and finishing processes: A case study. Desalination 258, pp. 229-232, 2010.

[17] A.Y. Zahrim, C. Tizaoui, N. Hilal, Coagulation with polymers for nanofiltration pre-treatment of highly concentrated dyes: a review. Desalination 266, pp. 1-16, 2011.

Investigation of Cheese Whey Wastewater Treatment Using Coagulation/Flocculation and Membrane Filtration: New Hybrid Process

Imen KHOUNI, Sana ABDELKADER, Latifa BOUSSELMI, Ahmed GHRABI

Laboratory of Wastewater and Environment, Water Research and Technologies Centre of Borj-Cedria (CERTE) BP 273, 8020 SOLIMAN-Tunisia.
imen.khouni@yahoo.fr

Abstract- In the food industry supply chain dairy applications are considered to be the most polluting ones, because of their large water consumption and wastewater generation. This study deals with the investigation of cheese whey wastewater treatment using membrane processes. Microfiltration (MF) and ultrafiltration (UF) treatments are used separately and combined in this study. Final results are compared with those of coagulation/flocculation (CF) treatment optimized through response surface methodology (RSM). A key objective is to assess the efficacy of pollutant removal performance during each process step. During phase I of this study, chemical precipitation methods were applied to raw cheese whey effluent by leveraging several coagulant agents: polymeric aluminum sulfate ($Al_2(SO_4)_3$), ferric chloride ($FeCl_3$), aluminum chloride ($AlCl_3$) and calcium hydroxide ($Ca(OH)_2$). COD removal efficiencies varied between 16% and 37%. The polymeric aluminum sulfate was the most effective method with 37% COD and 62% protein retention efficiency in the chemical treatment of cheese whey effluent. The use of a coagulant aid (flocculent) enhances the retention efficiency values. In addition, pH adjustment proved to sharply influence the treatment efficacy. Furthermore, response surface methodology (RSM) using central composite design (CCD) was successfully employed to model and to optimize the CF process.
Treatment by CF alone was inefficient in terms of COD removal (48.5 %), residual turbidity removal (6.32 NTU) and Protein retention (94.3%). Therefore, during phase II of this experimental study, the use of MF for cheese whey treatment was explored. It led to a retention efficiency of 99.9% for the fats, while the protein and COD removal rates were only around 15% and 18.5% respectively. Therefore, UF treatment was studied for optimizing the removal rate numbers. The use of an 8 KDa molecular weight cut-off UF membrane led to better treatment performance in terms of permeate flux, protein and fat retention efficiency and COD removal - 22.5 $L/h.m^2$, 81%, 99.9% and 29.5%, respectively. When the MF and UF treatments were combined, the process efficacy was enhanced since COD removal and protein retention rates reach, 50% and 99%, respectively.

Keywords: Cheese whey wastewater, Coagulation/flocculation, Ultrafiltration, Microfiltration, RSM.

I. INTRODUCTION

Dairy industry is a large scale food production Industrial process that is also heavily responsible for environmental (water) pollution. Cheese whey wastewater exhibits a sharp risk of environmental pollution due to its high organic load [1].
Cheese whey can cause an excess of oxygen consumption, eutrophication, toxicity etc in the host environments. The volume of effluents produced in the cheese manufacturing industry has increased with the increase in cheese production [2]. With their very high concentration of organic matter, these effluents may create serious problems of organic burden on the local municipal sewage treatment systems [3]. Since chemical precipitation has become a widely used technology for both industrial as well as municipal wastewater treatment, the principal aim of the present investigation was to verify the efficiency of the aluminum sulfate (Al2(SO4)3) or alum applied as coagulant for treatment of dairy industry wastewater. Maximum treatment efficiency was studied adopting a full range of response surface methodology (RSM) using central composite design(CCD) model to analyze the affectivity of the system under different conditions. Then, obtained CF efficiencies were compared to those achieved by the conventional optimization method.
Since membrane technology has several advantages including a high degree of reliability in removing dissolved, colloidal and particulate matter, it is widely used in the dairy industry wastewater treatment. In this study, an investigation of two hybrid treatments of cheese whey is carried out; the combination of microfiltration (MF) and ultrafiltration (UF) treatments and a hybrid treatment composed of the two aforementioned treatments followed by a coagulation-flocculation (CF) process.

II. MATERIALS AND METHODS

2.1 Cheese whey

Sweet cheese whey samples were obtained from a local cheese industry 'Cheese kzadri', Bizerte-Tunisia. The samples were cooled and conserved under a maximum temperature of 3°C until further analysis.

2.2 Coagulation/flocculation treatment and Response Surface Methodology (RSM)

Cheese whey coagulation/flocculation (CF) trials were realized on ambient temperature (24±2°C) using a "Jar test" according to the following principle: in a series of beakers containing sweet whey, different doses of the coagulating agent ($Al_2(SO_4)_3$) are introduced in the sweet whey and stirred for a short period at low speed (150 rpm for 3 min) ensuring a good spread of the coagulating agents and the colloids chemical destabilization. Then, the flocculent (CHT-Flocculent CV) was added, the whey was stirred gently (30 rpm for 20 min) to facilitate the contact of the particles and avoid breaking the flocks formed. Finally, these flocks were settled in a period of 30 min. The effectiveness of this treatment was evaluated analytically by monitoring the turbidity (measured in NTU), COD and protein removals.

Since the conventional method of optimization, "one factor at a time" approach is laborious, time consuming and incomplete response surface methodology (RSM) using central composite design (CCD) was applied to model the treatment process **[4]**. The RSM study was conducted to determine the relative contributions of three predictor variables (coagulant concentration, pH and flocculent concentration) for cheese whey CF treatment. The CCD model based on three factors was used as experimental design model. The factor levels were coded as −1 (low), 0 (central point) and +1 (high), **[5]**.

2.3 Membrane treatment

Three membrane modules were investigated for the enhanced treatment of the cheese whey wastewater. A ceramic microfiltration membrane module with a mean pore diameter of 0.2 µm and two organic ultrafiltration membranes with a molecular weight cut-off (MWCO) of 8 and 25 KDa.

III. RESULTS

3.1 Coagulation-flocculation treatment

Preliminary chemical precipitation studies were applied to the raw cheese whey effluent using different coagulant agents: polymeric aluminum sulfate (Al2(SO4)3), ferric chloride (FeCl3), aluminum chloride (AlCl3) and calcium hydroxyde (Ca(OH)2). COD removal efficiencies varied between 16% and 37%. The polymeric aluminum sulfate was the most effective coagulant with 37% COD and 62% protein removals efficiencies for CF treatment of cheese whey effluent under an optimal concentration of 0.3 g/L. Thus, the polymeric aluminum sulfate will be used to conduct the CF optimization through Response Surface Methodology (RSM).

3.2 Optimization of CF through RSM

The obtained results by RSM model show that CF treatment lows to good protein removal rates of about 94%. Besides, CF treatment gave about 48% of COD removal. Further RSM steps, the statistical analysis of CCD experimental results, response surface modeling and optimization of process variables were carried out using NemrodW software. These further studies will determine the influence of the different factors and the significance of the CF treatment.

According to the sequential model sum of squares, the models were selected based on the highest order polynomials where the additional terms were significant. The experimental results are evaluated and the different predicted responses (Y) for percent COD removal (Y1), turbidity (Y2) and percent protein retention (Y3) of samples treated were obtained in equations 1, 2 and 3, respectively:

$$Y1 = 48+5.625\ X3-21.375X3^2+3.25X1 \quad (1)$$

$$Y2 = -22.875X1-107.5X3+195.375X3^2-25X13 \quad (2)$$

$$Y3= 94+2.875X1+2.125X2+15.75X3-2.875X1^2-44.125X3^2+4.5X13+2.5X2.3 \quad (3)$$

Maximum rates of COD removal, protein retention and turbidity of the treated raw cheese whey by CF treatment are presented in Table 1. The removal rates were significantly higher than those obtained by the conventionally optimized CF process. The results illustrated by table 1 were achieved using 0.373g/L of the coagulant, 1.23 g/L of the flocculent under pH of about 9.6.

Table 1: Optimum values of responses variable.

Coded responses	Real responses	Maximum value
Y1	COD removal (%)	48.46
Y2	Turbidity (NTU)	6.32
Y3	Protein retention (%)	94.31

The statistical analysis of CCD experimental results showed that there was no significant interaction between the different factors (pH/coagulant concentration, pH/flocculent concentration and coagulant/flocculent concentrations) on the COD removal. Such interactions were more significant for the proteins removal.

3.3 Microfiltration (MF) of cheese whey wastewater

Microfiltration of the cheese whey wastewater under a pressure of 2.5 Bars led to high values of suspended solids and fats retentions, which reached 99.9% for both. The recorded average flux value was 37.3 $L/h.m^2$. However, the protein retention and COD removal values didn't exceed 15% and 18.5%, respectively.

3.4 Ultrafiltration (UF) of Cheese Whey wastewater

The UF experiments included a comparison between two UF modules having different molecular weight cut-off (MWCO) of 8 and 25 KDa. The results showed that the 8KDa membrane have better COD removal rates than

the 25 KDa membrane (29.5% and 22%, respectively). Besides, the 8KDa membrane module led to a protein retention of 66% compared to only 17% for the other UF module. Therefore, the 8KDa membrane unit was selected for the following treatment investigation.

3.5 Hybrid MF/UF for Cheese whey wastewater treatment

To enhance the COD and proteins removal rates, combining MF and UF processes was investigated. Results showed that the hybrid MF/UF can lead to better rates. The protein retention obtained was 95% with a COD removal of about 50% with 29.5 L/h.m^2 average recorded flux.

3.6 Hybrid CF/MF/UF of the cheese whey wastewater treatment

In order to study the influence of the combined multiples processes investigated in this paper, we analyzed the effluent obtained by the optimized CF process followed by the MF and UF treatments.

The results showed that a protein retention rate of 99% was achieved as well as a COD removal of 75% which led to a significant clarification of the cheese whey and a high improvement in its parameters (figure 1).

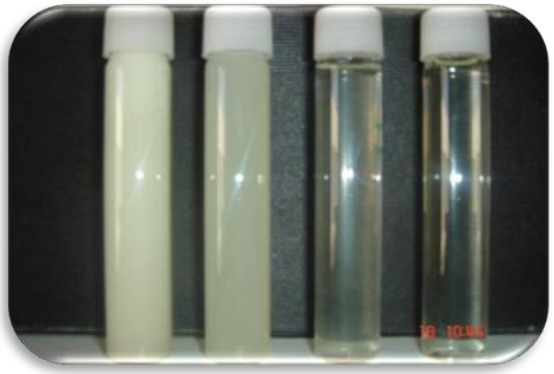

Figure 1: Four samples of cheese whey: (from left to right): raw cheese whey, cheese whey treated by CF, cheese whey treated by MF/UF, cheese whey treated by CF/MF/UF

IV. CONCLUSION

The final results demonstrated that the combination of several physical-chemical processes was preferred to improve the quality of cheese whey wastewater. The optimal concentrations of the coagulant and the flocculent as well as the optimal pH value calculated by several models established and validated under the Response Surface Methodology (RSM) led to improved protein retention efficiency, as well as COD and turbidity removals compared to the conventional optimization. The increase of COD removal was 37 % and that of protein retention rate was 61 %. Optimization of coagulant and flocculent concentrations and some pH adjustment gave rise to a significant improvement of the treated effluent quality. By combining CF with MF and UF treatments it was possible to further enhance the effluent quality. Hence, testing of the hybrid CF/MF/UF system was key to eliminate most proteins (retention 99.9%) and to sharply reduce the COD level (75%) when compared to an individual use of each process.

ACKNOWLEDGMENT

The authors are thankful to the staff of the dairy factory ‘Cheese kzadri’ for providing some cheese whey samples and for their kind assistance.

REFERENCES

[1] D.P. Harush, U.S. Hampannavar, M.E Mallik arjuna swami. "Treatment of dairy wastewater using aerobic biodegradation and coagulation", International Journal of Environmental Sciences and Research Vol. 1, No. 1, 2011, pp. 23-26.

[2] A. R. Prazeres, F Carvalho, J. Rivas, "Cheese whey management: A review" Journal of Environmental Management 110, 2012, 48-68.

[3] W Janczukowicz, M Zielin ski, M D bowski. "Biodegradability evaluation of dairy effluents originated in selected sections of dairy production." Bioresour Technol, 2008 ;99(10): 4199–205.

[4] G.E.P. Box, K.B. Wilson, "On the experimental attainment of optimum condition", J. R. Stat. Soc. B. 13, 1951, 1–38.

[5] M. Evans, "Optimization of Manufacturing Processes: A Response Surface Approach", Carlton House Terrace, London, 2003.

African Membrane Society
Water & Environment, Process, Energy
Sfax, Tunisia, May 3-5, 2016 - Membrane Water Treatment in Small Urban and Village Centers

Study of Ceramic Membrane from Naturally Occurring-Kaolin Clays for Microfiltration Applications

Sonia REKIK[1, 2], Semia BAKLOUTI[1], Jamel BOUAZIZ[1], André DERATANI[2]

[1]*Laboratory of Industrial Chemistry, National School of Engineers, University of Sfax, Sfax BP 1173, Route de Soukra km 4, 3018 Sfax, Tunisie*
[2]*Institut Européen des Membranes, Université Montpellier 2, cc 47, Place E. Bataillon 34095 Montpellier Cedex 5, France*
bouzidsonia@gmail.com

Absract: There is much current interest in the application of membranes in separation processes because of their potential for the treatment of large quantities of wastewater. The focus of this work is to assess the quality of porous membranes prepared from naturally occurring- kaolin clays and to evaluate the performance of tubular ceramic membranes treating integrated raw effluents from seafood industry. The preparation and characterization of porous tubular ceramic membranes, using kaolin powder with corn starch as poreforming agent, were reported. SEM photographs indicated that the membrane surface was homogeneous. The effects of material compositions, additives and the relatively lower sintering temperature, ranging from 1100° to 1250°C, on porosity, average pore size, pore-size distribution and mechanical strength of membranes have been investigated. A correlation between microstructure and mechanical properties of membranes has been discussed. The performance of the novel ceramic membranes obtained was determined by evaluating both the water permeability and rejection.

Keywords: ceramic tubular membrane, kaolin clays, sintering, filtration, cuttlefish effluent.

I. INTRODUCTION

Membrane separation processes extend more and more every day in industrial uses, with new requirements concerning the materials and preparation procedures. Due to their potential application in a wide range of industrial processes such as water and effluent treatments [1, 2], drink clarification [3], biochemical processing [4], inorganic membrane technology grows in importance.

The use of ceramic membranes has many advantages such as high thermal and chemical stability, pressure resistance, long lifetime, good resistance to fouling, and ease of cleaning [5]. The main process to prepare ceramic membranes includes first the obtaining of a good dispersion of small particles and then, the deposition of such dispersion on a support by a slip casting method.

Unfortunately, ceramic membrane fabrication, even though commercially available, still remains highly expensive from a technical and economic point of view due to the use of expensive powders such as alumina, zirconia, titania and silica [6, 7]. To reduce the cost of ceramic membrane fabrication,

recent research works are focused on the use of cheaper raw materials such as apatite powder [8], natural raw clay [9–11] and waste materials such as fly ash [12–14].

This study is related to the fabrication of tubular ceramic membranes using kaolin clays. Corn starch powder was added as pore-forming agent to produce sufficient porosity with acceptable Mechanical property. The properties of porous membrane were discussed as a function of sintering temperature in order to optimize the preparation conditions. Their structural and functional properties are determined by different techniques. The most important parameters used in the characterization of these substrates are: surface and internal morphology, mean pore size, pore size distribution, porosity and water permeability. Mechanical and chemical stability study of the membrane is also performed to verify its application in highly corrosive medium. The prepared microfilter membranes were used for the treatment and the decoloration of cuttlefish effluent.

II. EXPERIMENTAL

2.1 Materials

In this study, the supports were prepared from clay. The clay used in the present study is a kaolin Codex (notes as K), it was recommended by the L.P.M Cerina (Laboratoire des Plantes Medicinales, Tunisia).

2.2 Characterization of the kaolin powder

The chemical composition of the kaolin Powder was determined by spectroscopic techniques, such as X-

ray fluorescence for metals and by atomic absorption for alkaline earth metals.
Phase identification was performed by XRD analysis (Philips X″Pert X-ray) diffractometer) with Cu Kα radiation (λ= 1.5406 A°), and the crystalline phases were identified by reference to the International Center for Diffraction Data cards.
Thermogravimetric analysis (TG) and differential thermal analysis (DTA) were carried out from ambient temperature to 1300°C at a rate of 10 °C min^{-1} under air, using a setaram SETSYS Evolution 1750. The particle size distributions of kaolin (K) were determined by the Dynamic Laser Scattering (DLS) technique.

2.3 Elaboration of the membranes

The elaboration of membranes implies the following sequence of operations:

- preparation of a plastic ceramic paste;
- shaping by extrusion;
- Consolidation by thermal treatment.

The process of the ceramic preparation was described in Figure 1.

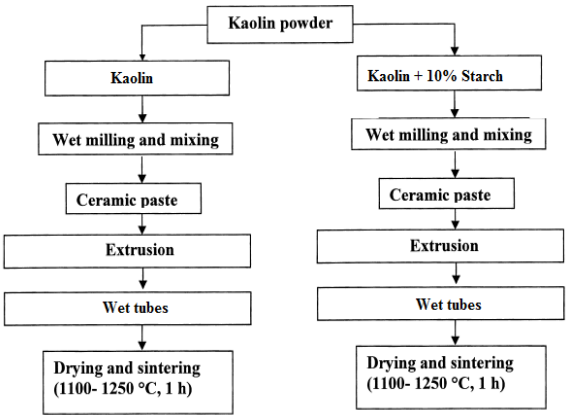

Figure 1. Schematic diagram describing the procedures, used in this work, for membrane preparation

The samples were synthesized from a mixture of kaolin and starch powders; this involves the preparation of a stable paste.
Before the extrusion phase, an ageing stage of the aqueous suspensions is necessary to obtain a good homogenous and to favor the formation of the porosity. This step is required to prepare a paste with rheological properties allowing the shaping by extrusion. To this end, the excess of liquid was eliminated and the obtained paste was kept in a closed plastic bag for 24 h under high humidity environment to avoid premature drying and ensure a homogeneous distribution of water.
After that, an extrusion technique is used to form tubular samples. For a good drying of these tubular samples, they are placed at room temperature on rotating aluminium rolls during 24h to ensure a homogenous drying and to avoid twisting and bending. Sintering was performed at a temperature ranging from 1100 to 1250 °C with a ramping rate of 2°C min^{-1} in order to avoid the formation of cracks during sintering of the samples. The temperature–time schedule not only affects the pore diameters and porous volume of the final product but also allows obtaining the final morphology and mechanical strength.
Tubular supports were elaborated with external/internal diameter of 10/5mm and the length of 150 mm.

2.4 Characterization of the membranes

The evolution of densification and surface quality of the membranes sintered at different temperatures were determined by scanning electron microscopy.
Porosity and pore size distribution were measured by mercury porosimetry. This technique is based on the penetration of mercury into a membrane″s pores under pressure. The intrusion volume is recorded as a function of the applied pressure and then the pore size was determined.
The mechanical resistance tests were performed using the three points bending method (LLOYD Instrument) to control the resistance of the membranes fired at different temperatures.
The corrosion tests were carried out using aqueous solutions of nitric acid (pH=2.5) and sodium hydroxide (pH=12.5) at 45 and 80°C, respectively. All the samples were ultrasonically rinsed in distilled water, dried at 110°C and stored in a dryer. The degree of corrosion was characterized by the percentage of the weight loss.
The tangential filtration experiments were performed using a home-made pilot plant at room temperature. It is equipped with a cross-flow filtration system implementing the tubular ceramic tubes of 15 cm length of this work. The transmembrane pressure (TMP) was controlled by the valve on the retentate side. The determination of the water membrane permeability was performed with distilled water.

2.5 Wastewater

Wastewater samples were taken from the effluents produced by a sea-product freezing factory located in Sfax, Tunisia. A large number of analyses were conducted on each sample and the following parameters were measured: turbidity, COD, temperature, pH and conductivity. The COD values of raw effluents from the production process ranged between 2000 and 3000 mgL^{-1} with an average concentration of 2615 mgL^{-1}. The turbidity measured for the raw effluent presents a very high value which is in the range of 335 NTU (Table 1).

Table 1. Turbidity, COD, conductivity and pH of raw effluents

Turbidity	COD ($mg.L^{-1}$)	Conductivity ($mS.cm^{-1}$)	pH
3	2615	204	7

III. RESULTATS AND DISCUSSION

3.1 Powder characterization

The chemical composition of kaolin is given in table 2, where the main impurities are CaO, K_2O and Fe_2O_3. It reveals that the major components were silica (SiO_2: 47.85%) and aluminium oxide (Al_2O_3: 37.60%).

Table 2. Chemical composition of the used kaolin (wt. %)

SiO_2	Al_2O_3	Fe_2O_3	MgO	K_2O	CaO	TiO_2
47.85	37.6	0.83	0.17	0.97	0.57	0.74

Phase identification is of great importance before any membrane manufacturing. For example, Figure. 2 presents the XRD patterns of the raw kaolin. It can be seen that kaolinite (K) was the major mineral component with a small amount of quartz (Q) and illite (I) impurities. No other components were observed, because the impurities are in so tiny quantity (table 2) and most of them are probably incorporated into the crystal structure of kaolinite.

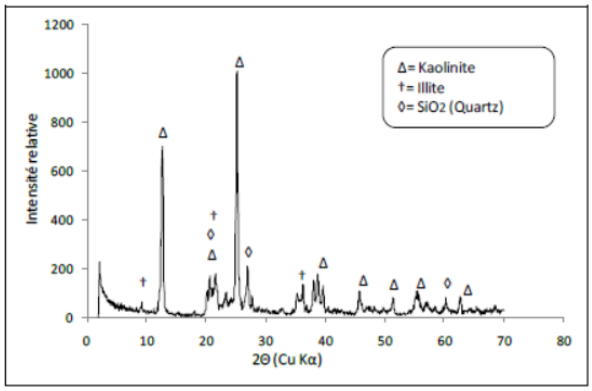

Figure 2. XRD pattern of the pure kaolin

A total weight loss is observed by TGA to be about 12% of kaolin (Figure. 3). In fact, the weight loss consists of two distinct stages: The first one is considered as a slight weight loss between room temperature and 150°C, because of the dehydration of the clay. The second mass loss detected between about 400 and 700°C is mainly due to the phenomenon of dehydroxylation of kaolinite confirmed by DTA which shows an endothermic peak at 560°C leading to the transformation of kaolinite to metakaolinite.
A third stage, which is characterized by an exothermic reaction appeared at about 975°C without any weight loss, might be attributed to the nucleus formation of spinel or mullite. The particle size distribution of kaolin was determined by the Dynamic Laser Scattering (DLS) technique, and the results shown in Figure 4. This method gave an average particle size in the order of 3, 8 µm.

3.2 Membrane Characterization

For the development of high-quality membranes, the following properties are of major importance: pore size distribution, porosity, surface texture, mechanical properties and chemical stability.

3.2.1. Scanning electron microscopy (SEM)

Figure 5 illustrates SEM pictures for the membrane sintered at the four different temperatures considered in this work. The optimal sintering temperature was determined by comparing the texture of the different obtained samples.

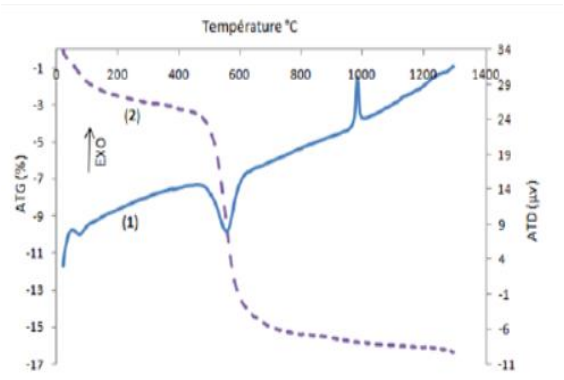

Figure 3 TGA–DTA data of the kaolin powder.

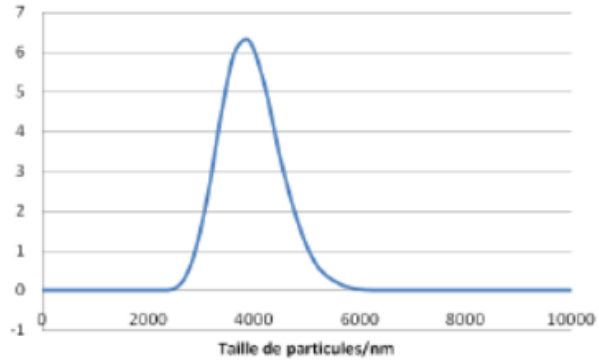

Figure 4. Particle size distribution of kaolin.

The ceramic substrates sintered at lower temperature (1100 °C and 1150 °C) show highly porous structure. Below 1100 °C, we detect the presence of intergranular contacts which are large enough to ensure ceramic cohesion (beginning of sintering).
The membrane sintered at 1200 °C and 1250 °C are more consolidated due to the fact that for sintering temperatures over 1200 °C, the particles agglomerate together creating more dense ceramic body. As a result the porosity of the membrane decreases with an increase in sintering temperature.
The obtained results (Figure. 6) show that the starch addition to kaolin has a positive effect on the porosity ratio of membranes compared to those prepared from kaolin alone.

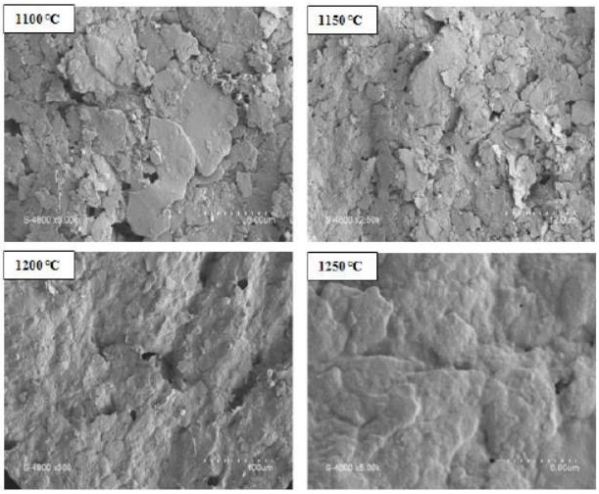

Figure 5. SEM of membranes sintered at different temperatures.

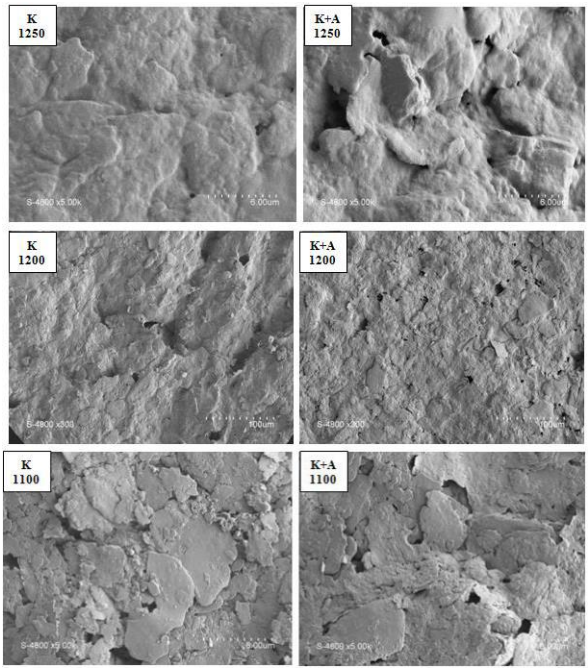

Figure 6. SEM micrographs of kaolin and kaolin +10 wt% starch samples

3.3 Mercury porosimetry

The evolution of the membrane characteristics (pore diameter and porosity) as a function of the sintering temperature is shown in Figures 7 and 8.

The evolution of the average pore diameter and the porosity reveals that the porosity decreases from 44 to 27% between 1150°C and 1250°C, while the pore diameter increased from 0.41 to 0.73 µm. This behavior corresponds to an opening of the pores in the same as a material densification occurring when the temperature increases.

Moreover, it can be said that both the mean average pore size and the porous volume are closely related to the preparation method.

The obtained results show that the starch addition to kaolin has a positive effect on the porosity ratio of membranes example, the kaolin (K) membrane had a porosity ratio of 27% and an average pore size of about 0.73 µm, whereas the kaolin + 10 wt% starch (K+S) membrane had a porosity ratio of 36% and an average pore size of about 1.41 µm, for samples sintered under the same conditions (at 1250°C for 1 hour).

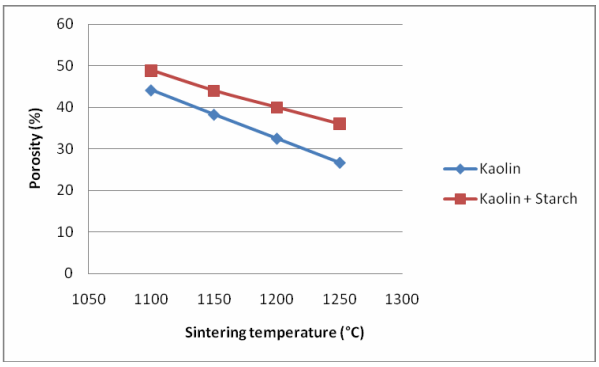

Figure 7. Porous volume (%) versus sintering temperature for kaolin (K) and kaolin +10% starch (K+S) samples.

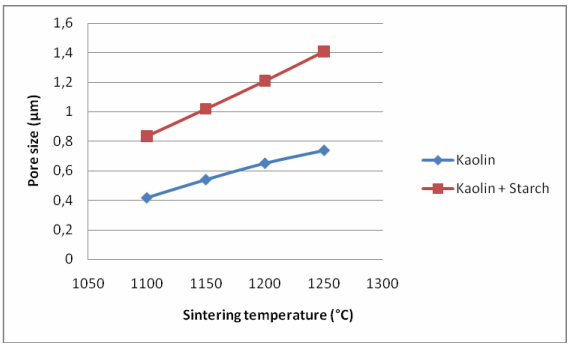

Figure 8. Average pore size versus sintering temperature for kaolin (K) and kaolin +10% starch (K+S) samples.

The membranes fired at 1250°C and tested by mercury porosimetry showed pore diameters centered near 0.73 µm and 27 % of porosity. Furthermore, the pore size distribution of the membrane is a single (mono) distribution modal as illustrated in Figure. 9. This is a clear indication that the samples have a uniform pore size distribution.

The average pore diameters of membranes are determined to be 0.4, 0.70, 0.8 and 1.41 µm for membranes (Kaolin and Kaolin+ Starch) sintered at 1100 °C, 1250 °C respectively corresponding to the micro-filtration range.

3.4 Mechanical resistance

Figure. 10 shows the variation of tensile strength with sintering. In accordance with the SEM pictures and the porosity values, the increase of the sintering temperature is accompanied with a densification phenomenon and consequently an increase in the tensile strength from 4 MPa at 1000 °C to 28MPa at 1250°C.

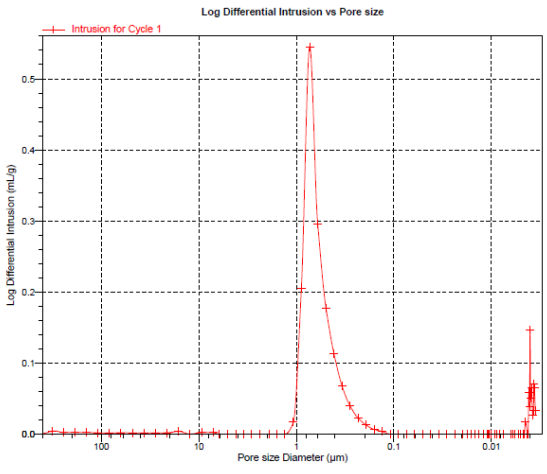

Figure 9. Pore size distribution in kaolin samples sintered at 1250°C for 1 hour.

As shown in Fig.10,the flexural strength values of the porous kaolin samples without pore former addition were higher than those of porous kaolin + organic additive samples. This figure shows that the flexural strength is closely related to the total porosity ratio whichisin turn sintering temperature-dependent.

For example, flexural strength was 28.41 MPa at a

porosity of 27% and an average pore size of 0.73 µm, whereas flexural strength was about 21 MPa for k+S supports having a porosity ratio of 36% and an average pore size of1.41 µm. Both K and K+S supports were sintered at 1250°C for 1 hour.

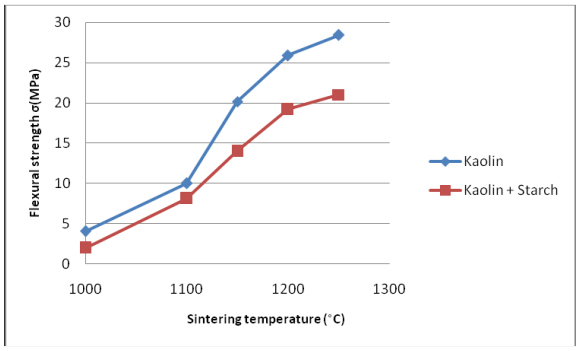

Figure 10. Flexural strength as a function of sintering temperature for kaolin (k) and kaolin + 10 wt% starch (k+S) samples

The strength of kaolin ceramic membrane sintered at 1250°C is about 28.41 MPa. Such resistance is high enough to achieve filtration. Thus, membrane support sintered at 1250°C for 1 hour (average pore diameter of 0.73 µm and 27 % of porosity) was retained for corrosion tests and filtration study.

3.5 Chemical resistance

The weight loss due to the corrosion byacids and alkali is shown in Figure 11. It can be seen that the membrane shows a better acid corrosion resistance, since itsmass loss is much lower than those of supports after alkali corrosion. Therefore, the observed results in weight loss during corrosion tests suggest that the prepared support possesses a good chemical corrosion resistance and it is suitable for applications involving acidic and basic media.

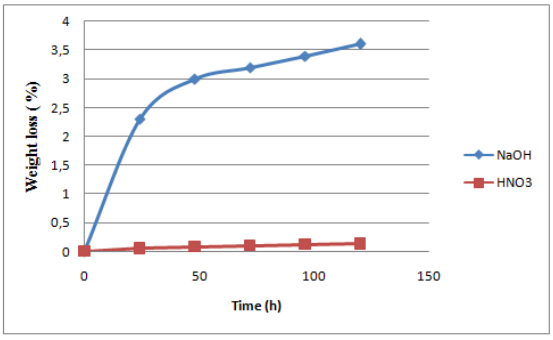

Figure 11. Weight loss of membranesin nitric acid (45°C) and soda solutions (80°C) as a function of time.

3.5 Determination of membrane permeability

The permeability of membranes was determined from the values of flux measured after stabilization for each operating pressure. It can be seen that the pure water flux increases with increasing the applied pressure (Figure 12). The membrane permeability ‘‘Lp’’ was found to be equal to 20 l/h m^2bar.

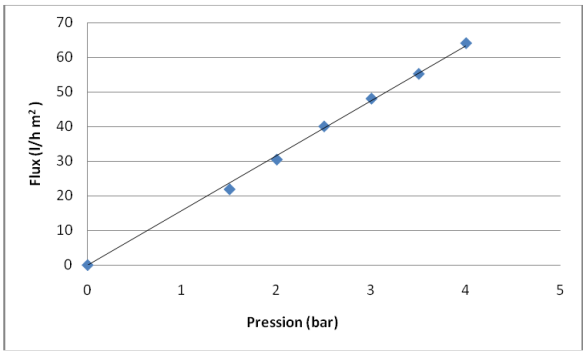

Figure 12. Pure water flux versus operating pressure.

IV. APPLICATION TO THE TREATMENT OF CUTTLEFISH EFFLUENTS

Microfiltration test carried out by keeping constant the initial concentration of the raw effluent by returning both permeate and retentateto the feed reservoir. Fig. 13gives the variation of permeate flux with transmembrane pressure. Permeate flux increased with transmembrane pressure until a value of 4 bars and then stabilized at a value of 25 l/h.m^2. This behavior can be explained by the formation of a concentrated polarization layer.

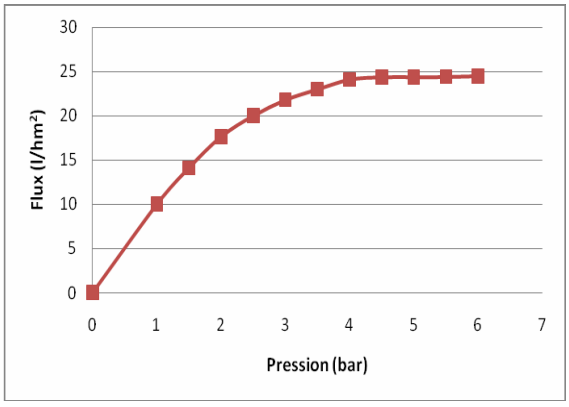

Figure 13. Variation of the permeate flux vs transmembrane pressure

The flux decreased slightly from 43 to 20 l/hm2 during 60 min when operated at 3 bar TMP (Fig. 14). Then it leveled off over time. The flux evolution corresponds to a decline of about 54%.

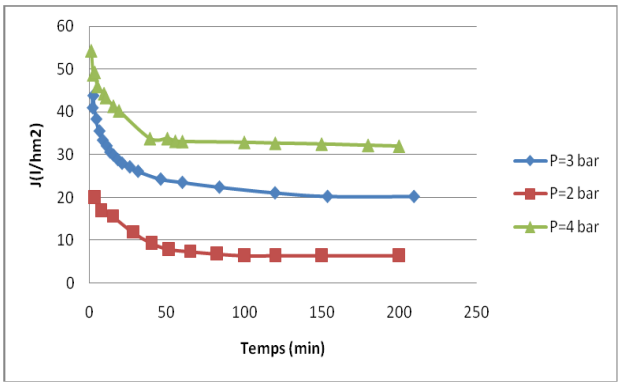

Figure 14. Variation of the permeate flux with time of filtration

Table 3 shows that the quality of permeate seems to be highly satisfactory in term of turbidity and COD reduction in the case of filtration using kaolin membranes. The retention of turbidity was about 99 % when operated at 3 bar TMP. It can be observed a very significant decrease of COD (70%). The conductivity is also reduced by almost 20%.

Table 3. Characteristics of the effluent before and after filtration on kaolin membranes.

	Pressure (bar)	Turbidity (NTU)	COD (mg L^{-1})	Conductivity (mS cm^{-1})
Raw effluents		335	2615	204
Filtrate	2	086	6995	150
	3	1;10	777.8	166
	4	2	862.6	170

IV. CONCLUSION

In this work, a comprehensive study on the fabrication and characterization of ceramic membrane from kaolinand starch mixtures were performed. The membranes were prepared by the extrusion procedure.

Ceramic membrane manufactured from kaolinand starch mixtures presented features of porosity (porous volume and average pore size) with values significantly higher than those elaborated from kaolin alone. It has also been found that the pore structure may be controlled by the sintering temperature.

The prepared membranes sintered at 1250 °C offer a better mechanical strength (28MPa compression strength), chemical stability (<5% weight loss in acidic media and negligible weight loss in acidicmedia),good porosity (27%) and a higher average pore size (0.73 μm). The application of this membrane to the washing cuttlefish effluent treatment shows good performances in term of permeate flux and pollutant rejection. These membranes can also be used as a support for ultrafiltration layer.

ACKNOWLEDGMENT

Authors would like to thank IEM (Institut Européen des Membranes), UMR 5635 (CNRS-ENSCM-UM), Université de Montpellierfor their help to carry out the analysis.

REFERENCES

[1] M. Ebrahimi, K. Shams Ashaghi, L. Engel,D. Willershausen, P. Mund, P. Bolduan, and P. Czermak, "Characterization and application of different ceramic membranes for the oil-field produced water treatment," *Desalination*, 2009, pp.533–540.

[2] S. Masmoudi, R. BenAmar, A. Larbot, H. El Feki, A. Ben Salah, L. Cot, "Elaboration of inorganic microfiltration membranes with hydroxyapatite applied to the treatment of waste water from sea product industry",*J. Membr.Sci.*247, 2005, pp.1–9.

[3] B.K. Nandi, B. Das, R. Uppaluri, M.K. Purkait, "Microfiltration of mosambi juice using low cost ceramic membrane", *J. Food Eng. 95*, 2009, pp. 597–605.

[4] P.M. Kao, S.C. Huang, Y.C. Chang, Y.C. Liu, "Development of continuous chitinase production process in a membrane bioreactor by Paenibacillus sp", *Process Biochem*. 42, 2007., pp.606–611.

[5] K. Li, "Ceramic Membranes for Separation and Reaction", *John Wiley and Sons Ltd*, West Sussex, England, 2007.

[6] Wang, Y.H., Tian, T.F., Liu, X.Q., Meng, G.Y., 2006. "Titania membrane preparation with chemical stability for very hash environments applications". *J. Membr. Sci.* 280, pp. 261–269.

[7] Yoshino, Y., Suzuki, T., Nair, B.N., Taguchi, H., Itoh, N., 2005. "Development of tubular substrates, silica based membranes and membrane modules for hydrogen separation at high temperature". *J. Membr. Sci*. 267, 8–17.

[8] S. Masmoudi, A. Larbot, H. El Feki, R. Ben Amar, "Elaboration and characterization of apatite based mineral supports for microfiltration and ultrafiltration membranes", *Ceram. Int*. 33, 2007, pp. 337–344.

[9] N. Saffaj, M. Persin, S.A. Younsi, A. Albizane, M. Cretin, A. Larbot, "Elaboration and characterization of microfiltration and ultrafiltration membranes deposited on raw support prepared from natural Moroccan clay: application to filtration of solution containing dyes and salts", *Appl. Clay Sci.31,* 2006, pp.110–119.

[10] L. Palacio, Y. Bouzerdi, M. Ouammou, A. Albizane, J. Bennazha, A. Hernández, J.I. Calvo, "Ceramic membranes from Moroccan natural clay and phosphate for industrial water treatment", *Desalination 245*, 2009, pp. 501–507.

[11] B.K. Nandi, B. Das, R. Uppaluri, M.K. Purkait, "Microfiltration of mosambi jui using low cost ceramic membrane", *J. Food Eng. 95,* 2009, pp. 597–605.

[12] S. Jana, M.K .Purkait, K. Mohanty, "Preparation and characterization of low-cost ceramic microfiltration membranes for the removal of chromate from aqueous solutions", Appl. Clay Sci.47 , 2010, pp. 317–324.

[13] P.K. Tewari, R.K. Singh, V.S. Batra, M. Balakrishnan, "Membrane bioreactor (MBR) for waste water treatment: filtration performance evaluation of low cost polymeric and ceramic membranes", *Sep. Pur. Technol.* 71, 2010, pp. 200–204.

[14] Y. Dong, X. Liu, Q. Ma, G. Meng, "Preparation of cordierite-based porous ceramic micro-filtration membranes using waste fly ash as the main raw materials", *J. Membr. Sci*. 285, 2006, pp. 173–181.

African Membrane Society
Water & Environment, Process, Energy
Sfax, Tunisia, May 3-5, 2016 - Membrane Water Treatment in Small Urban and Village Centers

Adoucissement des Eaux Saumâtres par Membrane de Nanofiltration NF270
Etude de la Rétention et des Mécanismes de Transport

Mohamed Aiman KAMMOUN[1], Sana GASSARA[2], André DERATANI[2], et Raja BEN AMAR

[1]*Faculté des Sciences de Sfax, Laboratoire des Sciences des Matériaux et Environnement, Route de Soukra km 4, 3018 Sfax, Tunisie*
[2]*Institut Européen des Membranes, Université Montpellier 2, cc 47, Place E. Bataillon, 34095 Montpellier, Cedex 5, France*
mohamadaymankamoun@gmail.com

Résumé : L'objectif de notre travail est de déterminer les performances et la sélectivité de la membrane commerciale de nanofiltration (NF270). Les résultats ont montré que la sélectivité de la membrane dépend respectivement par ordre de prédominance de l'effet de charge, de la pression et de la taille moléculaire des solutés traités : les ions divalents sont mieux retenus que les ions monovalents, la rétention est plus importante à des fortes pressions et les ions les plus petits sont les mieux filtrés. D'autre part, l'effet du taux de conversion sur le taux de rétention est étudié à faible et à forte pression. A basse pression, l'influence de l'augmentation du taux de conversion sur la rétention des ions Mg^{2+}, Ca^{2+} et Na^{+} était positive et plus visible pour les ions monovalents et les ions de grande taille. A forte pression, le taux de conversion n'avait pas d'influence sur les taux de rétention des ions SO_4^{2-}, Mg^{2+}, Ca^{2+} et Na^{+}. L'effet Donnan était présent dans membrane par le passage considérable des ions Cl^{-} aux perméats et des taux de rétention négatifs, à faible pression et à des taux de conversion supérieur à 30%.

Mots clés : nanofiltration, adoucissement, effet de charge, diffusion, convection.

I. INTRODUCTION

Les membranes de nanofiltration présentent une alternative au procédé d'osmose inverse. Plus que le gain en termes d'énergie, les procédés de nanofiltration ont montré une efficacité remarquable dans plusieurs domaines d'application tels que le traitement des eaux usées, des eaux potables, des eaux colorées et des eaux saumâtres [1]. L'adoucissement des eaux saumâtres fait partie des domaines qui font appel aux procédés de nanofiltration. Le but principal de ce travail est d'étudier les mécanismes de transfert dans le cas de l'adoucissement des eaux saumâtres par nanofiltration, évaluer l'influence des paramètres opératoires et des propriétés des solutés sur la sélectivité de la membrane et classer ses effets selon l'ordre d'importance. Pour ce fait, une membrane commerciale de nanofiltration, N270, a été choisie pour filtrer une solution aqueuse modèle contenant un mélange de sels avec des proportions très proches des celles d'une eau saumâtre de la région de Sfax.

II. MATERIELS ET METHODES

2.1 Produits chimiques

Des solutés neutres de types poly éthylène glycol PEG de faibles masses molaires (de 62.06 à 194,23 Da) ont été utilisés pour la détermination du seuil de coupure de la membrane utilisée. Ces produits ont été fournis par Sigma-Aldrich. La solution saline modèle a été composée de NaCl et $CaCl_2$ (CARLOERBA group), Na_2SO_4 (SDS) et $MgSO_4$ (Merck eurolab). Tous ces produits chimiques sont de grade analytique.

2.2 Boucle de nanofiltration

Le pilote de nanofiltration tangentielle est présenté sur la Fig. 1. Il est composé d'une cellule de filtration SEPA CF (Sterlitech) accueillant des membranes planes de 9.5 cm de largeur et de 13.5 cm de hauteur, ce qui correspond à une surface utile de 140 cm². Les membranes sont toujours positionnées la surface active en contact avec la solution d'alimentation. Le système de filtration est constitué aussi d'un réservoir thermostaté de capacité de 5 L, une pompe volumétrique pour assurer le transport de la solution d'alimentation du réservoir vers la cellule de filtration et deux manomètres P1 et P2 pour contrôler les pressions d'entrée et de sortie de la solution d'alimentation au et de la cellule de filtration. On trouve aussi une vanne pour régler la pression transmembranaire appliquée. Le débit de l'eau pure était fixé à 7.9 L min^{-1}.

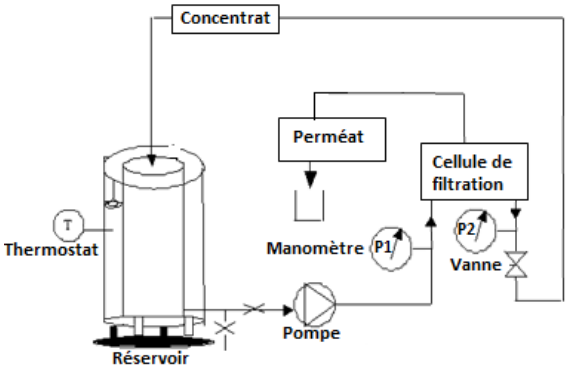

Figure 1. Représentation schématique du pilote de nanofiltration

2.3 Analyses des solutions

Après chaque essai de nanofiltration, le perméat et le rétentat récupérés ont été analysés par réfractomètre dans le cas des solutés neutres et par chromatographie ionique pour le dosage des ions.

2.4 Caractérisations de la membrane

Une observation microscopique à balayage électronique (MEB) a été réalisée pour étudier la structure de la surface membranaire. L'appareil utilisé est Hitachi S-4500 avec effet de champ de résolution de 1,5 nm à 15 kV. Une vue transversale d'une coupe de membrane a été faite aussi pour observer les propriétés structurales de la membrane telle que l'épaisseur de sa couche active et sa morphologie. Les images obtenues ont été traitées par un logiciel appelé Image J. En plus, une analyse de la charge de surface a été faite en utilisant un appareil de potentiel d'écoulement SurPass, Anton Paar.

2.4 Mesures de la performance de la membrane :

2.4.1 Perméabilité hydraulique : D'après Darcy, la perméabilité à l'eau pure. (LP en L h^{-1} m^{-2} bar^{-1}) se définit par la relation suivante [2]:

$$L_p = \frac{J_v}{\Delta P} \quad (1)$$

où ΔP est la pression transmembranaire en bar et Jv est le flux volumique de l'eau en $Lh^{-1}m^{-2}$.

2.4.2 Taux de rétention et taux de conversion

Le taux de rétention R(%) caractérise la sélectivité d'une membrane. Il est déterminé par l'équation (2) :

$$R = \left(1 - C_p / C_R\right) * 100 \quad (2)$$

Avec C_P et C_R représentent les concentrations du perméat et du rétentat respectivement.

Le taux de conversion Y (%) est définit par l'équation (3) :

$$Y = \left(Q_p / Q_o\right) * 100 \quad (3)$$

Avec Q_P et Q_0 représentent respectivement le débit du perméat et le débit initial.

2.4.3 Seuil de coupure : Le seuil de coupure d'une membrane correspond à la masse molaire d'un soluté retenu à 90 %. Ce paramètre a été étudié pour la membrane NF270 en filtrant des solutions simples de 1 g.L-1 de PEG de masses molaires pour déterminer leurs taux de rétention.

2.5 Mécanismes de transport

Les mécanismes de transport dans la nanofiltration sont le transfert par convection et le transfert par diffusion. Ainsi, on peut exprimer le flux de soluté Js comme la somme d'un terme de diffusion et d'un terme de convection forcée :

$$J_s = J_{diff} + J_v C_{conv} = C_p J_v \quad (4)$$

$$Cp = J_{diff} / J_v + C_{conv} \quad (5)$$

Où *Jv* et *Js* représentent respectivement les flux de solvant et de soluté, J_{diff} est le flux de soluté transporté par diffusion et C_{conv} est la concentration de soluté dans le perméat due à la convection forcée. Le flux de solvant peut être calculé à l'aide de l'équation suivante :

$$J_v = L_p\left(\Delta P - \sigma \Delta \pi\right) \quad (6)$$

Avec Δπ (en bar) est la différence de pression osmotique de part et d'autre de la membrane, σ (en m/s) est le coefficient de réflexion de la membrane.

Ainsi, pour déterminer la concentration dans le perméat due à la convection forcée et le flux diffusionnel d'un soluté dans le perméat, on trace la courbe CP = *f*(1/ JV). On obtient une droite dont l'ordonnée à l'origine représente la concentration C_{conv} et la pente représente le flux diffusionnel J_{diff}. Cette représentation permet d'évaluer la contribution de chaque mécanisme dans le transport des solutés.

III. RESULTATS ET DISCUSSION

3.1 Caractérisations physico-chimiques de la membrane NF270

Une série de caractérisations a été réalisée sur la membrane NF270 pour connaitre ses propriétés physico-chimiques et estimer ses performances de filtration.

3.1.1 Observation MEB : La Fig. 2 présente les photos MEB réalisées sur une surface et une section de la membrane NF270. Ces images ont été faites à deux grandissements différents (2500 et 50000 fois).

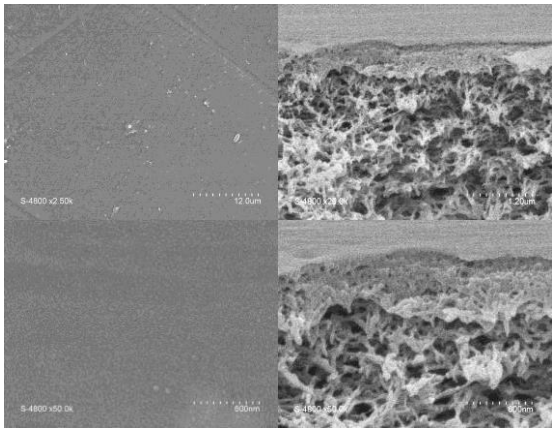

Figure 2 : Photos MEB de surface filtrante (à gauche) et une section (à droite) de la membrane NF270 à deux grandissement 2500 et 50000 fois.

D'après la Fig. 2, la membrane NF270 est caractérisée par une surface filtrante lisse et homogène. Avec la limitation du champ de résolution du MEB, aucun pore n'a été détecté même à un fort grandissement. En regardant les photos MEB de section, cette membrane possède une structure asymétrique avec une couche superficielle fine et dense superposée sur un support

contenant des macrovides. La couche dense est appelée couche active et elle a une épaisseur d'environ 480 nm.

3.1.2. Potentiel zêta de la membrane NF270 : Comme on peut voir dans la Fig. 3, la membrane NF270 est caractérisée par sa charge négative sur presque toute la gamme de pH utilisée avec un point isoélectrique à un pH proche de 3.

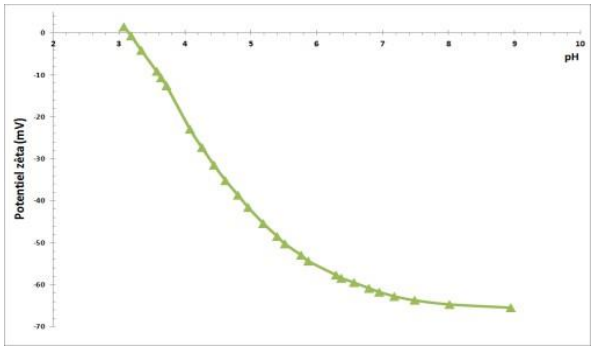

Figure 3. Évolution du potentiel zêta de la membrane NF270 en fonction du pH.

3.1.3. Perméabilité hydraulique : La perméabilité à l'eau pure de la membrane est déterminée à une température égale à 25°C. La figure 4 exhibe l'évolution du flux à l'eau en fonction de la pression. L'augmentation linéaire du flux avec la pression prouve bien la bonne stabilité de la membrane à des pressions plus élevée. La membrane utilisée dans ce travail est caractérisée par une perméabilité à l'eau de 19.8±0.2 L h^{-1} m^{-2} bar^{-1}.

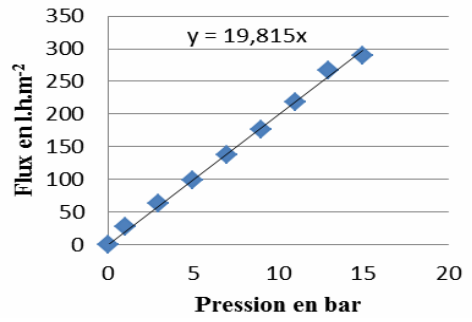

Figure 4. Perméabilité hydraulique de la membrane NF270 à 25°C.

3.2 Adoucissement des eaux saumâtres par NF270

Une solution saline modèle a été préparée contenant une concentration en sels de 2.215 gL^{-1} et de pH égal à 6.2. Sa composition ionique a été détaillée dans le tableau 1.

Table 1. Composition ionique de la solution saline

Ions	Na^+	Cl^-	SO_4^{2-}	Ca^{2+}	Mg^{2+}
mgL^{-1}	570.5	500	1000	74	77

3.2.1. Effet de la pression : La figure 5 présente l'évolution du taux de rétention de chaque soluté ionique en fonction de pression. Dans tous les cas des ions utilisés, le taux de rétention augmente progressivement avec la pression pour atteindre un plateau à 10 bar. Ce phénomène est caractéristique des expériences de NF. En effet, le mécanisme de transport en NF fait intervenir la diffusion et la convection : la participation de la diffusion intervient à faible flux de perméat (pression faible) alors que celle de la convection devient prépondérante avec des flux forts provoqués par une forte pression appliquée. Dans ce dernier cas, la rétention est plus élevée car le phénomène de diffusion dans les pores est limité.

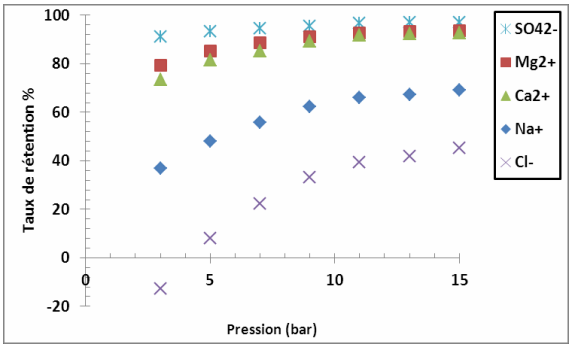

Figure 5. Evolution du taux de rétention en fonction de la pression pour les différents ions

Dans ce dernier cas, la rétention est plus élevée Dans le but de confirmer ce mécanisme de transfert, la concentration des ions transmis par convection dans le perméat et du flux de diffusion ont été déterminés pour chaque type d'ion et à chaque pression appliquée et les résultats obtenus ont été présentés dans la Fig. 6. Dans le but de confirmer ce mécanisme de transfert, la concentration des ions transmis par convection dans le perméat et du flux de diffusion ont été déterminés pour chaque type d'ion et à chaque pression appliquée et les résultats obtenus ont été présentés dans la Fig. 6.

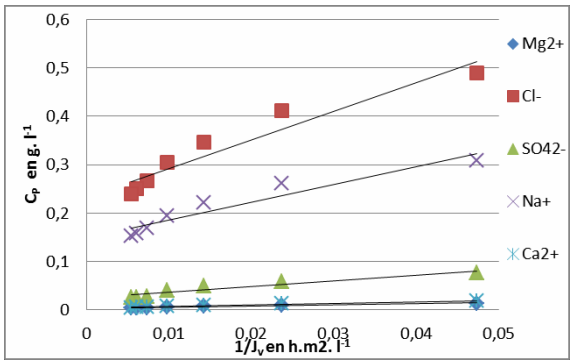

Figure 6. Évolution de la concentration des ions dans les perméats en fonction de l'inverse du flux de solvant.

D'après la Fig. 6, la Cp augmente d'une manière linéaire avec la diminution du flux du solvant. Le flux de chaque ion transporté par diffusion (J_{diff}) correspond à la pente chaque droite tracée dans la Fig. 6 et l'intersection de ces droites avec l'axe des ordonnées donne la concentration C_{conv}. Le tableau 2 rassemble toutes les valeurs de J_{diff} et C_{conv} déterminées pour chaque type d'ion.

D'après le tableau 2, les ions monovalents sont beaucoup mieux transportés par diffusion que les ions

divalents : (Cl^{-}>Na^{+}>$SO4^{2-}$>Ca^{2+}>Mg^{2+}). Ces résultats sont cohérant avec ceux présentés dans la Fig.5 où on voit bien la grande sensibilité de la rétention des ions monovalents avec l'augmentation de la pression (dans la zone de faible pression) par rapport à la rétention des ions bivalents. Donc, à basse pression, le transport des solutés se fait principalement par diffusion.

Table 2. Valeurs expérimentales du flux de diffusion et de la concentration due à la convection

Ions	C_{conv} (g.l^{-1})	J_{diff} (g.h^{-1}.m^{-2})
Cl^{-}	0.234	5.9
Na^{+}	0.1502	3.6
SO_4^{2-}	0.0241	1.2
Ca^{2+}	0.0041	0.3
Mg^{2+}	0.0036	0.23

Par contre, à une pression supérieure ou égale à 10 bar, l'augmentation du flux de solvantest plus important que l'augmentation du flux desolutés. Lessolutésse partagentdans un volume plus important. Le perméat est alors moins concentré et le taux de rétention plus important. A partir de la pression 10 bar, le terme de transport par convection devient plus significatif, l'augmentation du flux de solutés suit l'augmentation du flux du solvant. D'où la stabilisation des valeurs des taux de rétention. Le transport des ions suit l'ordre de l'énergie d'hydratation (Cl^{-}> Na^{+}> $SO4^{2-}$> Ca^{2+} > Mg^{2+}). En effet, le flux de diffusion est fonction de l'énergie d'hydratation et l'ion possédant l'énergie d'hydratation la plus faible est le mieux transporté [3]. Ainsi, on a remarqué que les valeurs des termes de transport ne suivent pas celles des taux de rétention pour le cas des ions $SO4^{2-}$ vis-à-vis aux ions Ca^{2+}et Mg^{2+}. Cela peut être expliqué par l'effet de la concentration initiale élevé des ionsSO42-etparl'effet de la pression[4].

3.2.2 Effet de charge : Ions monovalents et divalents
Pour des ions de même charge et de tailles moléculaires presque égales (Mg^{2+} et N^{a+}), on a vu que la rétention des cations Mg^{2+} est plus importante que celle des cations N^{a+} (figure 5). On peut conclure que la rétention des ions divalents est plus importante que celle des ions monovalents.
Ceci est d'autant plus vrai que la pression est plus faible. Cette constations s'explique par le fait que les ions divalents possèdent une énergie d'hydratation plus importante entraînant ainsi une augmentation de rétention. Dans la Fig. 5, on observe aussi que les sulfates sont les ions les plus retenus avec un taux de rétention maximal de 97 % à 15 bar. Or, d'après la Fig. 3, la surface de la membrane NF270 est chargée négativement avec une valeur de -60 mV à pH 6.2, le pH de la solution à filter. Donc, le fort rejet de cet anion peut être expliqué par sa favorisation en tant que co-ions de la membrane. Par contre, la forte rétention des cations bivalents Mg2+ et Ca2+ qui sont des contre-ions de la membrane peut être due essentiellement au phénomène d'électroneutralité des charges de part et d'autre de la membrane.

3.2.3 Effet de la taille moléculaire : Pour deux ions de même charge et de même polarité, la masse molaire de Mg^{2+} est inférieure à la masse molaire Ca^{2+} est inférieure à la masse molaire Ca^{2}. Cependant, la rétention des ions Mg^{2+} est légèrement supérieure à celle des ions Ca^{2+} (fig 5). On peut conclure que les petits ions sont mieux retenus. Ceci est plus visible pour les faibles pressions.

*3.2.4 Effet Donnan :*Pour respecter l'électroneutralité du milieu, certains ions doivent passer à travers la membrane au perméat (mécanisme de Donnan) ; les ions monovalents passeront préférentiellement aux ions multivalents. Nous avons observé, dans notre cas, un taux de rétention des ions Cl- négatif à faible pression (fig5). Les ions Cl- vont assurer l'électroneutralité du milieu. Ils sont repoussés par le gradient électrique qui est négatif à l'intérieur de la cellule. Un équilibre doit être donc atteint entre le gradient chimique et le gradient électrique.

*3.2.5 Effet du taux de conversion :*Pour étudier l'effet du taux de conversion, nous avons choisi de travailler sur deux niveaux de pression.
A : à faible pression: P=5 bar

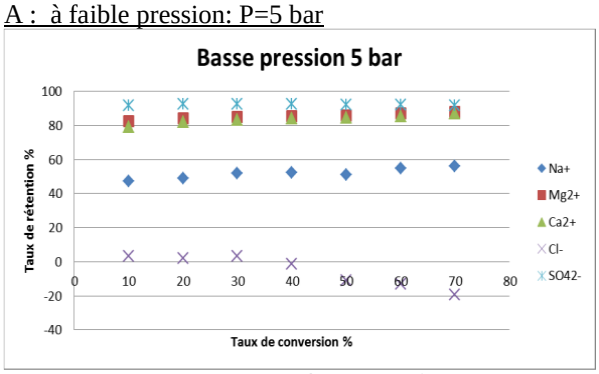

Figure 7.Evolution du taux de rétention en fonction du taux de conversion à faible pression pour les différents ions

La rétention des cations augmente avec l'augmentation du taux de conversion (fig 7). Cette augmentation est plus visible pour les ions monovalents (Na^{+}) et les ions de grandes tailles (Ca2+). D'autre part, la rétention des cations SO_4^{2-} ne dépend pas du taux de conversion. Elle garde une valeur constante au tour de 92%. Cette tendance montre l'efficacité de cette membrane vis-à-vis l'élimination des ions SO_4^{2-}. Cependant, la rétention des ions Cl-diminue en augmentant le taux de conversion jusqu'à atteindre des valeurs négatives. C'est l'effet Donnan. L'augmentation du taux de conversion favorise le déséquilibre de charge entre les deux milieux de la cellule membranaire.
B : à forte pression: P=15 bar

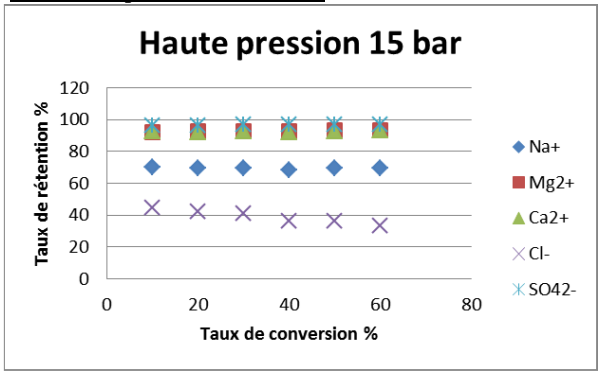

Figure 8.Evolution du taux de rétention en fonction du taux de conversion à faible pression pour les différents ions

A haute pression, les taux de rétention des ions Na^+, Mg^{2+}, Ca^{2+} et de SO_4^{2-} se sont stabilisés des valeurs maximales. A ce niveau de pression, le taux de conversion n'a pas d'effet considérable sur la rétention de cesions(fig 8). En revanche, nous remarquons l'absence du phénomène d'écrantage même pour des taux de conversion important.
Néanmoins, pour les ions Cl-, on a observé une diminution du taux de rétention en fonction du taux de conversion.Ceci est expliqué L'augmentation du taux de conversion favorise le déséquilibre de charge entre les deux milieux de la cellule membranaire.

3.2.5.3 Influence du taux de conversion sur le mécanisme de transport
L'augmentationdu taux de conversion favorise le transport par convection à lafaveur du transport par diffusion (fig 9).

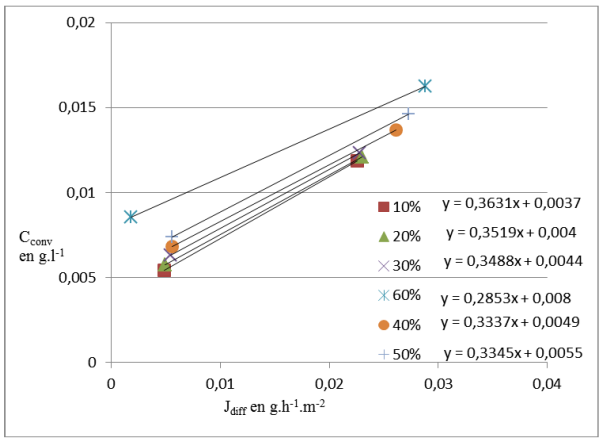

Figure 9.Évolution de la concentration du perméat en fonction de l'inverse du flux de solvant pour le Mg^{2+}aux différents taux de conversion

3.2.6 Ordre d'importance des effets étudiés :
Effet de la taille moléculaire VS Polarité des ions:
La rétention des ions Mg^{2+} et Ca^{2+} est plus importante que celle des ions Na^+. Les ions Na^+ sont plus petits que les ions Na+. L'effet de charge est dominant sur l'effet de la taille moléculaire. Tous les essais de nanofiltration ont montré que les ions bivalents SO_4^{2-}, Ca^{2+}, Mg^{2+} sont mieux retenus que les ions monovalents Cl^- et Na^+.

Effet de la pression VS Polarité des ions :
La rétention de l'anion SO_4^{2-} est plus importante que celle de Cl-. La rétention de SO42-à basse pression est plus importante que la rétention de l'anion Cl-à haute pression. Tous les essais de nanofiltration ont montré que la rétention des ions bivalents à basse pression est plus importante que la rétention des ions monovalents à hautes pression. L'effet de charge est plus considérable que l'effet de la pression.

Effet de la pression VS la taille moléculaire:
Dans le cas des deux ions Mg^{2+} et Ca^{2+}, la rétention des ions Mg^{2+} les plus petits, est plus importante pour la même gamme de pression. Néanmoins, la rétention des ions Ca^{2+} devient plus important que celle de Mg^{2+} si on utilise une basse pression pour Mg^{2+} et une forte pression pour Ca^{2+}. L'effet de la pression est plus considérable que l'effet de la taille moléculaire.

IV. CONCLUSION

Pour conclure, on peut classer les critères de sélectivité de la membrane NF270 en ordre de prédominance: l'effet de charge, la pressionet la taille moléculairedu soluté. La membrane NF270 est caractérisée par une haute sélectivité pour les ions divalents. La sélectivité de la membrane vis-à-vis aux ions monovalents et aux ions de grandes tailles est meilleur à faible pression.
Cette membrane peut adoucisse une eau de salinité 2.215 g.l-1à une eau potable de salinité égale à 0.47g.l-1à une moyenne pression qui ne dépasse pas 10 bar.

REFERENCES

[1] A. Lhassani, M. Rumeau, D. Benjelloun, M. Pontie, *Water Res*. 35, 3260, 2001.
[2] R. Bird. W. Stewart,E. Lightfoot, *"Transport Phenomena (Chapter IV)",* Wiley, New York, USA, 1960
[3] K. Mehiguence, G. Garba, S. Taha, N. Gondrexon, G. Dorange, Sep. *Purif. Technol*. 15, 181, 1999.

African Membrane Society
Water * Environment, Process, Energy
Sfax, Tunisia, May 3-5, 2016 - Membrane Water Treatment in Small Urban and Village Centers

L'Appoint des Energies Renouvelables au Dessalement

Nachida KASBADJI MERZOUK, Zahia TIGRINE et Djillali TASSALIT

Unité de Développement des Equipements Solaires, UDES Centre de Développement des Energies Renouvelables, CDER Bou Ismail 42415, W. Tipaza, Algeria
nkmerzouk@gmail.com

Résumé : La présente étude porte sur l'analyse du coulage du dessalement avec les énergies renouvelables. Pour cela, un état des capacités en énergie renouvelable dans le monde sera présenté en mettant en relief l'évolution en matière législatif, investissement, environnement et énergie en Afrique. Par ailleurs, plusieurs pays qui souffrent de stress hydrique se sont tournés vers le dessalement des eaux de mer. Malheureusement cette technologie est énergivore et non respectueuse de l'environnement. Les possibilités offertes par ces dernières pour répondre à la demande en énergie des unités de dessalement seront mis en évidence. Il sera montré que le couplage énergie renouvelable et dessalement reste rentable dans certain cas et dépend essentiellement de la capacité de production de l'unité de dessalement, de la technologie renouvelable choisie et de la disponibilité de la ressource. Ces aspects seront développés, avec comme exemple concret le cas de l'unité de dessalement membranaire couplé au solaire photovoltaïque mis en place à l'UDES.

Keywords : Energie renouvelable, Dessalement, membranaire, Photovoltaïque.

I. INTRODUCTION

La croissance de la population mondiale augmente les besoins en eau de 64 milliards de mètres cubes chaque année, soit plus de 2 millions de litres chaque seconde, [1]. Certaines régions sont plus touchées que d'autres. En figure 1 sont est donnée la carte du stress hydrique publié en 2014 par L'institut mondiale des ressources.

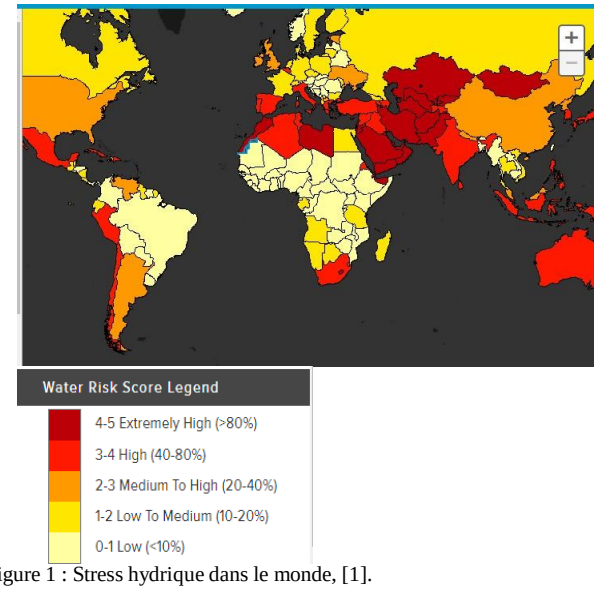

Figure 1 : Stress hydrique dans le monde, [1].

Il est montré clairement que parmi les pays touchés figurent ceux de l'Afrique du nord qui vont souffrir d'une diminution notable de l'approvisionnement des populations en eau, d'irrigation, urbaine ou industrielle.
Au vu de leurs positions géographiques, ces pays possèdent un avantage sérieux lié à leur frontière avec la mer méditerranée. En effet, l'une des solutions prometteuse pour réduire le déficit est de se tourneré vers le dessalement des eaux de mers. Certains, à l'instar de l'Algérie ont lancé un programme de grande envergure d'installation d'unités de dessalement d'eau mer pour alimenter les populations en eau potable.
On estime la production des usines de dessalement en Méditerranée à 10 millions de m^3/j, sur les 47 millions de m^3 d'eau/j production totale fin 2015, [2].
Le coût du dessalement de l'eau de mer dépend essentiellement de la taille de l'unité de dessalement ainsi que de la technologie utilisée. Il est estimé à partir des frais financiers induis, du coût de l'énergie et des coûts de transport, d'exploitation et de maintenance. Pour exemple, le coût de dessalement membranaire des eaux saumâtres est nettement plus faible que celui du dessalement des eaux de mers. Il passe d'une gamme de (0.2 to 0.3 €/m^3) à 0.4 to 0.6 €/ m^3 [3].

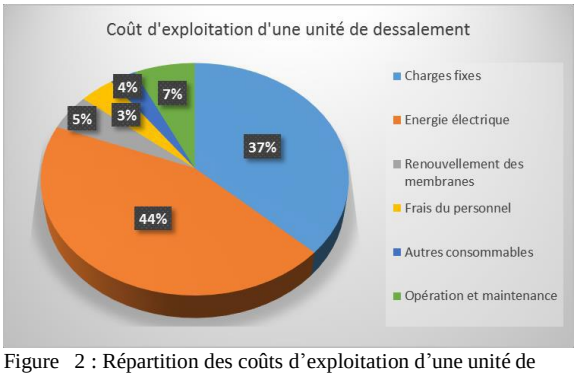

Figure 2 : Répartition des coûts d'exploitation d'une unité de dessalement, [3]

La figure 2 représente la répartition des coûts d'exploitation d'une unité de dessalement. Par ailleurs, les unités de dessalement sont énergivores et entraine un cout représentant 45% du cout d'exploitation, [4].

Le marché du d essalement ne fait que croitre et va entrainer une nette augmentation mondiale de la demande en électricité. Sans oublier que ces unités ont un impact néfaste sur l'environnement et dégagent des quantités de CO2 non négligeable.

Si on considère la projection donné en figure 3 effectué par « Global Water Intelligence/IDA » [5], le nombre d'unité de dessalement va nettement augmenter de 2020 à 2030 ou la capacité rajoutée sera de l'ordre de 150 Mm^3/j. ce qui va entrainer une augmentation vertigineuse de la demande en électricité qui avoisinera les 720 TWh/ jour.

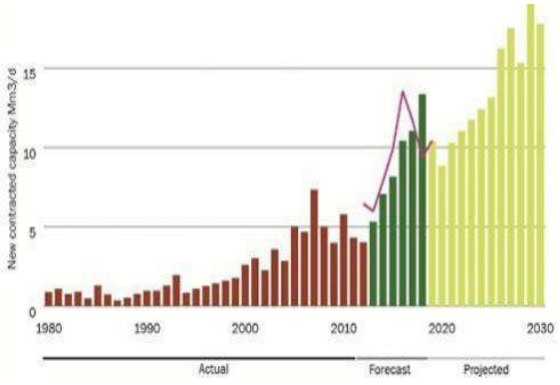

Figure 3 : Projections sur le marché de la désalinisation dans le monde © http://desaldata.com, [5]

C'est pour cela plusieurs pays producteur d'eau dessalée, développent des axes de recherche dans le domaine du dessalement de l'eau de mer couplé aux énergies renouvelables.

Ces dernières années, plusieurs études ont été effectuées sur le couplage des unités de dessalement avec les énergies renouvelables. Certains d'entre elles portent sur la réalisation d'unité de dessalement alimentée par des panneaux solaires photovoltaïque sans stockage Thomson [12] et avec stockage sur batterie pour augmenter le temps de production, Keefer et al [6], Maurel, [7], Kehal [8] and Fritzmann et al, [9]. Hanafi [10] a étudié le couplage d'une unité de dessalement par osmose inverse couplée à différentes technologies renouvelables, solaire éolienne et géothermie. Il a recommandé le couplage avec l'énergie éolienne qui demeure le plus rentable au vu des avantages du cout qui demeure en deca des autres technologies renouvelables.

En effet, la seule unité de dessalement alimentée installée en Australie à Melbourne d'une capacité 450 000 m^3/j couplée à l'énergie éolienne, est fonctionnelle depuis 2011, [11].

Par ailleurs, la plus grande usine de dessalement couplé au PV solaire d'une capacité de production de 30.000 m^3/j en utilisant une nouvelle technologie nano-membrane est en cours de construction dans la ville de Al Khafji, en Arabie Saoudite, [11].

2. CAS DE LA TUNISIE, LE MAROC ET EN ALGERIE

2.1. Etat du dessalement

En 2008, la capacité de dessalement produite en méditerranée était de 100 000 m^3/j pour la Tunisie de 20 000 m^3/j au Maroc et 200 000 m^3/j en Algérie, [12]. Parmi les trois pays cités, l'Algérie est le pays qui a lancé un programme de grande envergure pour répondre à la demande en eau de la population. En effet, la capacité de production d'eau de mer dessalée est passée de 152 500 m^3/j en 2006 à 1.3 M m^3/j en 2012 et a atteint 2.27 M m^3/j en 2014.

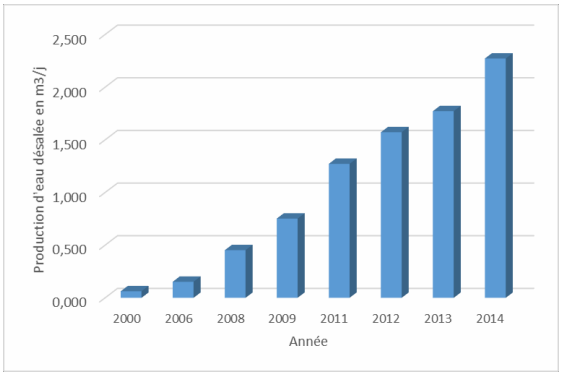

Figure 4: Evolution des capacités installées en Algérie de 2000 à 2014 [13,14].

Sur les 13 stations de dessalement prévues dans le programme du gouvernement Algérien, 11 sont fonctionnelles et répondent largement aux besoins en eau potable de la population du nord. La technologie adoptée étant celle de l'osmose inverse dont le coût de production du m^3/j dessalée reste plus faible que celle du procédé flash ou multiples effets. Toutefois, l'Algérie souffre d'une augmentation continue de la demande en énergie qui s'est accentuée par l'installation des unités de dessalement et le transfert des eaux les zones arides.

La consommation d'énergie par technologies de dessalement est importante est avoisine 3.5 à 5 kWh/m^3 pour l'osmose inverse qui est considérée faible comparée à celle du multiple effet et multi flash qui avoisinent respectivement les 5.7 à 7.5 kWh/m^3 et 15 à 18 kWh/m^3, [14]. En Algérie, technologie d'osmose inverse est devenue la plus utilisée pour le dessalement. Elle est passée de 14% en 1970 à 95% en 2014. Ce qui a classée l'Algérie comme second pays producteur d'eau à partir du dessalement des eaux de mers en 2016, (Voir figure 5) [12].

2.2. Etat des énergies renouvelables dans le monde

La capacité totale en énergie renouvelable installée en 2014 est de 81 GW. La capacité la plus faible a été enregistrée en Afrique.

Le retard enregistré dans ces pays à fort potentiel énergétique revient à plusieurs facteurs notamment celui lié à la législation pour la promotion des énergies renouvelables qui a mis beaucoup de temps pour se mettre en place.

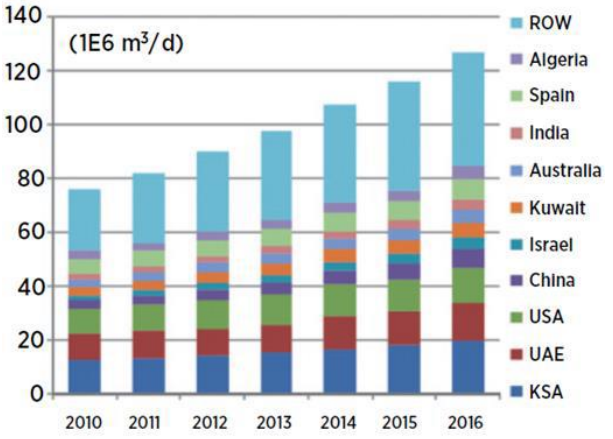

Figure 5 : Classement des pays selon la capacité de production d'eau à partir du dessalement, [12].

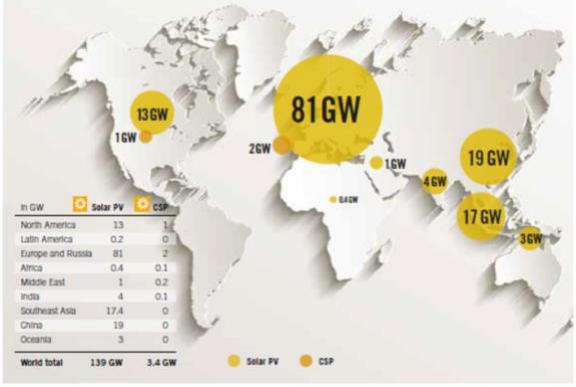

Figure 6 : Capacité en énergie renouvelables installée dans le monde.

Les seuls pays africains classés parmi les tops 5 dans le monde sont :

- le Kenya qui occupe la première place dans la production d'électricité par géothermie
- l'Algérie à la cinquième place pour le CSP
- et l'Afrique du sud qui fait partie des 5 pays émergents.

Le Kenya doit cela au fort potentiel énergétique géothermique disponible du pays, alors que l'Algérie le doit à la concurrence du PV qui a vu le prix du kWh produit baissé, [18]. Toutefois, il est prévu un changement en 2016 lors de l'intégration dans les capacités mondiales les 200 MW de la centrale CSP du Maroc et les 400 MW photovoltaïque de l'Algérie.

Il faut souligner que les investissements annuels sont passés de 45 milliards de dollars en 2004 à 232 milliards en 2013 et 270 milliards 2014. En figure 6 sont affichées les nouveaux investissements dans l'énergie renouvelable par technologies et pays développés et en développement. Ces dernières années, les pays en développement ont beaucoup investis dans 43 technologies, solaires, éoliennes, géothermiques et hydroélectriques. Ceci dénote de la place de ces pays dans le futur sachant que le Maroc et l'Algérie affichent des programmes ambitieux en matière de capacités installées d'ici 2030 qui avoisinent les 20 GW.

2.3. Couplage Dessalement/Energie renouvelable

Les unités de dessalement couplées aux énergies renouvelables sont généralement de petites capacités et ne dépassent pas les 100 m^3/j. Ce sont des installations qui répondent aux populations des zones arides à fort potentiel solaire, éolien ou géothermique.

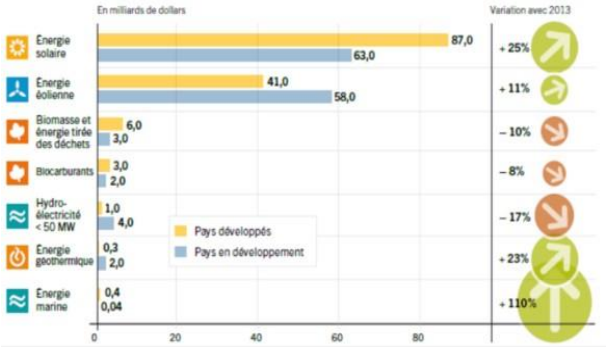

Figure 6: Nouveaux investissements dans l'énergie renouvelable par technologie (pays développés et en développement)

Plusieurs combinaisons de couplage sont possibles, (voir tableau 1), mais 43% des installations sont des unités de dessalement par osmose inverse couplées à la technologie photovoltaïque.

Tableau 1 : Combinaison possible de couplage des énergies renouvelables aux unités de dessalement [11].

Thermal Technologies	Membrane Technologies				
	MSF	MED	VC	RO	ED
Renewable Technologies	●	●	●	●	●
Solar thermal			●	●	●
Solar PV			●	●	●
Wind	●	●	●	●	●
Geothermal	●	●	●	●	●

Pour la région méditerranéenne, on peut citer trois installations de dessalement par osmose inverse réalisées en Tunisie, au Maroc et en Algérie.

En Tunisie, le Projet OPEN-GAIN portant sur la conception optimale de systèmes viables de production d'eau et d'électricité, destinés aux sites isolés utilisant les énergies renouvelables et une automatisation intelligente, a permis la réalisation à l'Institut National de Recherche scientifique et technique Bordj Cedria d'une station de dessalement d'eau saumâtre couplée à un système hybride renouvelables.

Le système de production d'énergie est composé d'un générateur photovoltaïque de 15 kWc, composé de 81 modules, d'un aérogénérateur de 15 kW installé à 25 m de hauteur, d'un groupe diesel de 19 kV A utilisé comme secours et d'un système de stockage d'énergie sur batteries et de convertisseurs DC/AC.

L'unité d'osmose inverse produit une capacité de 24 m^3/j d'eau douce à 0.6 g/litre à partir d'une eau brute hautement saumâtre (16 g/litre).

Le taux de conversion utilisé avoisine 60 %. Toutes les données de ces équipements sont mesurées et recueillies dans un système d'acquisition pour des besoins de contrôle, de monitoring et d'évaluation technique, [15].

Figure 7: Unité de dessalement de Bordj Cedria, Tunisie.

Au Maroc a été inaugurée en 2014, une station de dessalement d'eau et de dénitratation à Kénitra. Un projet installé avec le concours de la chaine SIMEV-UNESCO et de l'université. L'objectif principal de cette unité de dessalement est de produire grâce à un « mix-énergie », ie couplage de l'éolien et du solaire, une quantité d'électricité suffisante pour les besoins quotidiens d'un lycée et pour le fonctionnement de l'unité membranaire de traitement d'eau. Cette installation est composée de 158 panneaux photovoltaïques de type « couche mince » et dont la puissance est de 23.22 kWc pour une production estimée de 40 MWh, une éolienne avec un design hautement efficace de type Darius et Savonius qui capte des vents de toutes les directions ainsi que les vents turbulents dont la production annuelle est estimée à 4 MWh, une unité de traitement d'eau membranaire d'une capacité de 500 l/h, soit 12 m^3/ jour. Le système est complété par un pack de batteries pour le stockage de l'énergie et couplé à un système intelligent qui gère l'énergie en temps réel, [16].

Figure 8 : Unité de Dessalement de Kenitra, Maroc

En Algérie, les années 2000, le Centre de Développement des Energies Renouvelables a mis en place une unité de dessalement membranaire d'eau saumâtre couplée à un système solaire photovoltaïque. L'installation fonctionnait par intermittence pour satisfaire les besoins de la population d'un village situé au sud de l'Algérie à Tindouf. L'ensemble était constitué d'un osmoseur comprenant un système de prétraitement par filtration, une pompe à haute pression, de modules membranaires placés en série, d'un système de post traitement ainsi que d'accessoires et appareils de mesure.

Le générateur PV comprenait un champ de captation constituée de 72 panneaux solaires PV. Un système de stockage comprenant 60 batteries, ainsi qu'un onduleur de stockage et un régulateur. Le système a connu beaucoup de problèmes liés essentiellement à l'indisponibilité de la main d'œuvre local qualifié,

Figure 9 : Unité de dessalement de Hassi Khebi, Algérie.

III. SYNTHESE

Au tableau 2 sont donnés un comparatif des technologies renouvelables couplées aux différentes technologies renouvelables, en matière de coût, de demande en énergie, de capacités et du degré du développement du processus, [11]. Il est clair que le processus qui semble le plus adapté au dessalement membranaire est la combinaison avec les sources productrice d'électricité, à savoir éolien et photovoltaïque. En effet, le coût de production du m^3 reste le plus faible. Par ailleurs, ces combinaisons ont déjà dépassé le stade de la recherche et certaines applications existent dans le monde. En matière de capacité de production de l'eau de mer ou saumâtre ou dessalée, l'énergie éolienne semble la plus avantageuse puisqu'elle permet la production à grande échelle, [11].

Tableau 2 : comparatif des technologies renouvelables couplées aux différentes technologies renouvelables, [17].

	Technical Capacity	Energy Demand (kWh/m³)	Water Cost (USD/m³)	Development Stage
Solar stills	< 0.1 m³/d	Solar passive	1.3–6.5	Application
Solar-Multiple Effect Humidification	1–100 m³/d	thermal: 100 electrical: 1.5	2.6–6.5	R&D Application
Solar- Membrane Distillation	0.15–10 m³/d	thermal: 150–200	10.4–19.5	R&D
Solar/CSP-Multiple Effect Distillation	> 5,000 m³/d	thermal: 60–70 electrical: 1.5–2	2.3–2.9 (possible cost)	R&D
Photovoltaic-Reverse Osmosis	< 100 m³/d	electrical: BW: 0.5–1.5 SW: 4-5	BW: 6.5–9.1 SW: 11.7–15.6	R&D Application
Photovoltaic-Electrodialysis Reversed	< 100 m³/d	electrical: only BW:3–4	BW:10.4–11.7	R&D
Wind- Reverse Osmosis	50–2,000 m³/d	electrical: BW: 0.5–1.5 SW: 4–5	Units under 100 m³/d, BW:3.9–6.5 SW:6.5–9.1 About 1,000 m³/d, 2–5.2	R&D Application
Wind- Mechanical Vapor Compression	< 100 m³/d	electrical: only SW:11–14	5.2–7.8	Basic Research
Wind-Electrodialysis	–	–	BW: 2.0–3.5	–
Geothermal-Multi Effect Distillation	–	–	SW: 3.8–5.7	–

Solar Stills: simple and old technology where the incident short wave radiation is transmitted and absorbed as heat

IV. CONCLUSION

Le dessalement des eaux de mer ou des eaux saumâtres constitue une bonne alternative pour répondre à la demande croissante des populations en eau potable. Toutefois, il reste énergivore et polluant par les émissions de gaz à effet de serre.

Par ailleurs, la capacité globale des usines de dessalement devraient croître à un taux annuel de plus de 9% entre 2010 et 2016, avec un investissement cumulé d'environ 88 milliards de dollars.

L'Agence internationale de l'énergie a montré que pour la région MENA, la demande totale en eau augmentera de 13,3 milliards de m3 en 2030, en raison de la croissance démographique et de l'épuisement des ressources en eaux souterraines et de la surface,

En conséquence, la capacité de dessalement dans la région MENA devrait croître de près de 110 millions de m^3/j d'ici 2030 (dont 70% est en Arabie Saoudite, les Emirats Arabes Unis, le Koweït, l'Algérie et la Libye), [18].

Le solaire et l'éolien sont les technologies les plus adaptées pour le couplage avec les unités de dessalement membranaire. Le CSP jouera un rôle important dans le futur lorsque le prix de production du kWh devient concurrentiel avec celui du PV et de l'éolien.

REFERENCES

[1] http://www.planetoscope.com/eau-oceans/

[2] http://www.wri.org/applications/maps/aqueduct-country-river-basin-rankings/#x=-58.74&y=12.41&l=2&v=home&d=bws&f=0&o=139&init=y

[3] P. G. Youssefa , R.K. AL-Dadaha, S. M. Mahmouda : Comparative Analysis of Desalination Technologies : Energy Procedia 61, 2604 – 2607 .The 6th International Conference on Applied Energy – ICAE2014, 2014.

[4] Etude environnementale d'une usine de dessalement, INP, Toulouse, http://hmf.Enseeiht fr/travaux/bei/beiere/book/export/html/2014

[5] http://geopolis.francetvinfo.fr/le-boom-de-la-desalination-2 3957

[6] B.G. Keefer, R.D. Hembree and F.C. Scharach: Desalination, 54 89–103, 1985.

[7] A. Maurel. Desalination by reverse osmosis using renewable energies (SolarWind), Proc. of the new technologies for the use of renewable energies sources in water desalination conference, Session II, Athens, Greece, 17-26, 1991.

[8] A Kehal A. Reverse osmosis unit of 0.85 m3 /h capacity driven by photovoltaic generator in South Algeria, Proc. of the new technologies for the use of renewable energies sources in water desalination Conference, Session II, Athens, Greece, (1991) 8e16.

[9] C. Fritzmann, J. Löwenberg, T. Wintgens, T. Melin, State-of-the-art of reverse osmosis desalination, Desalination 216 (2007) 1–76.

[10] A. Hanafi : Desalination, 97 (1994) 339–352.

[11] Water Desalination Using Renewable Energy Technology Brief, IEA-ETSAP and IRENA© Technology Brief I12 – March 2012, www.etsap.org – www.irena.org

[12] H. Boyé, « Eau, énergie, dessalement et changement climatique en Méditerranée », Plan Bleu Centre d'Activités Régionales, Sophia Antipolis Août 2008.

[13] Recuperation d'energie Dans Le Dessalement D'eau Mer Par Osmose Inverse. Journée Mondiale de l'Eau 19 Mars 2014.9http://www.cuniv-ntemouchent.dz/files/eau 2014.pdf

[14] Z. Tigrine, N.Kasbadji Merzouk, H. Abuhideh, M. Abbas, S.Hout,, D. Zioui, M. Khateb Membrane Desalination Technology in Algeria: Reverse Osmosis for Coastal Areas, The Seventth Intternattiionall Exerrgy,, Enerrgy and Enviirronmentt Symposiium, IIEEES7 - htttp:////www..uniiv-vallenciiennes..ffr//evenementts //iieee s7, April 27-30, , University of Valenciennes et du Hainaut-Cambrésis - ENSIAME - Valenciennes – France, 2015.

[15] A. Sadi, Projet OPEN-GAIN, Conception optimale de systèmes viables de production d'eau et d'électricité destinés aux sites isolés utilisant les énergies renouvelables et une automatisation intelligente, Bulletn des Energies Renouvelables, CDER, N° 021, 2009.

[16] http://www.green-magazine.fr/?p=8203

[17] A. Sadi and S. Kehal, Retrospectives and potential use of saline water desalination in Algeria. Desalination 152, 5 l-56n 2011;

[18] MENA Regional Water Outlook, Part II,Desalination Using Renewable Energy, 2011 World bank, 2011.

African Membrane Society
Water * Environment, Process, Energy
Sfax, Tunisia, May 3-5, 2016 - Membrane Water Treatment in Small Urban and Village Centers

Tannery Wastewater Treatment Using Hybrid Process: Coagulation-Flocculation/Nanofiltration

Cheima FERSI[1], Chiraz GORGI[2], A. IRMANI[2]

[1]*Material, Treatment and Analysis Laboratory, INRAP, Biotechpole Sidi Thabet 2020, Tunisia*
[2]*National Center of Leather and Shoes, CNCC, Megrine, Tunisia*
cheimafersi@yahoo.fr

Abstract: Large amounts of water are daily used in tanneries in different parts of their services such as pickling, quenching, liming, etc. This consumption generates a huge quantity of wastewaters, which could be reused after performed treatment. In the present work, the treatment of quenching wastewater was investigated using hybrid process (coagulation-flocculation/ nanofiltration) in the objective of its reuse. The results show that the treatment of tannery wastewater using coagulation-flocculation/ nanofiltration could shoot the ionic conductivity at 63% and this at a transmembrane pressure equal to six bars. Similarly for salinity where the abatement rate has not exceeded 60%. This hybrid process could however reduce the COD to 90% and eliminate the turbidity (R=100%). A total removal of magnesium was also recorded an appreciable retention and other major ions (63% for sodium, 77% for potassium, 71% calcium and 61% for chlorides).

Keywords: tannery wastewater, coagulation-flocculation, alginate, nanofiltration.

I. INTRODUCTION

Tannery wastewaters are characterized by their high concentrations in COD, high conductivities and the presence of trivalent chromium [1,2]. Independent of conventional treatment used for raw wastewaters (physicochemical or biological), conductivities are often so high that the wastewaters do not meet legal standards.

Despite the installation of wastewater treatment plants in most tanneries, the usual techniques of wastewater treatment have variable yields and therefore tanners still confronted with environmental problems. The coagulation/flocculation process using inorganic coagulants is the most common pre-treatment in the removal of organic matter [3,4]. However, these type of coagulants presents two major drawbacks related to the addition of chemicals and to the increase of the ionic conductivity of the treated wastewater [5,6]. This paper investigates the performance of hybrid process with coupling the coagulation-flocculation using biopolymer to nanofiltration for the treatment of a tannery wastewater sample supplied from quenching process.

The objective of this work is the permeate reuse in different stages of the tannery process. The optimization of the coagulation-flocculation pre-treatment and nanofiltration treatment was established.

II. EXPERIMENTAL

2.1 Chemicals and analytical measurements

The biopolymer used as coagulant was alginate and it is analytical grade and purchased from Sigma Aldrich. The addition of this coagulant in the sample was in powder form (without adjustment of pH).

Ionic conductivity was measured using a conductivity/TDS/°C Meter Kit (model SenseLine F430T) and turbidity was measured using WTW 555IR turbid-meter.

The COD concentrations were obtained using a Spectroquant Nova 60 from MERCK (Germany) type COD-meter. The main ions and the total dissolved solids were determined according to the Standard Methods [7].

2.2 Wastewater Characteristics

Table 1 illustrates the physico-chemical characteristics of the wastewater sample collected at the outlet of the quenching wash process in a Tunisian tannery.

Table 1: Physico-chemical characteristics of the tannery wastewater sample.

Parameter	Value
Temperature °C	20.1
PH	6.58
Conductivity, mS/cm	41.81
Turbidity, NTU	984
Salinity, g/L	30.6
TDS, mg/L	21.2
COD, mg/L	29800
Na, mg/L	12363.21
K, mg/L	160.13
Ca, mg/L	13.43
Mg, mg/L	107.83

2.3. Jar test coagulation

Coagulation-flocculation treatment was carried out in a conventional jar test apparatus (model JLT4 Floc tester QA1014X). The experimental procedure is as follow:

- rapid stirring after the addition of coagulant (200 or 300 rpm for 5 or 15 min),
- mild stirring without addition of any flocculent (30 rpm for 30 min),
- and settling for 30 min.

2.4. Membrane filtration experiments

A cross-flow stainless steel nanofiltration unit was used (Fig. 1). This nanofiltration unit was equipped with one membrane module with an effective membrane area of 140 cm^2 which can be operated in the pressure range of 3 to 7 bar.

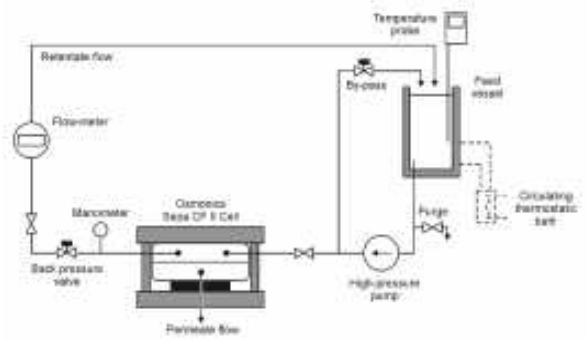

Figure 1. Membrane filtration experimental set-up.

The pure water permeability coefficient (L_o) was determined by measuring the pure water flux (J_o)versus transmembrane pressure (ΔP) for NF DL membrane. The Darcy law is used to fit the pure water permeability data defined by equation (1):

$$J_o = L_o \Delta P = \frac{\Delta P}{\eta_{water} R_{ff}} \quad (1)$$

Where R(m^{-1})) is the intrinsic resistance of the membrane and η_{water} (kg $m^{-1}s^{-1}$) represents the water dynamic viscosity.

The efficiency of the treatment was estimated by the retention rates using the following equation:

$$R\% = \frac{x_t - x_f}{x_t} * 100 \quad (2)$$

where R denotes the retention rate, x the experimental value (COD, conductivity, ionic concentration,…), i indicates the initial value (before coagulation-flocculation/nanofiltration process) and f indicates the final value (after treatment).

III. RESULTS

3.1. Coagulation optimization

The experiments were conducted with various dosages of the coagulant (100, 200 and 500 mg/L).

The two important parameters optimized were the mixing speed and coagulation time.

Figure 2 illustrates the reduction rates of turbidity of wastewater sample into various operating conditions using alginate as coagulant.

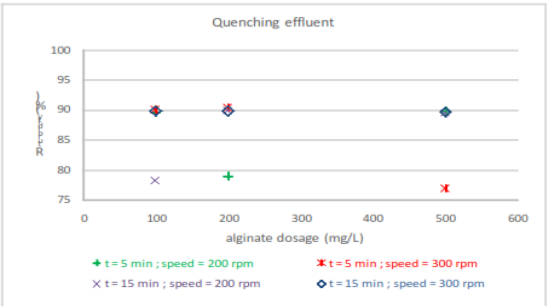

Figure 2. Variation of turbidity reduction of quenching effluent versus alginate dosage.

Figure 2 shows that 90% of turbidity reduction was obtained for several conditions. In order to minimize the alginate consumption, we opt for the dosage of 100 mg/L, 5 minutes for coagulation duration and 300 rpm for stirring speed.

3.2 Nanofiltration optimization

The transmembrane pressure was varied from 3 to 6 bar during the treatment of the tannery wastewater previously treated in the optimal conditions of coagulation-flocculation. Table 2 and figure 3 summarize the results of this study.

Table 2: The results of this study.

Parameter	Before treatment	After treatment			
		ΔP, bar			
Temperature °C	20.1	3	4	5	6
PH	6.58				
Conductivity, mS/cm	41.81	26.6	26.4	16.4	15.3
Turbidity, NTU	984	0.18	0.16	0.09	0.07
Salinity, g/L	30.6	15.7	15.2	12.5	12.1
TDS, mg/L	21.2	11.7	11.1	8.3	8.1
COD, mg/L	29800	5600	4900	2800	2600
Na, mg/L	12363.2	6400.7	6104.7	4890.1	4681.6
K, mg/L	160.13	54.9	46.8	38.7	35.9
Ca, mg/L	13.43	3.45	3.45	2.85	3.84
Mg, mg/L	107.83	0	0	0	0
Cl, mg/l	16140.1	8100.7	7950.8	6415.3	6219.9

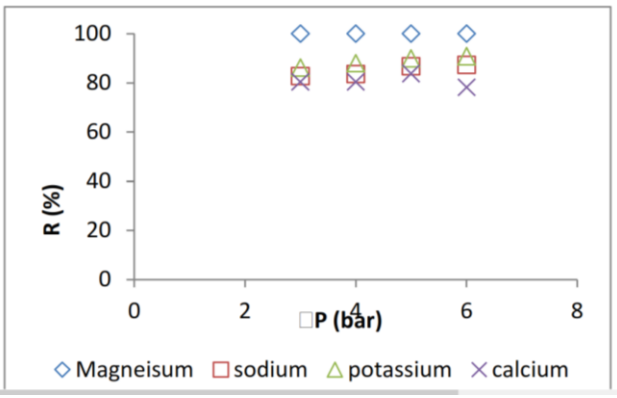

Figure 3. Variation of retention rates of major cations versus transmembrane pressure.

Table 2 and figure 3 show that the treatment of tannery wastewater using coagulation- flocculation/ nanofiltration could shoot the ionic conductivity at 63%

and this at a transmembrane pressure equal to 6 bar. Similarly for salinity where the abatement rate has not exceeded 60%.

This hybrid process could however reduce the COD to 90% and eliminate the turbidity (R=100%). A total removal of magnesium was also recorded an appreciable retention and other major ions (63% for sodium, 77% for potassium, 71% calcium and 61% for chlorides). The best abatement and retention rates were observed at transmembrane pressure higher than 5 bar.

IV. CONCLUSION

In conclusion, the results obtained in this study show that coagulation/flocculation process using natural polymer (alginate) seems to be a very good alternative as pre-treatment before membrane separation to attain considerable turbidity and ionic conductivity reduction of tannery wastewater.

The optimization of several parameters shows that best results were obtained for the dosage of 100 mg/L, 5 minutes for coagulation duration and 300 rpm for stirring speed in pre-treatment process and 5 bar for transmembrane pressure in nanofiltration treatment using DL membrane.

ACKNOWLEDGMENT

Authors would like to thank the National Center of Leather and Shoes (CNCC) and the Tunisian industry (Tannerie Megisserie du Maghreb (TMM))for funding this work.

REFERENCES

[1] O. Tünay, I. Kabdasli, D. Orhon and E. Ates, Characterization and pollution profile of leather tanning industry in Turkey. Water Sci. Technol., 32/12, 1–9, 1996.

[2] C. Collivignarelli, G. Barducci, Waste recovery from the tannery industry. Waste Manage. Res., 2 pp. 265–278, 1984.

[3] Z. Bajza, P. Hitrec, M. MuSic, Influence of different concentrations of Al2(SO4)and anionic polyelectrolytes on tannery wastewater flocculation, Desalination 171, 13-20, 2004.

[4] X. Zhi, F. Qingzhi, Z. Weilei, Research on orthogonal coagulated setting and coagulation-flotation test of tannery wastewater, Journal of Environmental Sciences Supplement S158–S161, 2009.

[5] J.A.M. Roca, M.V.G. Aleixandre, J.L. Garcia, A.B. Pia. Purification of tannery effluents by ultrafiltration in view of permeate reuse. Separation and Purification Technology 70, pp. 296-301, 2010.

[6] W.L. Ang, A.W. Mohammad, Y.H. Teow, A. Benamor, N. Hilal, Hybrid chitosan/FeCl coagulation–membrane processes: Performance evaluation and membrane fouling study in removing natural organic matter, Separation and Purification Technology152, 23–31, 2015.

[7] S.A. Díaz Santos, in : Standard Methods for Examination of Water and Wastewater. APHA/AWWA/WPCF. American Public Health Association. American Water Works Association. Water Pollution Control Federation. Madrid, pp. 1105, 1992.

African Membrane Society
Water & Environment, Process, Energy
Sfax, Tunisia, May 3-5, 2016 - Membrane Water Treatment in Small Urban and Village Centers

Performance Evaluation of an Autonomous Vacuum Membrane Distillation Unit Coupled With Solar Energy

Slimane GABSI[1], Nader FRIKHA[2], Béchir CHAOUACHI[3]

[1]*Unit of research: Environment, Catalysis & Processes Analysis, National School of Engineers of Sfax, Sfax University, Street Omar Ibn ElKhattab, 6029, Tunisia,*
[2]*Higher Institute of biotechnology, Sfax University, Street Soukra BP 261, 3038 Sfax,Tunisia*
[3]*National School of Engineers of Gabes, Gabes University, Street Omar Ibn ElKhattab, 6029, Tunisia*
naderfrikha@yahoo.fr

Abstract- The objective of this work is to estimate quantitatively the potential of membrane distillation of seawater technology coupled with solar energy. The unit presented in this paper is designed to provide high quality drinking water in remote coastal areas with low infrastructure and without connection to an electrical network. The designed installation is completely autonomous, indeed the only energy source is the sun. The electrical energy required to operate the plant is produced by a photovoltaic cells field, and the sea water heating is provided by a thermic solar collectors field. A model describing the operation of a desalination membrane powered by solar energy is developed. This model determines the performance of the unit over time and for any day of the year.
This model is established from the balance equations of mass and heat on the different units (membrane, exchanger, condenser, field of solar collectors). The model is used to evaluate the evolution of the distillate flow and temperature changes for different flows. The model also allows to estimate the productivity of the unit during the year. The simulation of the operation of the unit shows that the daily production of distilled water is between 63 kg/m^2 and 188 kg/m^2 for the days of December 21 and June 21.

Keywords: membrane distillation, solar collectors, photovoltaic cells.

I. INTRODUCTION

Desalination using solar energy coupled with membrane technology is considered an attractive alternative for the production of drinking water especially in rural and arid areas. Tunisia offers great opportunities for the development of solar applications through the exploitation of solar energy. Its geographical location, Tunisia has one of the highest solar radiations in the world [1].
The crisis of drinking water announced for the coming years raises the interest of rapid development of desalination technologies cheaper, simpler, more robust, more reliable and less energy intensive and environmentally friendly.
Vacuum membrane distillation (VMD) consists in applying a vacuum on the permeate side of a hydrophobic microporous membrane. A portion of the heated water will be vaporized and will then pass through the membrane pores while liquid is retained by the hydrophobicity of the membrane. The driving force for the process is due to the vapor partial pressure gradient between the two membrane sides. Vapor will then be condensed outside the module. VMD can be characterized by the following steps: vaporization of the more volatile compounds at the liquid/vapor interface and diffusion of the vapor through the membrane pores according to a Knudsen mechanism [2-3]. Permeate condensation takes place outside the module, inside a condenser or a trap containing liquid nitrogen.
The MD technique holds important advantages with regard to the implementation of solar driven stand-alone operating desalination systems [4-6]. The most important advantages are the operating temperature of the MD process in the range of 60 to 80°C.
This is a temperature level at which thermal solar collectors perform well, chemical feed water pre-treatment is not necessary, intermittent operation of the module is possible, contrary to RO, there is no damage occurs if membranes dry out, system efficiency and high product water quality are almost independent from the salinity of the feed water.

II. PRINCIPLE OF FUNCTIONING

The choice of unit design and dimensions of its components is the result of work carried out in the project MEDINA, [8].
These studies allowed to compare the performance of different configurations (membrane module integrated within the absorber, module separated from the solar collector ...) and to design the various organs of the plant chosen [8-9].
The unit was installed in the village of orphaned

children (SOS MAHRES). This is a set of houses located close to the city of Mahres in the region of Sfax. This is a non-governmental social, care and foster care of children without family support. It was created in 1949 to improve the living conditions of children in distress.

There are currently 13 family houses, a playground, a kids club, shops and services and domestic appliances. The capacity is 104 children: 8 children per family home. Figure 1 shows the desalination plant and various instrumentation and control regulation.

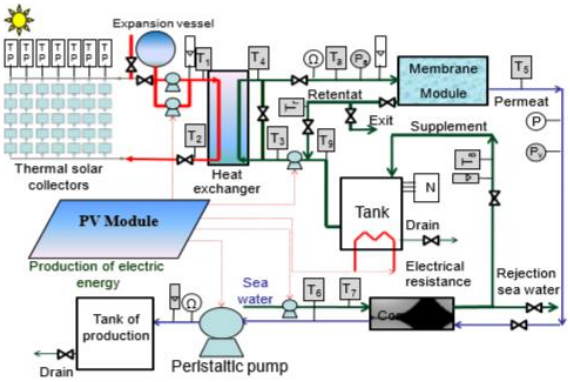

Figure 1: Design of the solar VMD desalination plant.

The main components of desalination plant are: given in table 1.

Table 1 : Components of desalination plant

1	A membrane module: (UMP 3247 R) with 806 fibers (PVDF) with an internal diameter of 1.4 mm. This module has a length of 1.129 m and offers a total area of 4 m^2.
2	Field of solar collector (7 rows and 5 collectors in series, total area : 70 m^2)
3	Field of solar photovoltaic modules (16 modules, peak power : 2.1 kW)
4	Flow pump ensuring the supply of seawater (Flow up to 2500 l/h, power: 1 kW)
5	Circulator pump circulates the coolant in the collector field (power: 0.5 kW).
6	Peristaltic pump used for the recovery the distillate product (power: 0.5 kW).
7	Plate heat exchanger with 27 titanium plates and offering an exchange area of 1.08 m^2 (maximal power of heat exchange: 26 kW)
8	Condenser used for the condensation of the steam produced
9	Instrumentation and control regulation
10	Mixing tank (volume: 80 liters)
11	Tank of fresh water production (volume: 2 m^3)

III. Characterization, selection and design collectors

3.1. Solar Thermal collector

The collector characteristics are given in table 2, collector efficiency and the field are presented respectively in figure 2 and 3.

Table 2 : Characteristics of the collector and the field

Collector			
Absorber:	-Type: Aluminum - Thickness: 1.3 mm - Tube: ø = 12/14 mm (number: 9)	- Collector: = ø 20/22 mm (number: 7) - Paint: Epoxy black matte	
Transparent cover:	-Number of windows: 1 -Thickness: 4 mm	- Nature: clear glass with high transparency and tempered safety	
Insulation:	Isolation and rear side panel: polyurethane covered with aluminum (	Thickness e = 30 mm).	
Framework and setting:	Aluminum		
Field of solar collector			
Collecting area of solar thermal collector	35 63 m² (7 rows of 5 collectors)	Safety valves	07
Circulation pumps	02	Drainers	07
Flow-meter,	01	Valves	07
Temperature sensors	07	Expansion tank,	01
Manometer	07	Isolating valves	02.

The collector efficiency is given in figure 3.

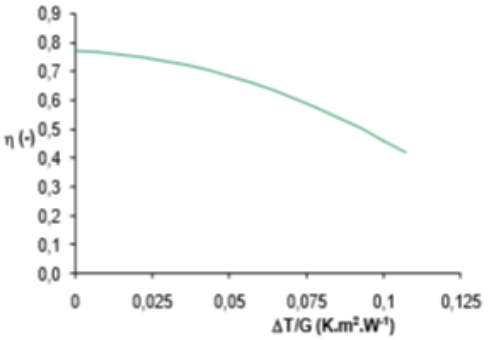

Figure 2: Collector efficiency

Figure 3: Field of solar collector thermal

3.2. Photovoltaic cells

The fact that the desalination systems will be operated as stand-alone systems requires a PV system as the supply for electrical auxiliary equipment. Most of the electrical power is consumed by the pump. Thus, the

efficiency of the pump is an important influence on the design layout of the PV area and therefore on the investment costs of the total system.
The pump can be connected to a PV module, and during outdoor tests current and voltage of the PV-module can be monitored. The photovoltaic field collector components are given in table 3.

Table 3: Characteristics of PV plant

1	16 modules of cells LC 120 WC,
2	02 voltage regulators 48 VDC 40A,
3	08 solar batteries tubulaire12V/230AH (4 rows of 2 batteries),
4	01 power inverter 220 / 2 kW,
5	01 electrical equipment box of power

Figure 4 : Photovoltaic collectors

3.3. Membrane

The chosen membrane module is a hollow fiber microfiltration module, provided by PALL Company. The membrane material is PVDF. Characteristics of the membranes are specified in table 4.

Table 1: Characteristics of the membrane module

Commercial reference	UMP 3247 R
Material	PVDF
Number of fibers	806
Thickness of the membrane (mm)	0.4
Module length (m)	1.129
Area (m^2)	4
Permeability at 20°C ($s.mol^{1/2}\ kg^{1/2}\ m)^{-1}$	$1.92\ 10^{-6}$
Tortuosity	2.1

IV. DESIGN EQUIPMENT INSTALLATION

4.1. Design of the flat plate heat exchanger

The plate heat exchanger is composed of a set of corrugated metal plates. The plates are mounted between a fixed frame and a mobile frame, the clamping being provided by bolts. The plates are equipped with seals that ensure the tightness of the heat exchanger and fluid flow. The number of plates is determined by the flow, fluid properties, pressure and temperature program. The specific corrugation plates promotes fluid turbulence and therefore heat exchange. The desired temperature levels of circulating fluid in the exchanger are deducted from the simulation model developed in Matlab. The coolant from thermal solar collector enter the heat exchanger at 77°C to heat the seawater from 55°C to 65°C. The coolant lives collectors at 60°C. The power exchanger calculated in terms of desired temperatures and insulation an average of 700 Wm/m^2 is about 26 kW. The heat exchanger coefficient is 3036 W/m^2K. The plates are made in titanium. The plate exchanger is properly sized and thermally, mechanically and later losses. The sizing of this device is about 13.4%.

4.2. Design of the condenser

Seawater at 25 °C ensures the condensation of vapor from the membrane module at 70°C. The temperature output desired is about 39.5°C. Similarly, the chosen material is titanium. The overall power of the condenser is 60 kW. The tubes number is 41 of internal diameter equal to 7 mm and thickness 1 mm. The over sizing of the condenser is 30%.

4.3. Circulation pumps

The coolant circulating in the solar system is provided by a circulation pump. The temperature range operation of the pump is -20 to 130 °C.

4.4. Peristaltic pump

This pump is able to carrying the steam produced in the membrane to the condenser, and then it ensures the flow of steam condensed to reservoir production. The vacuum level created is between 5000 and 7000 Pa.

4.5. Instrumentation and control

The pilot is also equipped with measuring equipment and control which characteristics are given in table 5.

Table 5 : Characteristics of measuring equipment

Equipment	Qt	Electrical box	Qt
Temperature sensors Pt100	11	Transformer 220 -24 V,	01
Pressure sensors	02	Frequency inverters: orders pumps (water supply, feeding membrane, peristaltic pump),	03
Vacuum meter	01	Regulators all or no level (02 electro-valves)	02
Flow-meters with digital display	01	PID controllers (control of 03 frequency inverters)	03
Flow-meters totalizer pulse	01	Temperature indicator,	01
Flow-meters with visual posting	02	Pressure indicator,	01
Levels sensor	03	Production flow indicator	01
Electro-valves	05	Switches lanes	01
Manual valves	10		

Acquisition of temperatures, pressures and flows as well as control of pumps and electro-valves is provided with a data logger Agilent technology.
In the proposed flowsheet (figure 1), the coolant fluid out of the field of solar collectors is routed to the heat exchanger to provide heat to the sea water at the inlet

of membrane module.

Figure 6: Electrical equipment box

Figure 7 : Acquisition system

The temperature of sea water at the outlet of the heat exchanger should not exceed 80 °C for the structure of membranes cannot resist high temperatures that can cause an alteration of their mechanical strength. The salinity of the supply of the membrane is controlled by a conductivity meter placed at the inlet of the membrane module. The salinity must not exceed a maximum permitted level and this to limit membrane fouling. If the maximum level of salinity is not exceeded, retentate exiting the membrane module is sent to the exchanger and is mixed with an addition of preheated seawater. If the maximum level is exceeded, the retentate will be rejected and feeding the membrane module is made from the mixing tank. The amount of vapor produced supplies the condenser. After condensation, a peristaltic pump mounted downstream of the condenser ensures the delivery of production of desalinated water. The condensation of vapor produced preheats the flow of sea water supplementary. A level switch installed on the tank controls the flow of seawater supplementary through a solenoid valve. The flow of seawater to the input of the condenser is of the order of 3000 l/h.

V. SIMULATION OF THE OPERATION OF THE INSTALLATION

The global model is established by taking into account the accumulation of matter and heat in the tank. It is assumed that the condensation is complete.

5.1. Influence of the vacuum pressure and the feed flow rate.

The global model developed allowed us to perform a parametric study quantifies the influence of different parameters. This study was useful in selecting appropriate operating conditions. Among the studied parameters we include the influence of coolant flow, the feed flow rate, the level of vacuum applied.

For example, Figure 8 shows the effect of the vacuum pressure applied to the flow of distillate collected. It follows from the analysis of these curves that the distillate flow rate gradually increases at the beginning of the day, reaches its maximum around midday and decreases gradually toward the sunset: It therefore follows the solar flux. The permeate flow increases with the increase of the pressure gradient which is the driving force of the transfer. Work with reduced pressures allows the evaporation of seawater for relatively low temperatures, this makes us increase the duration of production and especially earn in terms of daily production. Indeed, production passes from 48.6 kg at a vacuum pressure of 20000 Pa to 116.5 kg at a pressure of 5000 Pa.

Figure 9 shows the evolution of the distillate flow rate as a function of feed flow rate. These curves show that the flow of distillate is influenced by varying the feed flow rate. Distillate flows vary from 81 kg/h/m^{2}to 98 kg/h/m^2 for the feed rates 600 and 2400 kg/h, which represents a gain of 21% of daily production. This increase is due to the improvement of the transfer of heat and mass in the membrane following the increase of the flow rate of seawater. The feed flow rate must be sufficient to limit membrane fouling. On the other hand, the choice of an optimal flow must result from a technical and economic study taking into account the cost of pumping and the influence of flow increases about the longevity of membranes.

5.2. Estimation of productivity

The model describing the functioning of the collector field allows estimating the evolution of the temperature of the coolant during the day. The model describing the functioning of the plate heat exchanger is used to determine the temperature of the water

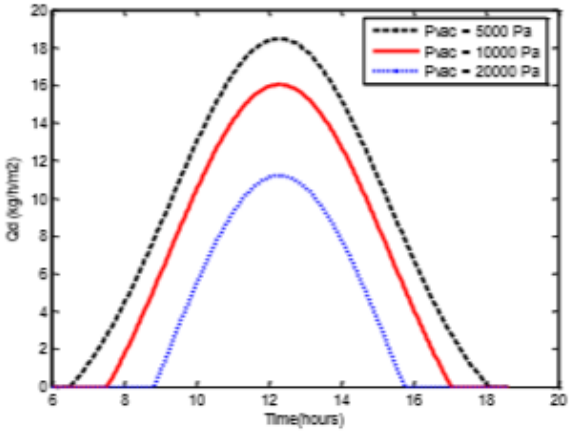

Figure 8: Variation of the distillate flow according to the vacuum pressure. m_{feed}= 1200 kg/h, Day : March 21

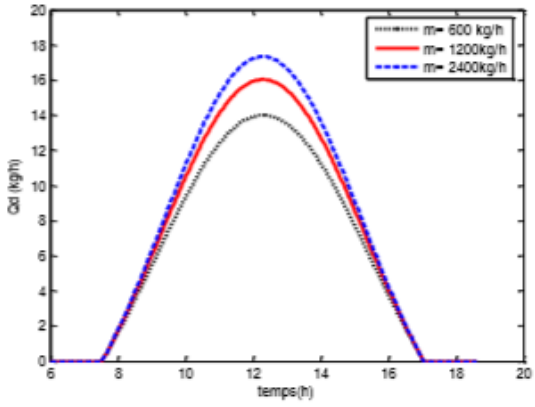

Figure 9: Variation of the distillate flow according to the feed flow.

P_{vacuum} = 10000 Pa, Day : March 21

feeding the membrane. The model describing the behavior of hollow fiber membrane module was used to evaluate, instantly and at each position, the steam and retentate temperatures, the flow of distillate and estimate the daily production.

Figure 10 shows an example of comparison between the variations of distillate flow determined experimentally and calculated by the model. The production begins when the required level of temperature is reached. We can notice the lag between the time corresponding to the maximum production (around 13h) and that corresponding to the maximum solar flux (around 12h), this difference is due to the effect of the thermal inertia. For all manipulations performed, the difference between the flow of distillate obtained experimentally and that estimated by the model is about 15%.

These relatively large differences between the experiment and simulation are due to disturbances in the solar flux and the vacuum pressure applied. Experimentally, it is very difficult to maintain a constant vacuum pressure along the manipulation, indeed the pressure varies between 10000 and 15000 Pa. On the other hand this difference can be justified by the change in permeability during the manipulation to the accumulation of salt on the membrane surface something that affects the porosity of the membrane. The Knudsen permeability of the membrane at 20°C is 1.92 10^{-6} s $mol^{-0.5}kg^{-0.5}m^{-1}$ which corresponds to k_{m0} = 1.505 10^{-8}s $mol^{-0.5}kg^{-0.5}m^{-1}$.

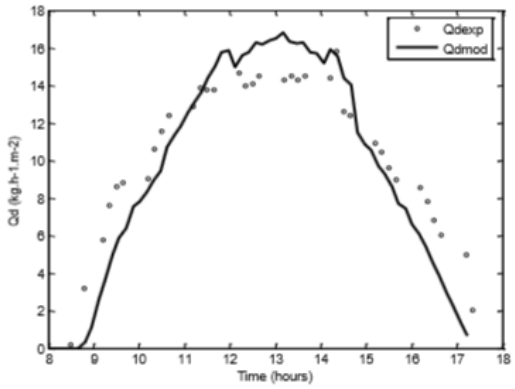

Figure 10: Temperature profile for the theoretical and experimental cold fluid
Day : June 9, 2011, $\dot{m}_{coolant}$ = 770 kg/h, $\dot{m}_{feed}$ = 1200 kg/h.

Four typical days representing the four seasons of the year were chosen: the equinoxes (March 21 and September 21) and solstices (June 21 and December 21). As an example Figure 11 present the instantaneous variation of desalinated water production for the four typical days of the year.

The flow of the distillate gradually increases at the beginning of the day and it decreases gradually at the end of the day.

Therefore, the production reaches its maximum value for June 21, it is around 22 kg/h m^2. The production is almost the same for both days of the equinox; it is about 17 kg/h m^2. For the December 21 (winter day) production is 10 kg/h m^2. Production varies in a remarkable manner throughout the day due to the variation of solar flux. The daily productivity is between 63 kg/m^2 and 188 kg/m^2 for the days of December 21 and June 21; this corresponds to average flow rates from 8 kg/h m^2 to 14 kg/h m^2 on the basis of the sunny period of the day.

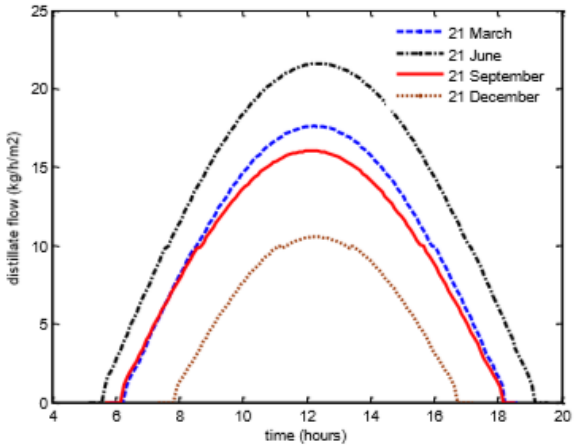

Figure 11: Variation of the simulated flow of distillate versus time for different year days. Pvacuum = 5000 Pa, m_{feed} = 1200 kg/h

VI. CONCLUSION

The designed installation is completely autonomous uses only solar energy as an energy source. The choice of solar collectors and their arrangement was made. The design of various required equipment to operate the plant was completed. The designed installation is carried out in a village of orphans in the coastal region Mhares. We developed calculation programs on the software MATLAB and this in order to simulate and study the functioning of the unit. The models developed are able to determine the evolution of temperatures at each organ in any position and over time and changes the flow of distillate during the day. The model allows studying the influence of various operating parameters such as flow rate of feed, coolant flow, inlet temperature. The study shows that the applied vacuum pressure is a key parameter; very extensive levels of vacuum pressure can increase considerably the flow of distillate product. This model determines the performance of the unit over time and for any day of the year. Simulations proved that pilot plant is able to provide average permeate flow ranging from 8 kg/h m2 to 21 December to 14 kg/h m^2 to 21 June.The models developed are very useful for controlling and regulating the installation. A system for regulating the inlet temperature of the membrane module is highly recommended for the maximum temperature that can support the membrane is 75 °C.

The prospects consist essentially in determining the optimal operating conditions and to carry a energetic study of the pilot. These conditions concern mainly the

flow of coolant and its regulation as a function of solar radiation, the flow of seawater and the rejection rate of the retentate.

ACKNOWLEDGEMENTS

The authors address their thanks to the European Commission for funding the cooperation project FP6 Membrane-Based Desalination: An Integrated Approach. MEDINA Project No: 036997

REFERENCES

[1] S. Bouguecha., B. Hamrouni, M. Dhahbi, Small scale desalination pilots powered by renewable energy sources: case studies Desalination 183, 151–165, 2005.

[2] J.P. Mericq, S. Laborie, C. Cabassud, Vacuum membrane distillation for an integrated seawater desalination process, Desalination and Water Treatment 9, pp 293–302, 2009.

[3] M.R. Qtaishat, F. Banat, Desalination by solar powered membrane distillation systems, Desalination 308, pp 186-197, 2013.

[4] A. Zrelli, B Chaouchi, S. Gabsi, Simulation of vacuum membrane distillation coupled with solar energy: Optimization of the geometric configuration of a helically coiled fiber, Desalination and Water Treatment 36, pp 41–49, 2011.

[5] F. Banat, N. Jwaied, Economic evaluation of desalination by small-scale autonomous solar-powered membrane distillation units, Desalination 220, pp 566–573, 2008.

[6] E. Mathioulakis, V. Belessiotis, E. Delyannis, Desalination by using alternative energy: Review and state-of-the-art , Desalination 203, pp 346–365, 2007.

[7] J-B. Gálveza, L. García-Rodríguezb, I. Martín-Mateosclination, Seawater desalination by an innovative solar-powered membrane distillation system: the MEDESOL project, Desalination 246, pp 567–576, 2009.

[8] S. Ben Abdallah, N. Frikha, S. Gabsi, Design of an autonomous solar desalination plant using vacuum membrane distillation, the MEDINA project, Chemical Engineering Research and Design 91, (2013), pp 2782-2788, 2009.

[9] N. Frikha, R. Matlaya, B. Chaouachi, S. Gabsi, Simulation of an autonomous solar vacuum membrane distillation for seawater desalination, Desalination and Water Treatment, pp. 1 -10, 2013.

African Membrane Society
Water & Environment, Process, Energy
Sfax, Tunisia, May 3-5, 2016 - Membrane Water Treatment in Small Urban and Village Centers

Improvement of Membrane Filtration Performances by Using Hydrophilic Polymers

Sanna GASSARA[1,2], Elsa DUFOUR[1], Watchanida CHINPA[3], Y.-J. SHIH[1,4], Damien QUÉMENER[1], Raja BEN AMAR[2], Yung CHANG[4], Olivier LORAIN[5] and Alain DERATANI[1]

[1]*Institut Européen des Membranes, Université Montpellier 2, cc 47, Place E. Bataillon, 34095 Montpellier Cedex 5, France*
[2]*Faculté des Sciences de Sfax, Laboratoire des Sciences des Matériaux et Environnement, Route de Soukra km 4, 3018 Sfax, Tunisie*
[3]*Department of Materials Science and Technology, Faculty of Science, Prince of Songkla University, Hat-Yai, Songkhla, Thailand,*
[4] *R& D Center for Membrane Technology and Department of Chemical Engineering, Chung Yuan ChristianUniversity, Chung Li, Taoyuan 320, Taiwan*
[5]*Polymem - 3 rue de L'industrie - Zone de VIC, 31320 Castanet-Tolosan - France*
Sana.Gassara@iemm-univ-montp2.fr

Abstract: This work describes several approaches to improve the fouling resistance of hydrophobic membranes fabricated by the phase inversion technique. The blending method which consist of the introduction of hydrophilic polymer additives in the dope solution was first investigated. In this work, poly(vinylpyrrolidone) and an amphiphilic block copolymer poly(methyl methacrylate)-*b*-poly(hydroxyethyl methacrylate) were used in fabrication of poly(vinylidene difluoride) (PVDF) hollow fiber membranes. Effectiveness of the method was evaluated by quantifying the additives using (Fourier Transform Infrared Spectrometer (FTIR) in new and aged PVDF hollow fibers. Physical and chemical membrane surface modifications are other approaches. Both approaches were explored by surface modification of poly(etherimide) membranes using poly(ethylene glycol) moieties and sulfobetaine amphoteric groups to prevent the fouling by biomolecules (proteins).

Keywords: membrane fabrication, fouling resistance, block copolymers, blending, surface modification

I. INTRODUCTION

Membrane filtration provides a physical barrier that effectively removes various materials from water such as particles, viruses, bacteria and other unwanted molecules. It widely recognized as the technology of choice for industries seeking to reuse their wastewater and reduce their water footprint to comply with increasingly stringent environmental legislation [1].

The most commercially available membranes used for water treatment are made of polysulfone (PSU), poly(ethersulfone) (PES) and poly(vinylidene difluoride) (PVDF). Their excellent chemical resistance and good thermal and mechanical properties [2] characterize these materials. However, these polymers are highly hydrophobic entailing an excessive fouling on membrane surfaces by biological and organic matter during practical application [3]. Membrane fouling is an undesirable phenomenon because it causes a sharp decline in permeation flux and loss of the efficiency of the membrane process. To overcome this problem, it is necessary to improve membrane hydrophilicity while retaining the bulk membrane properties.

Considerable efforts have been devoted to develop suitable techniques for surface modification of hydrophobic membranes. Generally speaking, the membrane with the desirable properties can be obtained either directly with an appropriate formulation of the dope solution or by surface modification of the formed membrane. The first technique is achieved by blending hydrophilic additives such as poly(vinylpyrrolidone) (PVP) and polyethylene glycol (PEG) in the polymer solution used to prepare the membrane. Recently, amphiphilic block copolymers with a hydrophobic block compatible with the membrane matrix material and a hydrophilic block have been specially designed to be used as additives [4]. The second technique, named post-treatment, is done by surface modification after membrane fabrication. This method can be classified into grafting reactions, surface coating and adsorption of polyelectrolyte layers.

Grafting modification enables to generate hydrophilic functional groups on the membrane surface [5]. For instance, membrane can be treated using plasma or UltraViolet (UV) laser ablation. However, these physical can be hardly implemented in hollow fiber fabrication. Therefore, modification by chemical solution is a versatile alternative to make the membrane surface hydrophilic provided that reactive groups are found on the surface.

This report gathers data obtained for different approaches of modifying hydrophobic membrane surface in order to increase their resistance to biomolecule fouling. Physico-chemical characterization of the modified membranes will be presented and advantages and disadvantages of each proposed method will be discussed along with.

II. BLENDING METHOD

Blending can be considered as a single-step method for preparing hydrophilic and anti-fouling membrane [6]. It was investigated to fabricate PVDF hollow fiber membranes. Two polymer additives were considered: (i) PVP, the most popular polymer additive that has been widely used to now more particularly in the case of PSU and PES membranes and (ii) an innovative additive being an amphiphilic block copolymer the characteristics of which will be presented in paragraph 2.2.

The amount of the additive remaining in the membrane is proportional to its hydrophilicity and consequently its fouling resistance. Therefore, it is of prime importance to quantify the additive amount in the membrane newly fabricated but also to follow it during its whole lifespan. This objective can be achieved by using PVDF fiber/KBr tablets analyzed by FTIR. The obtained results are presented in Figure 1 as normalized additives concentrations with respect to the initial additives concentrations setting in the casting solutions. As noted, a new membrane is a virgin membrane not used in a filtration process and ageing was conducted by accelerated action of sodium hypochlorite.

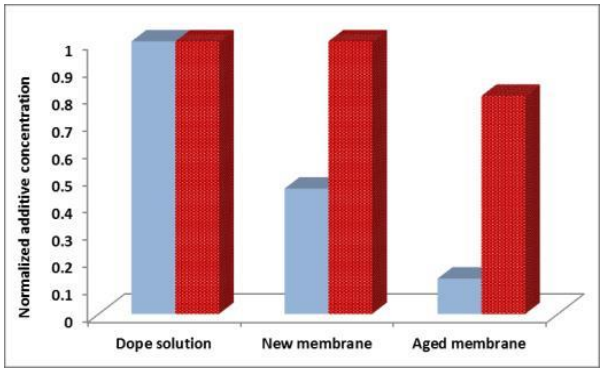

Figure 1. Normalized concentration of PVP (left blue) and amphiphilic copolymer (right red) in dope solution, new and aged membranes.

2.1 Adding a conventional hydrophilic additive

As can be seen in Fig. 1, the new and aged membranes have lost about 50% and 85% respectively, with respect to the initial PVP concentration present in the dope solution.

The PVDF hollow fibers were prepared by non-solvent induced phase inversion. The dope solution was coagulated in an aqueous phase enabling a fast exchange rate between the solvent and non-solvent which creates the porous membrane morphology [2]. During this stage, about 50 % of PVP leached out from the resulting membrane to the aqueous coagulation bath because it is not covalently bonded to the polymer matrix and it has a high affinity to water [7]. Actually, PVP also serves as pore forming agent since it is easily washed out during membrane preparation to control the morphology, pore size and distribution [6,8].

The remaining PVP (50 % in new membrane) stays entrapped due to the polymer precipitation and contributes to improve the hydrophilic character of the new membrane surface. However, PVP is susceptible to degradation by oxidizing agents (as sodium hypochlorite) commonly used during the cleaning steps. This phenomenon along with the continuous extraction during the filtration operations accounts for the drastic loss of PVP in the aged membrane.

2.2 Adding an amphiphilic block copolymer

In order to prevent the polymer additive from leaching to the aqueous solution, we proposed to use an amphiphilic block copolymer. As shown in Fig. 2, this additive is composed of both hydrophobic and hydrophilic chain segments which are poly(methyl methacrylate) (PMMA) and poly(hydroxyethyl methacrylate) (PHEMA), respectively. The PMMA block enables the polymer additive to be firmly anchored in the polymer matrix, thus avoiding its leaching out from the forming membrane. This assumption was confirmed by the concentration of the amphiphilic additive that remains identical in the new membrane compared to that in the dope solution (Fig. 1). Furthermore, it can be seen that its concentration in the aged membrane is only reduced of about 20 % owing to its much less susceptibility to degradation by oxidizing agents than PVP. It can then be concluded that the use of such an amphiphilic additive should allow the membrane surface to keep a hydrophilic character improving its resistance to biofouling.

Figure 2 presents also the proposed copolymer positioning within the membrane. The hydrophilic part of the PMMA-*b*-PHEMA block copolymer is assumed to present a brush-like structure on the membrane surface with the hydrophobic part strongly entangled in the PVDF matrix guaranteeing its durable stability.

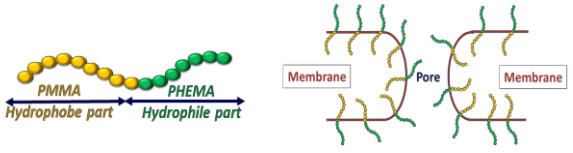

Figure 2. Amphiphilic block copolymer composition (left) and its expected position in the membrane (right).

III. POST TREATMENT SURFACE

A set of flat PEI membrane samples was prepared by the phase inversion method under similar conditions according to a previously described procedure [9]. The obtained membranes, named unmodified PEI, were then reacted with aqueous

solutions of various modifying agents such as aminated oligomers, anionic polyelectrolytes and zwitterionic block copolymers to generate modified PEI membranes. The aim of this chemical post treatment is to introduce hydrophilic functional groups on PEI membrane surface without the use of harmful compounds.

The anti-fouling properties of the obtained membranes were evaluated using bovine serum albumin (BSA) as model protein foulant. To do that, experiments were carried out by dead-end filtration of a feed solution containing 1 g/L of BSA in buffer phosphate at pH 7.4. The comparison between the pure water flux prior and after the BSA filtration through the flux recovery ratio (FRR) calculation, gives a clear insight of the fouling tendency for a given membrane.

3.1 Covalent modification

Actually, the covalent reaction route requires the presence of chemical groups at the membrane surface that can be easily activated. As shown in Fig.3, the backbone of PEI contains imide groups. In the presence of amino groups, the imide function undergoes ring opening by reaction with amine converting it into amide group [9].

This simple approach was used to attach covalently a hydrophilic function having PEG chains onto the surface of unmodified PEI membranes. To do that, Jeffamine M-2070, an amino terminated poly (propylene oxide)/poly (ethylene oxide) block copolymer (PEG-amine) was choosing as surface modifying agent. The obtained membranes were named PEGylated PEI membranes (PEG-PEI).

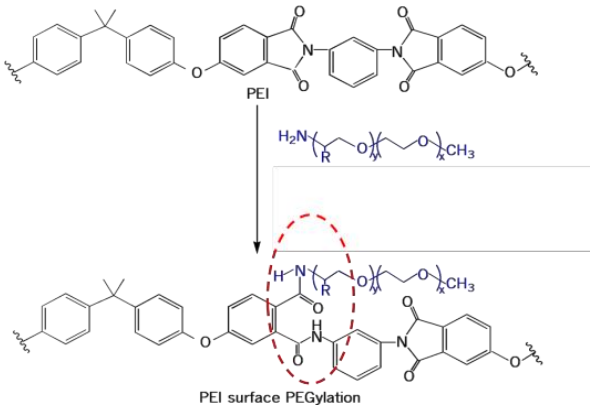

Figure 3. Schematic reaction of the PEI membrane post-treatment using amine groups.

Fig. 4 presents the effect of post-treatment time on BSA rejection and FRR of PEGylated PEI membranes. It can be seen that the BSA was completely retained by unmodified and modified PEI membranes indicating that all membranes have the rejection property with a molecular weight cut off of about 100 KDa (determined with PEG standards), according to our previous work [9].

It can also be seen that the FRR was significantly increased with the PEGylated time meaning a gradual coverage of the surface by PEG chains. A FRR value of about 95 % obtained after 2.5 h of PEGylated reaction proves that the procedure enables to limit strongly the protein fouling. This technique is very attractive due to its simplicity, efficiency and environmentally friendly condition of preparation. Moreover, the hydrophilic grafted function was stable with its covalent attachment to the PEI membrane matrix and it was not leached out over time.

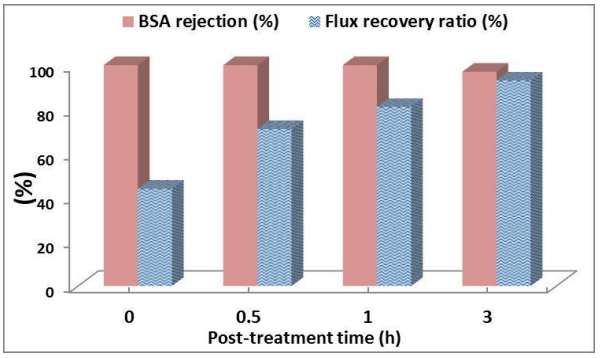

Figure 4. Influence of PEGylating time on BSA rejection and water flux recovery ratio for PEI membranes.

On the other hand, the same approach was used to design positively charged PEI membranes. As demonstrated in our previous work [9], unmodified PEI membranes were successfully modified using poly(ethyleneimine) oligomers having a molecular weight of 2 kDa. The obtained cationic membranes, named Cat PEI, may undergo surface fouling due to adsorption of biological matter which is negatively charged at neutral pH [10]. To solve the problem, a simple approach using a physical adsorption method was proposed for producing anti-fouling membrane surface.

3.2 Modification by physical adsorption

The adsorption approach used in this work is based on electrostatic interactions. It can be achieved by dipping a charged membrane into a dilute aqueous solution of an oppositely charged polyelectrolyte and allowing the polymer to adsorb and reverse the charge of the membrane surface [11-12].

The physisorption of anionic polyelectrolytes sodium poly(styrene sulfonate) (PSSNa) and sodium poly(vinyl sulfonate) (PVSNa) onto positively charged Cat PEI was investigated to prepare bipolar layered membranes Cat PEI-PSS and Cat PEI-PVS.

These membranes have both a negatively charged surface and positively charged pores.

Figure 5 displays the FRR for the modified membranes. As seen, only half of the water flux is recovered after BSA filtration by positively charged Cat PEI indicating severe membrane fouling.

It was then assumed that the fouling tendency of Cat PEI mainly occurs through electrostatic attraction between the positively surface charge and the BSA protein that is negatively charged at pH 7.4 [10]. By contrast, a quantitative FRR were obtained for both the negatively charged Cat PEI-PSS and Cat PEI-PVS

membranes.

3.3 Adsorption of zwiterionic block copolymer

In nature, cell membrane phospholipid bilayers is characterized by zwitterionic phosphate heads pointing "out" towards the physiological liquid and hydrophobic tails pointing "in" towards the core of the bilayer as shown in Fig. 6.

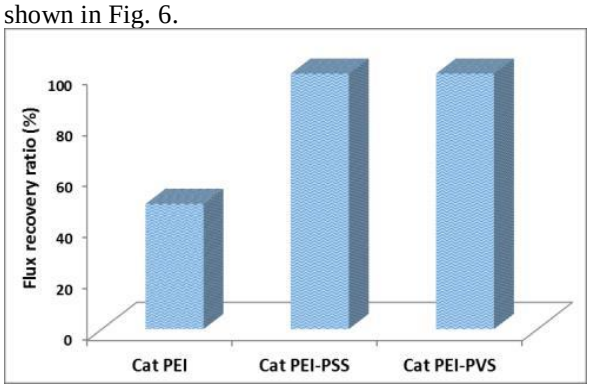

Figure 5. Water flux recovery ratio for Cat PEI, Cat PEI-PSS and Cat PEI-PVS membranes.

Our interest in this example is the remarkable resistance of the cell membrane phospholipid surface to protein adsorption and platelet adhesion owing to the zwitterionic headgroups. As definition, a zwitterionic molecule contains both positive and negative charges while maintaining overall charge neutrality within a wide pH range. So, inspired by fundamental aspects of the cell membrane phospholipid surface, many polymers bearing biomimetic zwitterionic groups including phosphobetaine, sulfobetaine or carboxybetaine can be synthesized. These polyzwitterionic materials can be explored into a platform strategy for development of membrane antifouling surfaces. A block copolymer poly(acrylic acid)-*b*-poly(sulfobetaine methacrylate) named PAA-b-PSBMA was designed for this study.

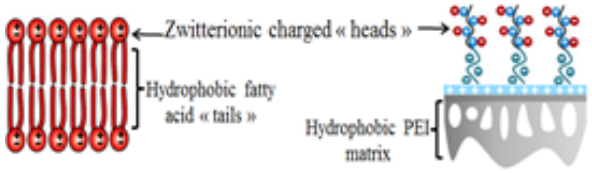

Figure 6. Schematic representation of a phospholipid bilayers membrane (left) and a Cat PEI covered with a zwitterionic block copolymer (right).

The negatively charged part PAA is expected to enable the physisorption by electrostatic interactions with positive charges of the membrane surface while the block bearing zwitterionic groups is assumed to be oriented to the feed solution (Fig. 6). Modification of Cat PEI membranes was carried out by dip coating.

A preliminary result showed that the BSA fouling resistance of the zwitterionic membrane was improved by about 85% compared to the unmodified and Cat PEI membranes.

Actually, the physical adsorption technique was effective to cover a membrane surface of hydrophilic and zwitterionic groups involving significant improvement of the protein fouling resistance. Among the several important advantages, it is a simple, relatively fast, environmentally benign, and potentially economical process. It should be mentioned that the obtained surface layer is not stable overtime by comparison with a covalent modification particularly in presence of high concentration of salts. However, the polyelectrolyte layer can be easily regenerated by repeating the adsorption procedure.

IV. CONCLUSION

The bending method can be an efficient approach to improve the hydrophilicity of PVDF hollow fiber membranes. Actually, PVP was found to be not the ideal additive to ensure long-lasting membrane surface hydrophilicity due to its high affinity to water and its susceptibility to degradation by chlorine compounds. Thus, most of the PVP amount added in the dope solution was leached out during membrane preparation and over the membrane lifespan. To overcome this problem, amphiphilic block copolymer with a hydrophobic part enabling the polymer additive to be firmly anchored in the polymer matrix and a hydrophilic that segregates and migrates to the membrane surface can an attractive alternative to provide long-term fouling resistance.

On the other hand, the chemical post-treatment method also provides an efficient mean for turning hydrophilic the membrane surface. This was successfully achieved in the case of hydrophobic PEI membrane surfaces. Covalent modification using mono and polyaminated groups, modification by physical adsorption of anionic polyelectrolyte layers and adsorption of zwiterionic block copolymer are the three used techniques in this approach. The obtained results showed a large improvement of BSA fouling resistance for the modified PEI membrane especially in the case of Cat PEI-PSS and Cat PEI-PVS membranes which have both a FRR close to 100%.

ACKNOWLEDGMENT

The authors are grateful for the financial support of this work provided by the Program AVERROES Erasmus Mundus from the European Commission (Sana Gassara's grant), and the Fond Unique Interministeriel (FUI) funded by Bpifrance that supported a part of this work through the project NEOPHIL.

REFERENCES

[1] S. F. E. Boerlage, "Scaling and Particulate Fouling in Membrane Filtration Systems," Delft, The Netherlands: Wageningen University and The International Institute for Infrastructural, Hydraulic and Environmental Engineering, 2001.

[2] E. Dufour, S. Gassara, E. Petit, C. Pochat-Bohatier, and A. Deratani, "Quantitative PVP mapping in PVDF hollow fiber membranes by using Raman spectroscopy coupled with spectral chemiometrics analysis", *Eur. Phys. J. Special*

Topics, vol. 224, pp. 1911–1919, 2015.

[3] A. Azaïs, J. Mendret, S. Gassara, E. Petit, A. Deratani, S. Brosillon, "Nanofiltration for wastewater reuse: Counteractive effects of fouling and matrice on the rejection of pharmaceutical active compounds", *Sep. Purif. Technol*, vol. 133, pp. 313–327, 2014.

[4] J. F. Hester, P. Banerjee, Y.-Y. Won, A. Akthakul, M. H. Acar, and A. M. Mayes, "ATRP of Amphiphilic Graft Copolymers Based on PVDF and Their Use as Membrane Additives", *Macromolecules*, , vol. 35, pp. 7652–7661, 2002.

[5] W. Chinpa, D. Quémener, E. Bèche, R. Jiraratananon, A. Deratani, "Preparation of poly(etherimide) based ultrafiltration membrane with low fouling property by surface modification with poly(ethylene glycol)", *J. Membr. Sci.*, vol. 365, pp. 89–97, 2010.

[6] F. Liu, Y.-Y. Xu, B.-K. Zhu, F. Zhang and L.-P. Zhu, "Preparation of hydrophilic and fouling resistant poly (vinylidene fluoride) hollow fiber membranes", *J. Membr. Sci*, vol. 345, pp. 331–339, 2009.

[7] N. Pezeshk, D. Rana, R. M. Narbaitz and T. Matsuura, "Novel modified PVDF ultrafiltration flat-sheet membranes", *J. Membr. Sci.*, 2012, vol. 389, pp. 280–286, 2012.

[8] F. Liu, N. A. Hashim, Y. Liu, M.R. M. Abed and K. Li, "Progress in the production and modification of PVDF", *J. Membr. Sci*, vol. 375, pp. 1–27, 2011.

[9] S. Gassara, W. Chinpa, D. Quemener, R. Ben Amar and A. Deratani, "Pore size tailoring of poly(ether imide) membrane from UF to NF range by chemical post-treatment using aminated oligomers", *J. Membr. Sci*, vol. 436, pp. 36–46, 2013.

[10] S. Gassara, A. Abdelkafi, D. Quemener, R. Ben Amar, and A. Deratani, "Positively charged and bipolar layered poly(ether imide) nanofiltration membranes for water softening applications", *Eur. Phys. J. Special Topics*, vol. 224, pp. 1899–1910, 2015.

[11] W. Chen and T. J. McCarthy, "Layer-by-Layer Deposition: A Tool for Polymer Surface Modification," *Macromolecules*, vol.30, pp. 78-86, 1997.

[12] B. Seantier, A. Deratani, "Polyelectrolytes at interfaces: applications and transport properties of polyelectrolyte multilayers in membranes", *Ionic Interactions in Natural and Synthetic Macromolecules*, edited by A. Ciferri and A. Perico, Wiley, Hoboken, New Jersey, USA, 2012, pp. 683-726.

African Membrane Society
Water & Environment, Process, Energy
Sfax, Tunisia, May 3-5, 2016 - Membrane Water Treatment in Small Urban and Village Centers

Contribution to Understand $Caco_3$ Scaling of Ion Exchange Membranes during Conventional Electrodialysis

Ilhem BEN SALAH SAYADI, T. MANSOUR, H. BOUGHANMI, M. BEN AMOR

Laboratory of Natural Water Treatment, Water Researches and Technologies Center, Borj-Cedria, BP 273 Soliman 8020, Tunisia
ilhem_bensalah@yahoo.fr

Abstract: The democratization of electrodialysis (ED) that can be applied to more than 90% of Tunisian groundwater, is related to the control of scaling adhesion on membranes. In this study, the desalination performance and scaling resistance of two commercial membranes were tested: PCCell and Neosepta. Tests were performed using a pilot unit as a conventional ED in batch recirculation mode. PCCell membranes induce a rapid CaCO3 precipitation but they don't present affinity to the scaling, contrary to Neosepta ones. Neosepta affinity to scaling can be explained by the formation of CaCO3 layer on membranes. This formation opposes the ion transfer and decreases the abatement salinity rate. The local water dissociation phenomenon, caused by the structure of certain membranes, may lead to a more rapid CaCO3 precipitation that can adhere to the membrane surfaces and provoke her scaling.

Keywords: electrodialysis, CaCO3, membrane scaling.

I . INTRODUCTION

Tunisia is a semi-arid to arid country which has turned in over a thirty year to the membrane desalination sector whose reliability is well established. Several worldwide technical and economic studies have determined the optimal desalination process according to water salinity. Although electrodialysis (ED) is the most suitable technology for water desalination of low to moderate salinities (≤ 5 g L^{-1}) [1-3], it remains far exceeded by the reverse osmosis, usually used for high salinity waters. This is due to the heavy tech pre-processing operations using to minimize $CaCO_3$ membrane scaling. The democratization of this process ~~that~~ can be applied to more than 90% of Tunisian groundwater and 26% of surface water (salinity ≤ 5 g L^{-1}), therefore, is related to the control of membrane scaling adhesion in order to minimize or prevent it. In this study, the desalination performance and scaling resistance of two commercial membranes were tested: PCCell (PC-SA and PC-SK) and Neosepta (CMX and AMX), in order to understand the mechanisms leading to $CaCO_3$ formation and adhesion.

II. MATERIALS USED AND METHODS

2.1 Work solutions

For the evaluation of membrane desalination performance, tested solutions are synthetic NaCl 5 g L^{-1} and for the evaluation of membrane scaling, synthetic solution of brackish water were prepared by adding $CaCl_2$ to $NaHCO_3$ solution under CO_2 bubbling. Carbonate and calcium ions concentrations were maintained at 10×10^{-3} and 5×10^{-3} M respectively. The solutions ionic strength was kept at 845×10^{-4} M, adjusted by adding NaCl. All reagents were from analytical grade.

2.2 Electrodialysis equipment

The ED setup consists of a power DC, a concentrate reservoir, a diluate reservoir, a rinsing electrode reservoir 100 and three pumps (Heidolph D-93309) equipped each with a flow-meter (PCCell GmbH). Figure 1 shows a simplified scheme of ED setup.

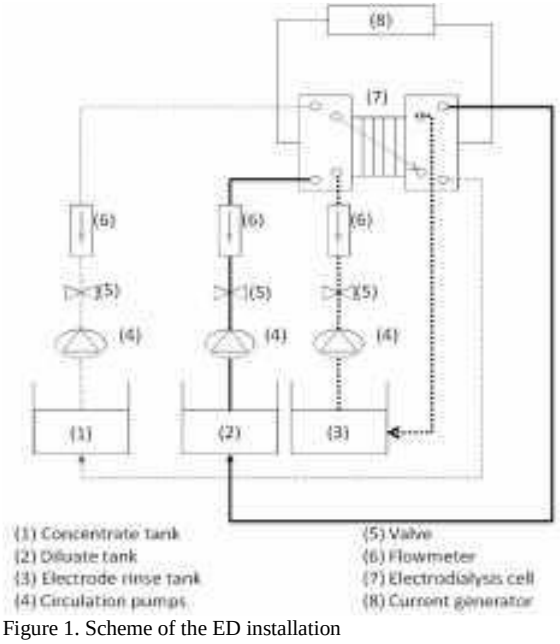

Figure 1. Scheme of the ED installation

2.3 Experimental procedure

During all experiments, the volume of diluate, concentrate and rinsing electrode solution was 1 L each. Rinse solution was 0.1 M Na2SO4 in order to prevent generation of toxic gas. Before the onset of the desalination test, the same solution of brackish water was introduced in diluate and 135 concentrate compartments. Flow rate of electrode rinse solution was fixed at 100 L/ h throughout the test and for all experiments. For concentrate and diluate solutions, only the initial values of flow rates were fixed (60 L/h). The experiment starts at time of the potential application (10V; 140~1V/cell). For this potential, the system operates under the limiting current (maximum value fixed by membrane constructor and verified at laboratory scale was 2 V/cell). The solutions pH, conductivity and flow rate were recorded in time. pH was measured with a pH meter (model pH 320/ 145SET, WTW, Arles, France). Conductivity was measured using conductivity meter (model LF320/SET, WTW, Arles, France). The pH and conductivity electrodes were immersed in each tank (concentrate and diluate). When the conductivity of the product water reaches 0.5 ± 0.1 mS cm−1, a value of high-quality drinking water, voltage is cut and only the dilute solution is replaced by a new working solution. This corresponds to batch duration of 25 min. This operation was repeated several times until detecting stack scaling. After every experiment, ED cell was cleaned with circulation of 0.1 M HCl solution during 30 min followed by three successive rinsing of 15 min each with ultra-pure water.

III. RESULTS AND DISCUSSION

3.1 Evaluation of membranes performance desalination

The superposition of diluate and concentrate conductivity curves show that the two membrane types have close desalination performance: the value of 0.5± 0.1 mS cm-1 is reached after 25 min for the two tests. This result is expected since the two membranes have very close characteristics (exchange capacity and permselectivity) as shown by Table 1.

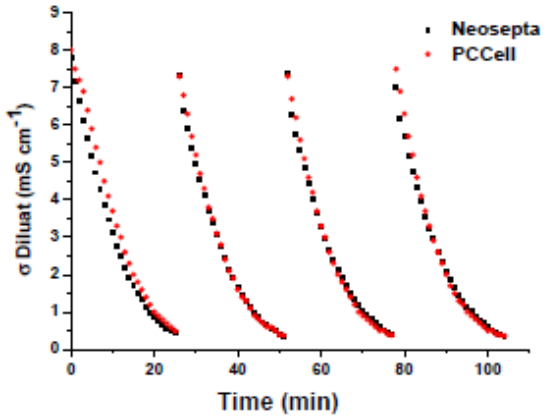

Figure 2: Conductivity (σ) profiles in the diluate during desalination of synthetic brackish water ([NaCl]= 5g L-1)

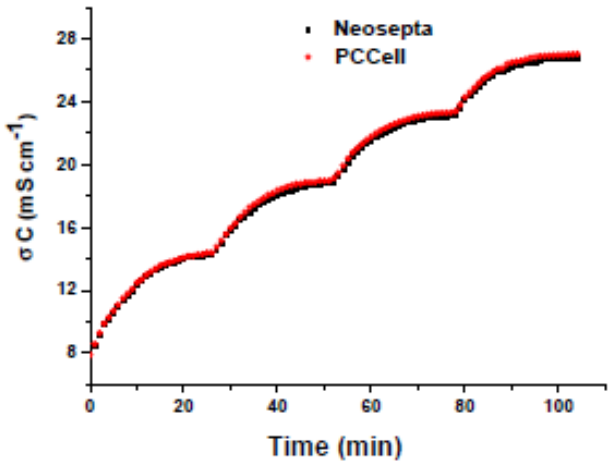

Figure 3: Conductivity (σ) profiles in the concentrate during desalination of synthetic brackish water ([NaCl] = 5g L-1)

Table 1. Countries and cities

Membrane	Thickness (µm)	Exchange Capacity (meq g^{-1})	Stability (pH)	Permsel ectivity	Specific Resistance (Ω cm^{-2})
PC-SK	130	≈1	0-11	>0.96	0.75-3
PC-SA	90-130	≈1.5	0-9	>0.93	1-1.5
CMX	170-190	1.5-1.8	0-12	0.98	2.5-3.5
AMX	160-180	1.4-1.7	0-12	0.98	2.5-3.5

3.2 Evaluation of membranes scaling resistance

The pH of working solutions was fixed at 7±0.1, corresponding to a supersaturation coefficient (Ω ≈ 3), (determined using equation 1) superior to the unity for which spontaneous precipitation of calcium carbonate cannot be induced [4-6]. As for the monovalent salt solution, the behavior of the membranes is similar since one obtains the same cycle duration (25 min) to achieve ≈ 0.4 mS cm^{-1} as the final diluate conductivity.

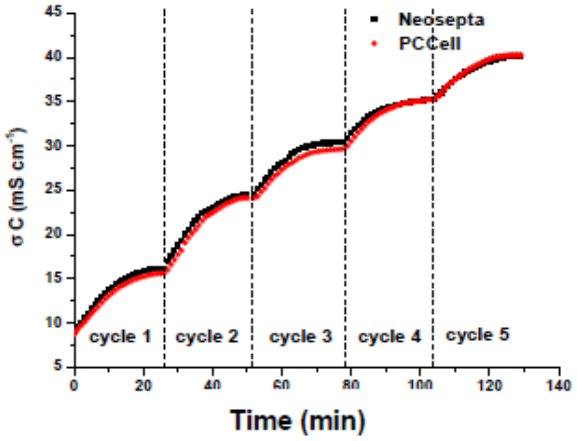

Figure 4: Conductivity (σ) profiles in the concentrate during desalination of synthetic brackish water ([Ca2+] = 10^{-2} M; [HCO3 –] = 5×10^{-3} M)

$$\Omega = \frac{\left(Ca^{2+}\right)\left(CO_3^{2-}\right)}{KSP_{calcite}} \qquad (1)$$

Where :
(Ca^{2+}) : Calcium ions
(CO_3^{2-}) : Carbonate ions
KSP : calcite solubility product

Figure 5 shows that precipitation is detected from the second cycle for the test using PCCell membranes and from the fourth cycle for the test using Neosepta ones. The more rapid precipitation occurred with PCCell membranes is also observed on flow-rate curve by pH increase since the second run. However, it is observed from the fourth run with Neosepta membranes. In fact, in previous study [7], we have detailed the link between the pH evolution and $CaCO_3$ precipitation during desalination test. We have also shown that the flow-rate fall is due to precipitation into solution (homogeneous precipitation) and that the decrease of the water produced conductivity is due to precipitation on membranes (scaling).

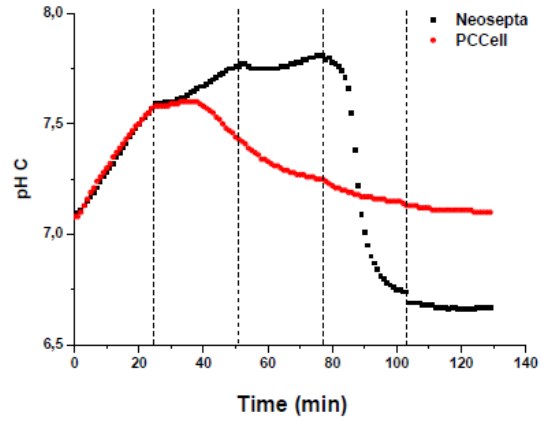

Figure 5: pH profiles in concentrate compartment during desalination of synthetic brackish water ([Ca2+] = 10^{-2} M; [HCO_3 –] = 5×10^{-3} M)

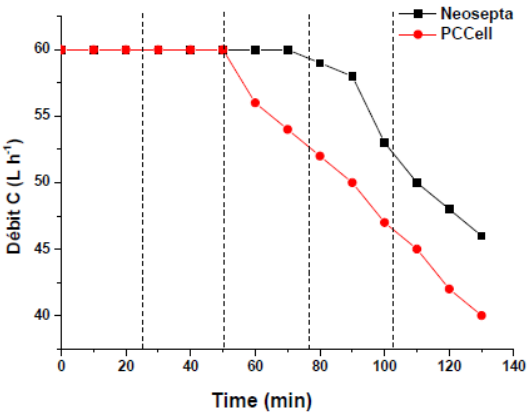

Figure 6: Flow-rate profiles in concentrate compartment during desalination of synthetic brackish water ([Ca^{2+}] = 10^{-2} M; [HCO3–] = 5×10^{-3} M)

Then, we suggest that the faster precipitation observed with PCCell explains the non superposition of conductivities curves during the fourth and the fifth runs (Figure 7). The curve relative to the test using PCCell membranes is slightly below that using Neosepta ones.

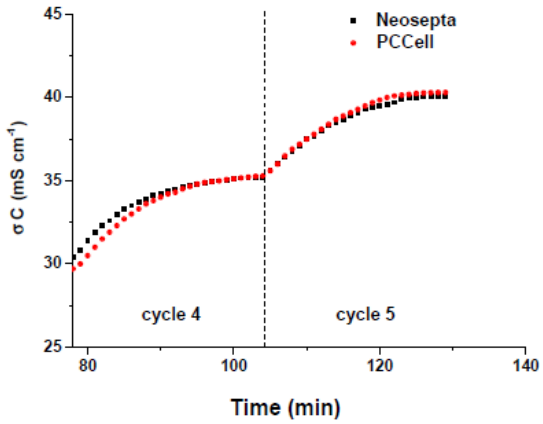

Figure 7: Conductivity (σ) profiles in the concentrate during the 4th and 5th runs of synthetic brackish water water ([Ca^{2+}] = 10^{-2} M; [HCO3–] = 5×10^{-3} M)

The differences observed on the conductivity curves of tests carried out with the two types of membranes are due to different start of precipitation, and not to a difference in membranes performance. However, during the fifth cycle, the order is reversed again and the conductivity values for the test performed with Neosepta are slightly below those recorded with the PCCell.

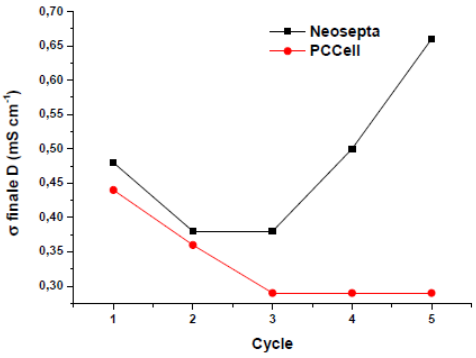

Figure 8: End diluate conductivities during desalination of synthetic brackish water water ([Ca^{2+}] = 10^{-2} M; [HCO3–] = 5×10^{-3} M)

The decrease in the variation of the conductivity observed from the fourth run for test using Neosepta membranes could be explained by the early onset of scaling formation on the membranes. Figure 8 shows that end conductivity values reached respectively to the tests carried out with Neosepta and PCCell membranes are very close for the first and second runs. From the third cycle, water produced quality is improved for the test performed with PCCell despite a faster precipitation, and degraded for the other test. This behavior is not recorded when membranes are tested with monovalent salt solutions. The formation of an adherent layer of $CaCO_3$ to Neosepta membranes may explain this decline in quality of produced water. We can, therefore, conclude that the two types of membranes have different roles in the initiation of the $CaCO_3$ precipitation and its adhesion: scaling occurs only during the test performed with Neosepta

membranes. However, the affinity of PCCell membrane to scaling is relatively low. A surface
phenomenon of membrane/solution may be the cause of the start nucleation which tend to precipitate in
solution or onto membranes. The conductivity reached in the diluate is influenced by the scaling occurrence. Indeed, for
PCCell membranes, abatement rate (τ_{TDS}) increases from 95.7% in the first run to 97.2% in the third one and , stabilize at this level for the last two runs (Figure 9). However, for Neosepta membranes, abatement rate is about 95.5% in the first run. It increases to 96.2% in the second and third runs and significantly decreases during the last two runs to
reach 93.4% at the end test. The formation of scaling layer on Neosepta membranes opposes the ion transfer from the diluate to the concentrate.

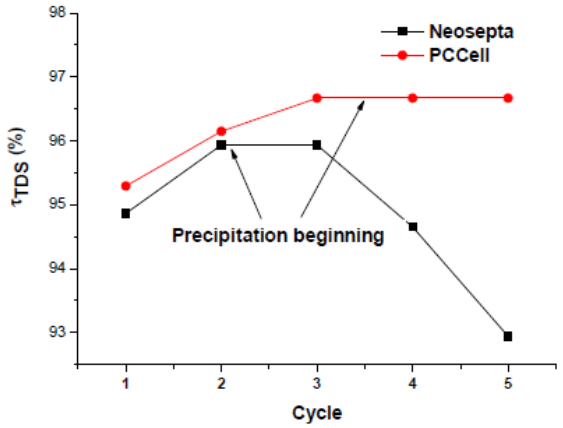

Figure 9: Evolution of salinity abatement rate during desalination of synthetic brackish water water ([Ca^{2+}] = 10^{-2} M; [HCO3–] = 5×10^{-3} M)

IV. CONCLUSION

In this study, two types of commercial membranes used for electrodialysis desalination were compared (Neosepta and PCCell). Results have shown that the two types of membranes have similar desalination performance with monovalent salt work solution ([NaCl]= 5g L-1). However, for the desalination ofhard ([Ca^{2+}] = 10^{-2} M; [HCO3–] = 5×10^{-3} M), they play different roles in the initiation of $CaCO_3$ precipitation and its adhesion: scaling takes place only during the test with the Neosepta membranes. The affinity of PCCell [8]
membrane to scaling is relatively low. According final diluate onductivities, the required quality of produced water is achieved with PCCell throughout the test: 5runs, but only during three runs with Neosepta. We have shown that in the same operating conditions, some membranes have a tendency to scale and not others. The constitution of the membranes, usually not announced by the manufacturers and very difficult to determine by users, do not explain mechanisms leading to the membranes scaling. Nevertheless, laboratory studies allow to assess desalination performances and scaling resistance of membranes.

REFERENCES

[1] F. Valero, R. Arbos, “Desalination of brackish river water using Electrodialysis Reversal (EDR) Control of the THMs formation in the Barcelona (NE Spain) area”, *Desalination* 253, pp. 170-174, 2010.

[2] M. D. Afonso, O. J. Jaber, S. M. Mohsen, “Brackish groundwater treatment by reverse osmosis in Jordan”, *Desalination*, pp 164-157, 2004.

[3] A. Maurel, “Dessalement de l’eau de mer et des eaux saumâtres et autres procédés non conventionnels d’approvisionnement en eau douce”, Edi Tec & Doc, Paris, 2001.

[4] J.Y. Gal, Y. Fovet, N. Gache, “Mechanisms of scale formation and carbon dioxide partial pressure influence: Part I. Elaboration of an experimental method and a scaling model”, *Water Res* 36, pp. 755-763, 2002.

[5] H. Elfil, H. Roques,” Contribution à l’étude des mécanismes de l’entartrage. Étude de la signification physique de la droite limite de précipitation”, *Tribune de l’eau* 599:3, 1999.

[6] J.Y. Gal, J.C. Bollinger, H. Tolosa, N. Gache, “Calcium carbonate solubility: a reappraisal of scale formation and inhibition”, *Talanta, vol.*43, pp. 1497–1509, 1996.

[7] B.S. Sayadi, P. Sistat, M. M. M. Tlili,”Assess of physical antiscale-treatments on conventional electrodialysis pilot unit during brackish water desalination”, Chemical Engineering and Processing: Process Intensification 88, pp. 47–57, 2015.